The syntheses and characterization of nickel complexes; investigation of $Ni(dppp)_2$ and $[NiX(dppp)_n]_x$, potentially catalytically active nickel(0)/(I) species for cross-coupling reactions

By

Rozan Hassan Mehder

A thesis submitted to the Department of Chemistry
in conformity with the requirements for
the degree of Master of Science

Queen's University
Kingston, Ontario, Canada
May, 2016

Copyright © Rozan Hassan Mehder, 2016

Abstract

This thesis describes an investigation in which we compare Ni(0), Ni(I) and Ni(II) complexes containing 1,3-bis(diphenylphosphino)propane (dppp) as a phosphine ligand for their abilities to effect three types of cross-coupling reactions: Buchwald-Hartwig Amination, Heck-Mizoroki, and Suzuki-Miyaura cross-coupling reactions with different types of substrates. The Ni(0) complex $Ni(dppp)_2$ is known and we have synthesized it via a new procedure involving zinc reduction of the known $NiCl_2(dppp)$ in the presence of an excess of dppp. The Ni(0) complex was characterized by NMR spectroscopy and X-ray crystallography. Since Ni(I) complexes of dppp seem unknown, we have synthesized what at this stage appear to be $NiXdppp_n/[NiX(dppp)_n]_x$ (X = Cl, Br, I; n = 1, 2, x = 1, 2) by comproportionation of molar equivalents of $Ni(dppp)_2$ and NiX_2dppp, X= Cl, Br, I.

Acknowledgements

In these acknowledgements, I would like to express my very great appreciation to a number of people for their assistance and encouragements throughout my master studies. I would like to offer my special thanks to my supervisor Professor Michael Baird for his valuable and constructive suggestions during the planning and development of this research work. I appreciated for his cooperation and his willingness to give his time so generously. Working with his group gave me a valuable experience.

In addition, grateful thanks to Dr. Françoise Sauriol for all her support, advice and explanation in NMR experiments. Also, special thanks to Dr. Gabriele Schatte for X-ray crystallography, Also, thank you for my friends Anfal and Adeela in Baird lab, and all colleagues in the Department of Chemistry for making my work more productively and efficiently.

I wish to thank my lovely parents, Hayat Abid, and Hassan Mehder, for their recommendation, encouragement, and support. Special thanks to my dear brother Amar Mohdar for his help throughout my study in Canada. I would like you to know how thankful I am for having you as my brother. Thanks for my dear sister and brothers for their assistance and endless love. Words will never be enough to show my appreciation to them

Last and most important, I would like to thank ministry of education in Saudi Arabia, and Saudi Cultural bureau in Canada for their financial support and cooperation with me.

Table of Contents

List of Figures

List of Schemes

List of Tables

List of Abbreviations

Å…….. Ångström

br…… broad

°C……..….Degrees Celsius

C_6D_6 ……Deuterated benzene

$CDCl_3$ ..... Deuterated chloroform

CD_2Cl_2.....Dichloromethane-d_2

δ…… Chemical shift

dppe……....1,2-Bis(diphenylphosphino)ethane

dppf ……..…….....…… 1,1'-Bis(diphenylphosphino)ferrocene

dppp ……..……...1,3 Bis(diphenylphosphino)propane

EPR…….....……...… Electron paramagnetic resonance

eq ……Equivalents

g ……..……...……Grams

GC ……..……Gas chromatography

η…….……Hapticity

h ……..……Hour

HMBC……Heteronuclear Multiple Bond Correlation

Hz..…….. Herz

J…….. Coupling constant (NMR)

M..……...Metal

m ……multiple

Me ……methyl group

MeCN .....…….....Acetonitrile

mg ……milligram

MHz ……..……megahertz

min ……..……..……..……minutes

mL ……..……milliliter

mmol ……..……mililimoles

Mw.....Molecular Weight

NMP…… N-Methylpyrrolidone

NMR……..…….. Nuclear magnetic resonance

NR……..…No reaction

PPh_3……..…….... Triphenylphosphine

R ……Alkyl group

RT……..……..……..…Room temperature

s ……..…..……Singlet

SSB ……..……..…….....Spinning side bands

t ……..……..……...…Triplet

THF……..……Tetrahydrofuran

Chapter 1

Introduction

1.1 Cross-Coupling Reactions

Transition-metal catalyzed-cross-coupling reactions are highly potent synthetic tools for creating a carbon-carbon bond.[1,2] Organic electrophiles of the type R^2-X including organic halides and pseudohalides (triflates, mesylates, tosylates) react with organometallic reagents of the type R^1-m (m = Mg, B, Sn, Al, Li, Si, Zr, Zn), catalyzed by transition metals such as Ni and Pd, with formation of carbon-carbon bonds R^2-R^1 and generating salts m-X as a result (Figure 1).

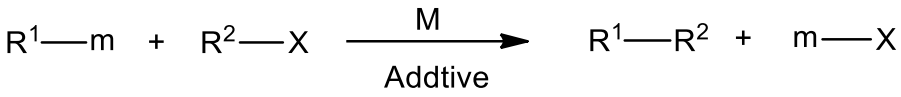

Figure 1. General cross-coupling reaction for C-C bond formation

R^1 = R^2 = alkenyl, aryl, alkyl, etc., m = Mg, B, etc; M = Ni, Pd; X = Cl, Br, I, etc.

Transition metal catalyzed cross-coupling reactions have several uses in the agricultural, medicinal and liquid crystals industries, in addition to the syntheses of macromolecules and natural products. They are widely used because of their high selectivity and functional group tolerance in the synthesis of natural products with complicated chemical structures.[1,2]

1.1.1 A General Catalytic Cycle for Cross-Coupling Reactions

A generally accepted mechanism for the cross-coupling reaction is shown in Scheme 1.[2] In the case of carbon-carbon coupling reactions, this involves the oxidative

addition of organic halides (RX) to the metal(0) complex, thus producing the organometal halide (R-M-X) complexes. This step is followed by the transmetalation involving R'm, and the final step involves reductive elimination to form the carbon–carbon bond accompanied by regeneration of the catalyst.

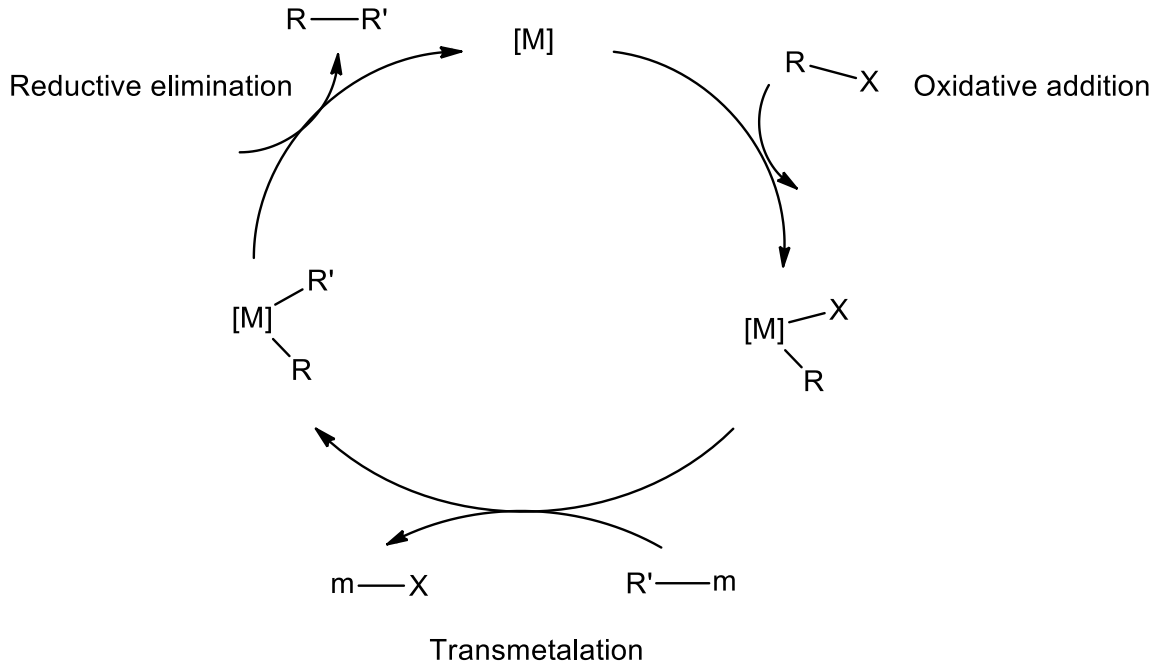

Scheme 1. General mechanism of the metal-catalyzed cross-coupling reaction.

1.1.2 General Catalytic Cycles for Palladium and Nickel

The development of Pd-based catalysts has proceeded further than the Ni-based catalysts.[1-3] Numerous cross-coupling reactions are catalyzed by Pd(0) species of the type PdL_2 (L = phosphine ligand) and Pd(II) species of the type $PdRXL_2$ which lie on the catalytic cycle (Scheme 2). As in the general cycle shown in Scheme 1, the catalytic cycle[2] begins with the oxidative addition of aryl halides to the catalytic species PdL_2, a two-electron process in which the Pd(0) is oxidized to Pd(II). The next step is the transmetalation involving species m-nuc (m = Mg, Si, Sn, Zn, etc.; nuc = alkyl, aryl,

amide, alkoxy, etc.). The organic group is transferred from the nucleophile to produce $PdR(nuc)L_2$. The final step is the reductive elimination of R-nuc to regenerate the catalytically active species PdL_2 and form the carbon-carbon bond.

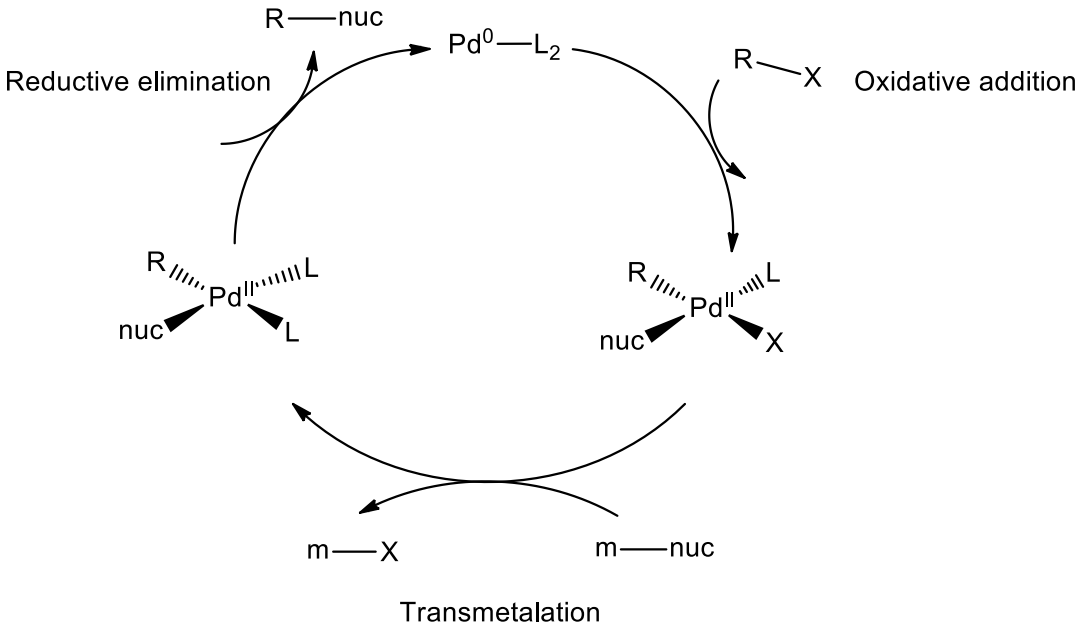

Scheme 2. Generalized mechanism for palladium-catalyzed cross-coupling reactions.

Nickel(0) catalysts can also be used in many cross-coupling reactions as in Schemes 1, 2.[3] Nickel possesses several advantages over palladium as it is less expensive and more environmentally benign.[3a,c] Nickel(0) systems also carry out more facile oxidative additions of alkyl halides and better avoid the β-hydrogen elimination from alkyl intermediates which would stop the catalytic cycle. Radical pathways are also accessible.[4]

1.1.3 Catalytic Cycles involving Nickel(I) and Nickel(III)

Nickel readily occurs in several oxidation states, 0, +1, +2, +3 and +4, giving rise to more than one type of catalytic cycle, including the M(0)/M(II) two-electron processes shown in Schemes 1 and 2.[3a,d] It has also been established that Ni(0) and Ni(II)

complexes can undergo comproportionation to Ni(I) complexes sufficiently readily that the presence of both can result in comproportionation of reactant and product to give Ni(I) compounds.[5]

A currently popular catalytic cycle involving a Ni(I)-based mechanism is shown in Scheme 3.[6,7] This catalytic cycle begins with transmetalation of a halonickel(I) compound, $NiXL_n$, with a species m-R' (m = Mg, Si, Sn, Zn, etc.; R'= alkyl, aryl, amide, etc.) to produce an intermediate of the type $NiR'L_n$. The second step involves reaction with an organic halide RX to form the Ni(II) species $NiR'XL_n$ plus an organic radical R•. The $NiR'XL_n$ intermediates then combine with the organic radical to produce $NiXRR'L_n$, and the final step involves reductive elimination to regenerate the catalyst, $NiXL_n$, and the cross-coupling product R-R'.

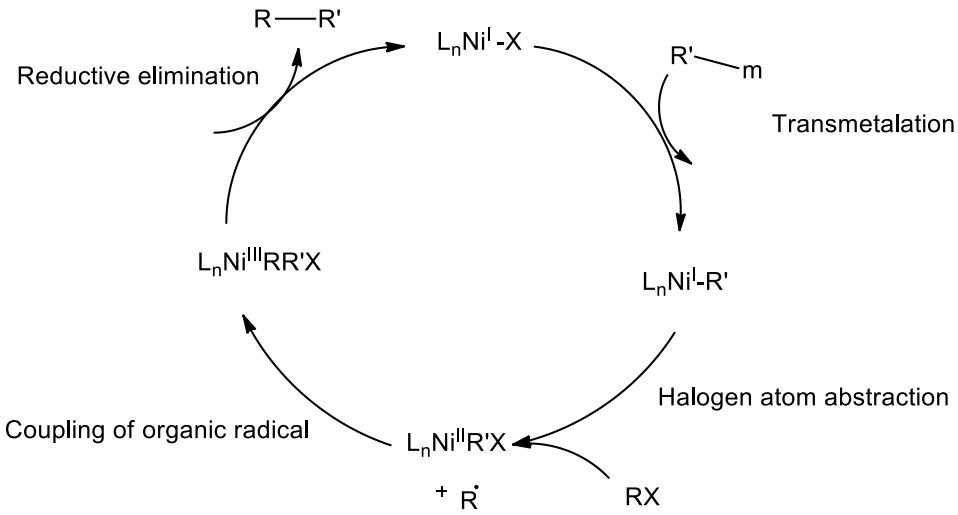

Scheme 3. Proposed mechanism for nickel catalyzed cross coupling reaction via transfer of one electron.

1.2 Catalytic Activities of Ni(II) Complexes of Chelating Diphosphines for Cross-Coupling Reactions

1.2.1 Kumada-Tamao-Corriu Cross-Coupling Reaction

Kumada cross-coupling reactions, discovered in 1972 by Kumada et al,[8] play an important role in organic synthesis; they involved coupling of Grignard reagents with organic halides such as aryl- and vinyl halides in the presence of a phosphine-nickel catalyst to form carbon-carbon bond and generate the salt.[8] (Figure 2).

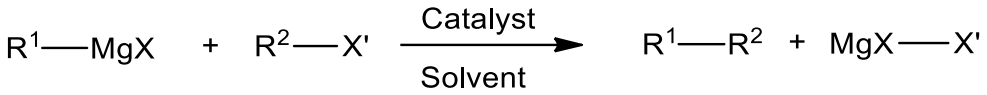

Figure 2. General Kumada cross-coupling reaction

Catalyst: NiX_2L_2 (L_2 = diphosphine); Solvent: THF or Ether

For instance, 1,2-dibutylbenzene has been prepared[9] in just a single step by using a mixture of Grignard reagent with an organic halide in the presence of a phosphine-nickel catalyst shown in Figure 3.

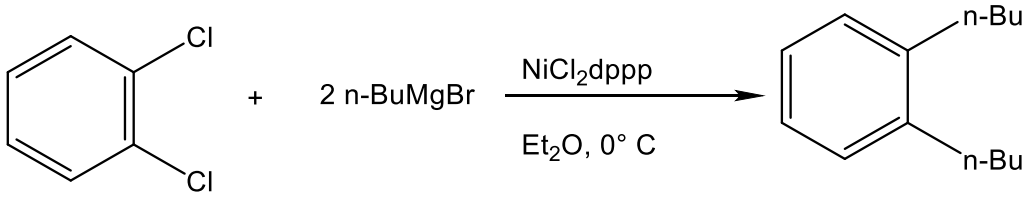

dppp= 1,3bis(diphenylphosphino)propane

Figure 3. Preparation of 1,2-dibutylbenzene

In 2015, the nickel-phosphine catalysts, $NiCl_2$dppe, $NiCl_2$dppp and $NiCl_2$dppf, were used in the Kumada cross-coupling reactions[10] and it was found that $NiCl_2$dppf with an

excess of PPh_3 ligand was the most reactive followed in the order [$NiCl_2$dppe]> [$NiCl_2$dppp] as shown (Table 1). The reasons for this trend are not known.

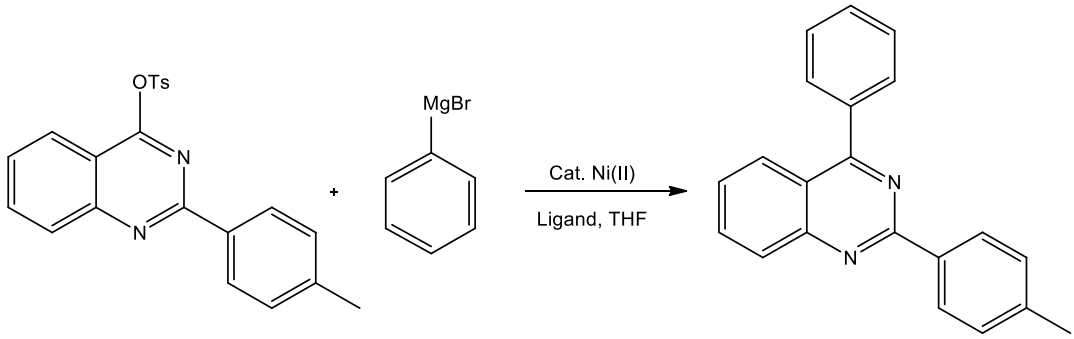

1a 2a 3a

Cat. Ni(II) = $NiCl_2$dppe, $NiCl_2$dppp, $NiCl_2$dppf

Figure 4. Synthesis of 4-Phenyl-2-p-tolyl-quinazoline

Table 1. Percent composition of Kumada cross-coupling products

Entry	Ni(II) catalyst	ligand	Yield(%)
1	$NiCl_2$dppe	dppe	71
2	$NiCl_2$dppp	dppp	65
4	$NiCl_2$dppf	dppf	79
3	$NiCl_2$dppf	PPh_3	80

Thus 4-phenyl-2-p-tolyl-quinazoline (3a) was successfully synthesized by reaction of 2-(p-methyl phenyl)quinazoline-4-tosylate (1a) and phenyl magnesium bromide (2a) in the presence of phosphine-nickel catalysts and excess ligands.[10] Similarly reactions of vinyl chlorides with aryl Grignard reagents in the presence of $NiCl_2$dppp in THF resulted in a high yields of coupled products as shown in Figure 5-6.[9,11]

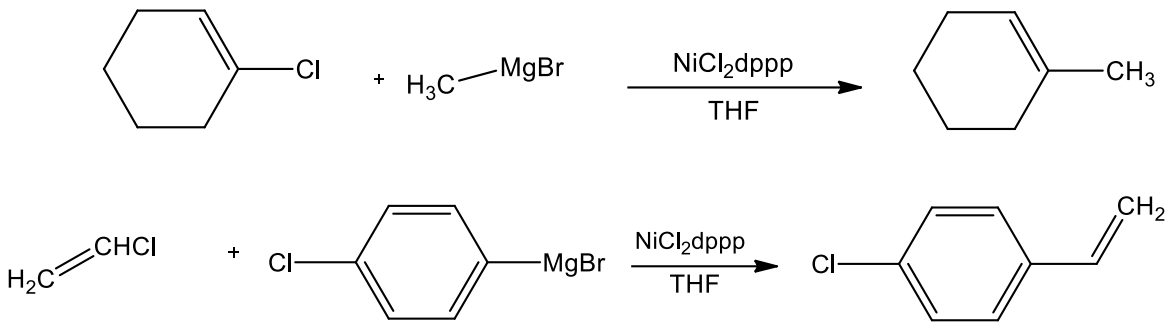

Figure 5-6. Examples of Kumada cross-coupling reactions.

The catalytic activities of the phosphine-nickel complexes depend on the nature of the ligands (Figure 7, Table 2), with bidentate phosphine complexes exhibiting relatively high catalytic activities. The efficiency of the bidentate phosphine ligands decreases in the order dppp > dmpf > dppe > dmpe > dppc > cis-dpen,[11,12] for reasons unknown at present.

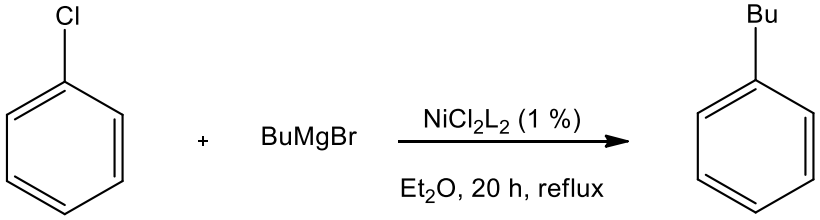

Figure 7. Cross-coupling of chorobenzene with Grignard reagents catalyzed by various $NiCl_2L_2$

Table 2. The catalytic activity of various nickel-phosphine catalysts.

L_2	Yield (%) of PhBu
dppp	100
dmpf	94
dppe	79
dmpe	47
dppc	28
cis-dpen	20

Other examples of Kumada cross-coupling reactions include coupling of vinyl chloride and Grignard reagents catalyzed by $NiCl_2$dppp;[11] yield:100% (Figure 8).

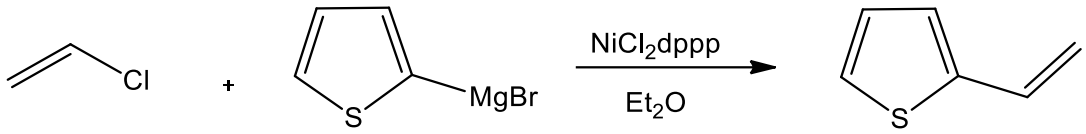

Figure 8. Synthesis of 3-ethenylthiophene

1.2.2 Suzuki-Miyaura Cross-Coupling

Suzuki–Miyaura cross-coupling, involving the reaction between an organoboron compound and an organic halides or pseudohalide (OTf, OTs, OMs) in the presence of nickel catalyst and base is one of the most powerful methods for the construction of biaryls and heterobiaryls.[13] The nickel-catalyzed cross-coupling reaction of phenyl boronic acids with chloroarenes was first reported by Miyaura and his colleagues in early 1996.[14]

The Suzuki coupling has several advantages. The reactants are highly stable to air, water, moisture, and exhibit low toxicity.[15] Gao et al. reported the use of the $NiCl_2$dppp as a catalyst for the coupling of aryl mesylates and tosylates with only 1 mol% loading without excess of ligands. The coupling between 1-naphthyl tosylate (1b) and 4-methoxylphenylboronic acid (2b) in the present of the most promising catalyst ($NiCl_2$dppp) produced the biaryl in 91% yield (Figure 9).[13]

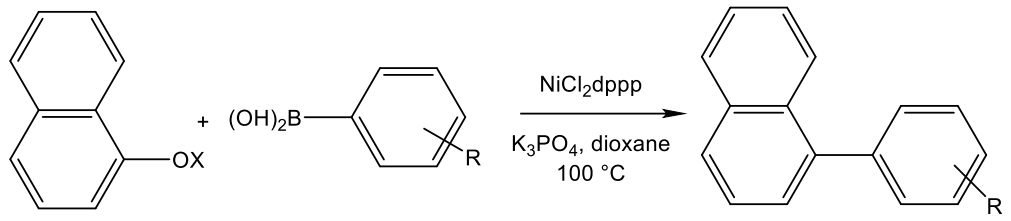

(1b) X = Ts; (2b) R = *p*-OMe; (3b) X = Ms; (4b) R = *m*-NH_2

Figure 9. Suzuki–Miyaura cross-coupling of 1-naphthyl mesylate (1b) with 4-methoxylphenyl boronic acid

Similarly, coupling of 1-naphthyl mesylate (3b) with 4-methoxylphenyl boronic acid (2b) gave the desired product in 99%. These reactions can be viewed as references in the optimization of reaction conditions[13] because researchers tested the feasibility of the transformations using various organoboron reagents. In general, cross-coupling of both 1-naphthyl tosylate and mesylate (1b and 3b) react with various boronic acids in the presence of $NiCl_2$dppp formed the products in very high yields as shown in Figure 9. In addition, the authors tested the applicability of a broad range of phenols by using various aryl tosylates and mesylates; giving good yields as shown in Figure 10, 11.

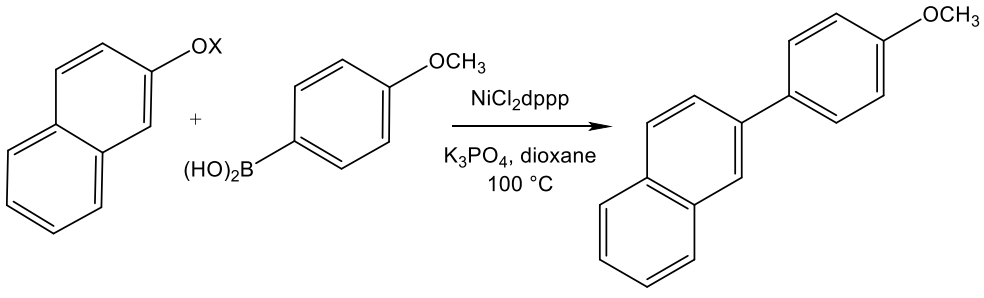

X = Ts 97%; X = Ms 98%

Figure 10. Suzuki cross-coupling reactions.

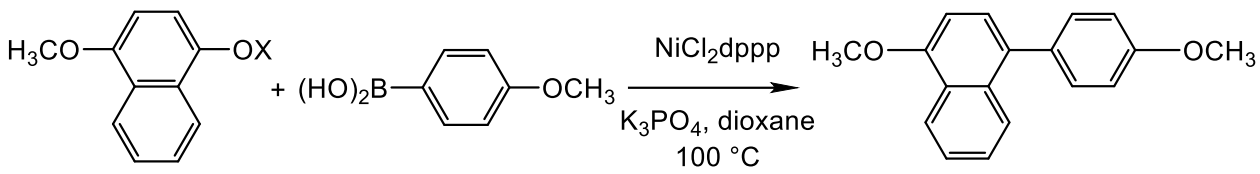

X = Ts 73%; X = Ms 78%

Figure 11. Suzuki cross-coupling reactions.

1.2.3 Heck-Mizoroki Cross-Coupling (henceforth the Heck reaction)

The Heck cross-coupling reaction, involving cross-coupling reaction of an aryl or vinyl halide with an alkene in the presence of a base and a catalyst (Figure 12), is one of the most significant processes in synthetic organic chemistry and has been applied to many substrates.[16]

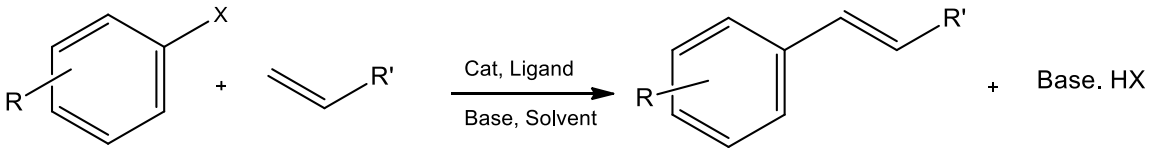

Figure 12. General Heck cross-coupling reaction

Palladium is the most widely used catalyst for the Heck reaction, but nickel can be a good replacement for palladium.[16] In 1986, coupling reactions between activated olefins and aryl/vinyl halides were carried out using $NiCl_2(PPh_3)_2$ reduced by zinc in THF as shown in Figure 14.[17] Excess zinc powder was needed to ensure catalytic results[17] (Figure 13, 14). The products are formed depending on the activated group in the olefin and the nature of the organic halogen.

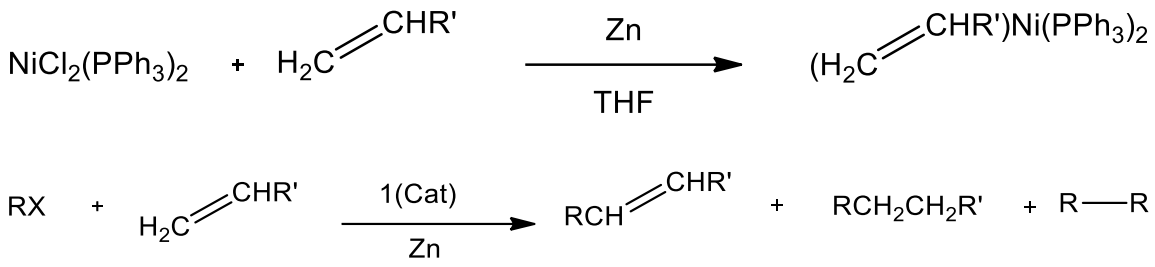

Figure 13-14: Heck cross-coupling reactions.

In 2006, nickel acetate catalyzed cross-coupling of iodobenzene and methyl acrylate in the present of triethylamine was reported in a variety of solvents such as toluene, ethanol, and N-methylpyrrolidone.[18a] It was found that polar solvents produced better yields than non-polar solvents.

The mechanism of the Heck reaction[16] involves four steps, oxidative addition of organic halide (RX) to form a *cis*-$RMXL_n$ species, alkene coordination to the metal, insertion of the alkene into the C-M bond and β-hydride elimination to form the substituted olefin product, which dissociates. The final step is the regeneration of the catalyst after the removal of HX from the species $MHXL_n$. M=Pd, Ni (Scheme 4). Thus there are similarities between the mechanisms of the Ni- and Pd-catalyzed Heck reactions (Scheme 4) although it is found with nickel systems that alkyl halides undergo oxidative addition more readily and that the resulting alkyl-nickel species undergo β-elimination less readily. The reasons for the differences are not clear.

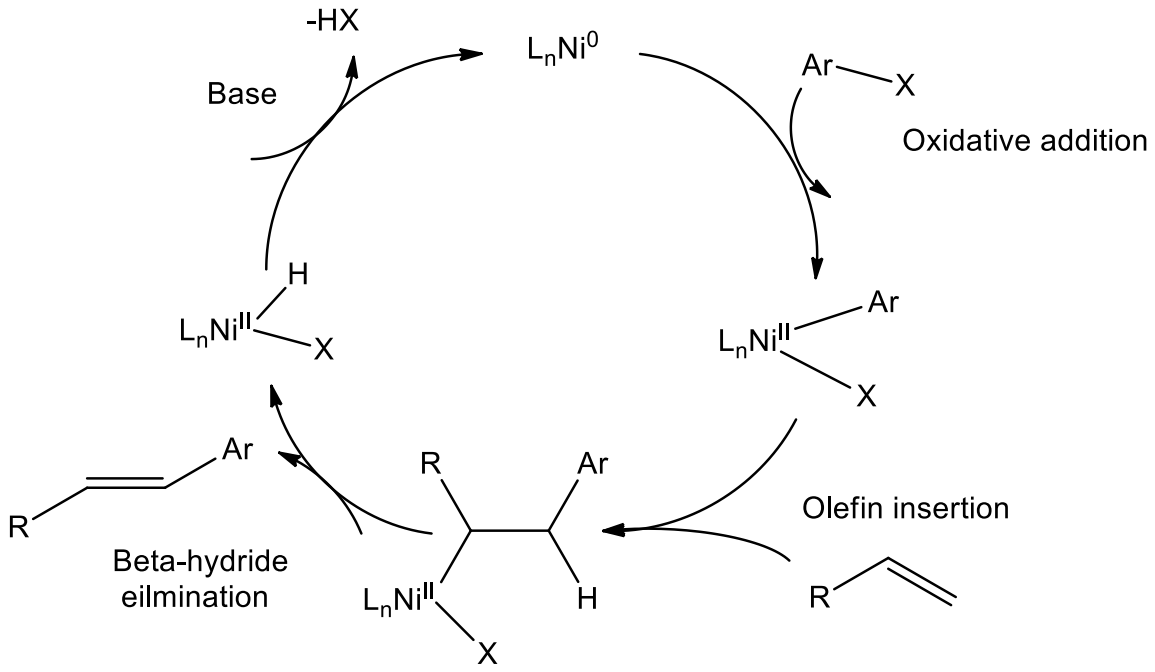

Scheme 4. General Mechanism of the Heck reaction

1.2.4 Buchwald-Hartwig Amination Cross-Coupling Reactions

The Buchwald-Hartwig cross-coupling reaction is one of the most important processes for the formation of carbon-nitrogen bonds, this is a cross-coupling reaction of aryl haildes with an amine in the presence of a catalyst and a strong base.[19a]

The catalytic cycle starts with oxidative addition of aryl halides (RX) to the metal (L_nM^0) to form $L_nM^{II}(Ar)X$ complex, this complex coordinate with the amine. Then, the deprotonation occurs when the base removes a proton from the amine. The final step is the reductive elimination to regenerate the catalyst and form a carbon-nitrogen bond. It has been applied to aryl chloride substrates with primary or secondary amines in the present of nickel as a catalyst (Figure 15).[19b, c]

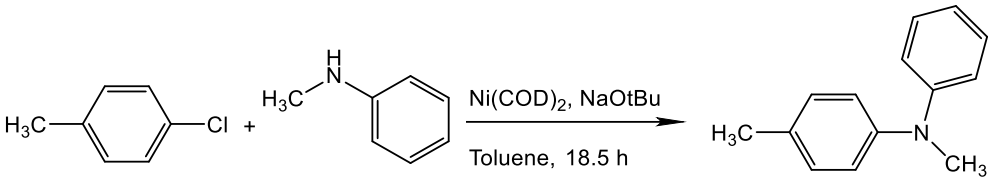

Figure 15. Amination cross-coupling reaction.

For example, the coupling of 4-chlorotoluene with N-methylaniline in the presence of 2 mol % of $Ni(COD)_2$ (COD = 1,5-cyclooctadiene) and 4 mol % of dppf (1,1`-bis-(diphenylphosphino)ferrocene) with excess of NaOtBu at 100 °C in toluene formed the high yield of tertiary amine in 80% yield.[19a]

1.3 Ligand

1.3.1 (1,3-Bis(diphenylphosphino)propane (dppp))

1,3-Bis(diphenylphosphino)propane (dppp) is the ligand used in this research. It is a slightly air sensitive, white solid with a chemical formula $(CH_2)_3(P(C_6H_5)_2)_2$ and a molecular weight of 412.2. It has been used to tune the reactivities of complexes of nickel and palladium.[20,21]

The compound dichloro[1,3-bis(diphenylphosphino)propane]nickel ($NiCl_2$dppp) was prepared by combining dppp and nickel(II)chloride hexahydrate.[22] This nickel complex has been used as a catalyst in a very small number of cross-coupling reactions.

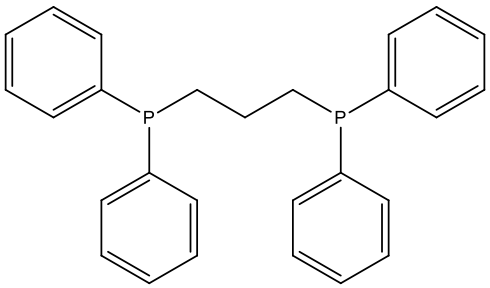

Scheme 5. Structure of 1,3-Bis(diphenylphosphino)propane (dppp)

1.4 Objectives of this research

Although phosphine complexes of palladium have been much used as catalysts for cross-coupling reactions,[1,2] relatively little has been done with analogous phosphine nickel complexes. The general aim of this research was therefore to explore nickel catalysis utilizing a typical ligand, dppp. It was anticipated that catalysis by the known nickel(0) complex $Ni(dppp)_2$[23] could be studied, and that new nickel(I) species such as $NiX(dppp)_n$ (X = halide, n = 1, 2) might also be synthesized and studied.

The first target was a synthesis and characterization of the Ni(0) complex $Ni(dppp)_2$[23], and this was accomplished by a novel procedure involving reduction of $NiCl_2(dppp)$ with zinc dust in the presence of excess of dppp. The second target was synthesis of a Ni(I) complex and a Ni(I) compound of unknown structure was obtained by a comproportionation reaction using equimolar amounts of Ni(0) and Ni(II) complexes. The third target was to investigate Ni(0), Ni(I) and Ni(II) complexes for their abilities to catalyze Heck and Suzuki-Miyaura reactions with different types of substrates.

Chapter 2

Experimental Section

2.1 General Procedures

All reactions were carried out using dry, deoxygenated argon with standard Schlenk line techniques. Argon was deoxygenated by passing through a heated column of BASF copper catalyst, and then dried by passing through a column of 3A molecular sieves. Anhydrous solvents (benzene, dioxane, hexane, toluene, diethyl ether, dichloromethane, acetonitrile, and THF) were dried over molecular sieves, which were activated by heating at 225 ^{o}C, 10^{-2} torr. The appropriate glassware had been stored in an oven overnight. The air sensitive compounds were stored and handled in an LCBT-1 Bench Top Glovebox.

Bruker AV 400, AV 500 and AV 600 spectrometers were used to record solution NMR spectra. ^{1}H NMR spectra were referenced to residual proton present in the deuterated solvents with respect to TMS (tetramethylsilane). Many of the spectra contained resonances which were very broad and which exhibited very unusual chemical shifts. Overlap in some cases was considerable and, as a consequence, integrations were often non-integral. They are reported here as such, and are discussed further and assigned in the Results and Discussion section.

^{13}C and ^{31}P NMR spectra were run in the solid state on a Bruker AV600 by Dr. Francoise Sauriol. Spectra were generally complicated by the presence of spinning side bands (SSB), and the chemical shifts given are for the centre peaks. GC experiment was carried out using a Varian 3900 GC equipped with a CP8400 autosampler, a 0.32 fused silica column (CP-Sil 8CB, 25 m x 0.32 mm ID, DF = 0.52) and an FID detector.

The column temperature was set at 140 °C, the injector and detector temperatures at 250 °C. Hexadecane was used as standard for the cross-coupling reaction.

EPR spectra were run on powdered solids at 77 K by Dr. Bruce Hill of the Department of Biochemistry, Queens University. An X-ray crystal structure determination was performed by Dr. Gabriele Schatte at Queen's University. Crystals were mounted on a glass fiber with grease and cooled to −93 °C in a stream of nitrogen gas controlled with Cryostream Controller 700. Data collections were performed on a Bruker SMART APEX II X-ray diffractometer with graphite-monochromated Mo K_α radiation (λ = 0.71073 Å) operating at 50 kV and 30 mA over 2θ ranges of 4.38 ~ 51.98º.

2.2 Chemical Supplies

Nickel(II) chloride hexahydrate ($NiCl_2.6H_2O$) and anhydrous nickel(II) iodide (NiI_2) were purchased from Sigma Aldrich, 1,3-bis(diphenylphosphino)propane (dppp; ^1H and ^{31}P NMR spectra Figure A1, A2) from Strem. NMR solvents were purchased from Cambridge Isotope Laboratories, anhydrous solvents from EMD Chemicals.

The compounds dichloro[1,3-bis(diphenylphosphino)propane]nickel ($NiCl_2$dppp), dibromo[1,3-bis(diphenylphosphino)propane]nickel ($NiBr_2$dppp) and diiodide [1,3-bis(diphenylphosphino)propane]nickel (NiI_2dppp) were synthesized as in the literature.[22a] Toluene-d_8, benzene-d_6, dichloromethane-d_2 and chloroform-d were dried over 3A molecular sieves under an argon atmosphere.

2.3 Synthesis of NiX_2dppp

2.3.1 Synthesis of $NiCl_2dppp$[22a]

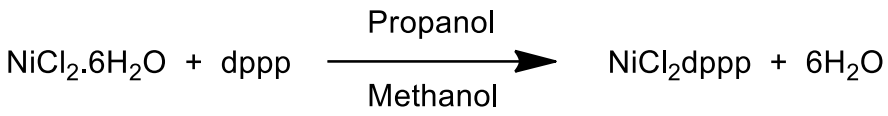

Figure 16. Synthesis of $NiCl_2dppp$.

A solution of dppp (3.01 g, 7.31 mmol) in 40 mL of warm 2-propanol was added to a solution of nickel(II) chloride hexahydrate (2.00 g, 8.39 mmol) in 35 mL of warm 5:2 2-propanol:methanol to give a red precipitate of $NiCl_2dppp$. The mixture was heated for 10 min, the air-stable product was collected by filtration and recrystallized from dichloromethane to give 3.36 g (yield 85%). A ^1H NMR spectrum was run in CD_2Cl_2 and is shown in Figure A3. ^1H NMR (CD_2Cl_2, 500 MHz): δ 0.24 (br, 2.0 H), 5.95 (br, 3.5 H), 6.85 (br, 8.0 H), 9.32 (br, 8.0 H), sharp singlets at δ 5.36 and 1.57 are attributed to $CHDCl_2$ and HDO respectively. Because $NiCl_2dppp$ is paramagnetic, the ^{31}P resonance is too broad to be observed in solution (Figure A4).^{13}C and ^{31}P NMR spectra were therefore run in the solid state on a Bruker AV600 (Figures A5, A6). ^{13}C NMR, δ (ppm): 120-142 (m, Ph), 16-22 (m, CH_2), ~57 (partially obscured by spinning side bands, CH_2). ^{31}P NMR, δ (ppm): 0.59.

2.3.2 Synthesis of $NiBr_2dppp$[22a]

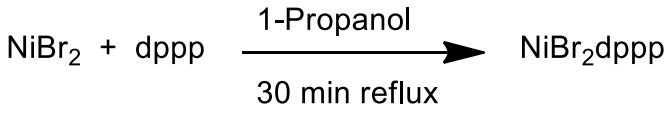

Figure 17. Synthesis of $NiBr_2dppp$

A solution of anhydrous nickel(II) bromide (2.36 g, 10.80 mmol) in 80 mL hot 1-propanol was combined with a solution of dppp (4.11 g, 10.0 mmol) in 40 mL of hot 1-

propanol to give a deep red precipitate. The mixture was refluxed for 30 min, and filtered to give 5.11 g (81% yield) of air-stable product. ^{1}H NMR spectra were run in $CDCl_3$ and CD_2Cl_2 on a Bruker AV 500 (Figures A7a, A7b). ^{1}H NMR ($CDCl_3$): δ –4.83 (s, 2H), –0.29 (br, 3.3 H), 1.55 (br, 2.7 H; HDO), 2.61 (br, 6.2 H), 7.27 (s, $CHDCl_3$), 7,74 (w, m), 16.21 (br, 6.8 H). ^{1}H NMR (CD_2Cl_2): δ –3.09 (br, 2.0 H), 0.40 (w, br), 1.59 (br, 2.30 H), 1.85 (br, 3.2 H), 4.08 (br, 5.7 H), 7.57, 7.81 (w), 14.0 (br, 6.5 H), 20.4 (w, br). Because $NiBr_2$dppp is paramagnetic, the ^{31}P resonance is too broad to be observed in solution. ^{13}C and ^{31}P NMR spectra were therefore run in the solid state on a Bruker AV600 (Figures A8, A9). ^{13}C NMR: δ 15-26 (m, CH_2), 120-135 (m, Ph). ^{31}P NMR: δ 17.6 (br), 2.3 (br).

2.3.3 Synthesis of NiI_2dppp[22a]

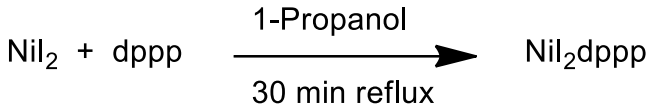

Figure 18. Synthesis of NiI_2dppp.

A solution of anhydrous nickel(II) iodide (3.45 g, 10.75 mmol) in 80 mL of hot 1-propanol was combined with a hot solution of dppp (4.11 g, 9.99 mmol) in 40 mL of 1-propanol to give a dark purple solution. The mixture was refluxed for 30 min, and the solvent was removed under reduced pressure to give 5.19 g of dark purple, air-stable solid (70% yield). ^{1}H NMR ($CDCl_3$, 500 MHz): δ – 4.14 (br, 2.0 H), –1.76 (br, 6.5 H), 1.0-3.8 (several broad resonances, 101.7 H), 7.34, 8.05 (two br resonances, 244 H), 18.2 (br, 8 H) (Figure A10). Because NiI_2dppp is paramagnetic, the ^{31}P resonance is too broad to be observed in solution. ^{13}C and ^{31}P NMR spectra were therefore run in the

solid state on a Bruker AV600 (Figures A11, A12). ^{13}C NMR: δ ~16.82 (m, CH_2), 120-140 (m, Ph). ^{31}P NMR: δ ~26 (br).

2.4.1 Synthesis of $Ni(dppp)_2$ via reduction of $NiCl_2dppp$

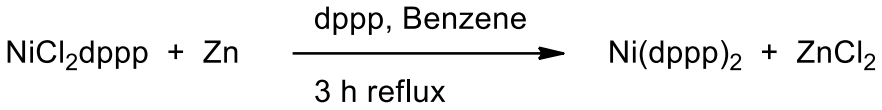

Figure 19. Synthesis of $Ni(dppp)_2$ via reduction of $NiCl_2dppp$.

Under an argon atmosphere, a mixture of 1.79 g $NiCl_2dppp$ (3.30 mmol), 1.36 g dppp (3.30 mmol) and 1.2 g zinc dust (18.40 mmol) in 90 mL of anhydrous benzene was refluxed for 3 h, the colour of the solution changing from red to orange-yellow. The mixture was filtered to remove the zinc, and the solvent was removed under reduced pressure to give 1.98 g of air-sensitive, orange-yellow product (68% yield). ^{1}H, ^{31}P and ^{1}H-^{31}P HMBC experiments were carried out in benzene-d_6 on a Bruker AV 500 and 600 (Figures A13, A14, A15). ^{1}H NMR (C_6D_6, 500 MHz): δ 1.58 (br, 4.0 H), 2.34 (br, 7.0 H), 7.11 (br m, 17 H), 7.27 (br, 4.67 H), 7.61 (br, 11 H). ^{31}P NMR (C_6D_6, 500 MHz): δ 13.6, lit. 12.7 in toluene.[23] Complementing these spectra, a ^{1}H-^{31}P HMBC experiment was run and the resulting spectrum is shown in Figure A15. As can be seen, the ^{31}P resonance correlated strongly with the ^{1}H resonances at δ 7.61 and 2.34, weakly with that at δ 7.11 and not at all with that at δ 1.58. An EPR spectrum of a powder sample of one batch of crude material (77 K) is shown in Figure A16.

A sample was recrystallized under argon by dissolving 1.0 g in 90 mL hot anhydrous benzene in a Schlenk tube; 2 mL of anhydrous hexane were added dropwise and the mixture was left for 3 days in the glove box to give orange-yellow crystals which were characterized crystallographically at −93 °C. The structure is shown in Figure A17,

important bond lengths and angles in Tables B3 and B6 where comparisons are made with the corresponding data for an earlier room temperature structure determination.[24]

2.4.2 Synthesis of $Ni(dppp)_2$ via reduction of $NiBr_2dppp$

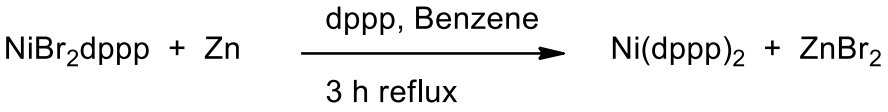

Figure 20. Synthesis of $Ni(dppp)_2$ via reduction of $NiBr_2dppp$.

Under an argon atmosphere, a mixture of 2.08 g $NiBr_2dppp$ (3.30 mmol), 1.36 g dppp (3.3 mmol) and 1.2 g zinc dust (18.4 mmol) in 90 mL of anhydrous benzene was refluxed for 3 h, the colour of the solution changing from red to bright yellow. The mixture was filtered to remove the zinc, and the solvent was removed under reduced pressure to give 1.61 g of air-sensitive, orange-yellow product (55 % yield). ^{1}H NMR (C_6D_6, 500 MHz): δ 0.39 (w, br, 1.2 H), 1.56 (br, 4.0 H), 2.32 (br, 7.1 H), 2.47 (br, 1.5 H), 7.08 (br, 21 H), 7.25 (br, 5.9 H; C_6D_6), 7.59 (br, 11.4 H), 7.88 (br, 3.0 H) (Figure A18). ^{31}P NMR (C_6D_6, 500 MHz): δ 12.3 + a weak, broad resonance at δ ~30 (Figure A19).

2.4.3 Attempted Synthesis of $Ni(dppp)_2$ via reduction of NiI_2dppp

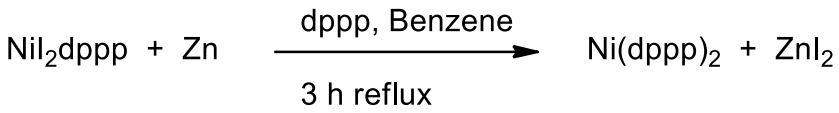

Figure 21. Synthesis of $Ni(dppp)_2$ via reduction of NiI_2dppp.

This reaction was carried out as described above with $NiCl_2dppp$ and $NiBr_2dppp$, and produced an orange-yellow product (0.30 g, 10% yield) and a black precipitate. The ^{1}H NMR spectrum (C_6D_6, 500 MHz; Figure A20) exhibited several broad resonances in the regions δ 0-3 and 7-8.5, in addition to weak resonances at δ 6.1, 8.7, 13.2 (br) and

13.8 (br) while the ^{31}P NMR spectrum (C_6D_6, 500 MHz, Figure A21) exhibited resonances at δ 13.6 (sharp), 30.3 (br) and 36.6 (br, w).

2.5.1 Attempted synthesis of Ni(I) species $NiCl(dppp)_n$ in benzene

$$NiCl_2dppp + Ni(dppp)_2 \xrightarrow[3\ h\ reflux]{Benzene} NiCl(dppp)_n$$

Figure 22. Attempted synthesis of Ni(I) species $NiCl(dppp)_n$ (n=1, 2)

Under an argon atmosphere, a mixture of 0.54 g $NiCl_2dppp$ (1 mmol) and 0.88 g $Ni(dppp)_2$ (1 mmol) in 55 mL anhydrous benzene was refluxed for 3 h, the colour of the solution changing from reddish yellow to beige as a beige precipitate formed. The precipitate was collected by filtration, washed with benzene and dried under reduced pressure to give 0.61 g of air-sensitive material. The product was exhibited very low solubilities in several organic solvents, but ^1H and ^{31}P NMR spectra of of the material were run in CD_2Cl_2; as can be seen in Figures A22 and A23, the spectra obtained are not very informative. Anal Calcd for $Ni_4Cl_3C_{27}H_{26}P_2$: C, 43.03%; H, 3.48%; Cl, 14.11%. Found: C, 41.64%; H, 4.22%; Cl, 14.52%.

The filtrate from the above experiment was taken to dryness to give a small amount of pale yellow solid, and the ^1H and ^{31}P NMR spectra, run in C_6D_6 on a Bruker AV 400, are shown in Figures A24 and A25. The ^1H spectrum exhibits several broad resonances in the regions δ 0.4-2.5 and δ 7.0-8.0 while the ^{31}P spectrum exhibits sharp singlets at δ 30.3 (s) and 13.6 (w).

2.5.2 Attempted synthesis of Ni(I) species $NiBr(dppp)_n$

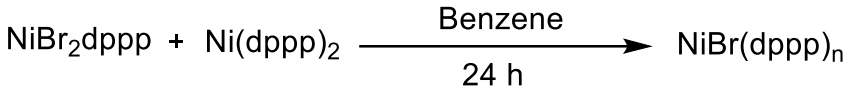

Figure 23 Attempted synthesis of Ni(I) species $NiBr(dppp)_n$ (n=1, 2)

Under an argon atmosphere, a mixture of 0.26 g $NiBr_2$dppp (0.41 mmol) and 0.36 g $Ni(dppp)_2$ (0.41 mmol) in 45 mL anhydrous benzene was refluxed for 6 h and then stirred at room temperature for 18 h; the colour changed from reddish yellow to beige as a beige precipitate developed. The precipitate was filtered to give 0.23 g of product but taking the filtrate to dryness resulted in very little solid product and no NMR spectra of the residue were run. The ^{1}H NMR and ^{31}P NMR spectra of the precipitate were run in benzene-d_6 using the Bruker AV400 (Figures A26, A27). The ^{1}H spectrum exhibits several broad resonances in the regions δ 0.1-2.5 and δ 6.5-8.8 and a very broad resonance at δ ~14, while the ^{31}P spectrum exhibits no resonances.

Alternatively, a mixture of 0.13 g anhydrous $NiBr_2$ (0.60 mmol) and 0.53 g $Ni(dppp)_2$ (0.60 mmol) in 45 mL anhydrous toluene was stirred for 23 h at room temperature as the colour changed from yellow to brown and a beige precipitate formed.

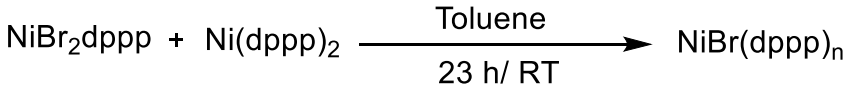

Figure 24. Attempted synthesis of $NiBr(dppp)_n$ in toluene (n=1, 2)

The precipitate was filtered to give 0.21 g of beige product and the solvent was removed from the filtrate under reduced pressure to give 0.02 g of a white solid. The ^{1}H

and ^{31}P NMR spectra of the precipitate were run in CD_2Cl_2 and are shown in Figures A28 and A29. As can be seen, the ^{1}H spectrum exhibits several broad resonances in the region δ 0-4 and δ 7-8 but the ^{31}P spectrum exhibits none. The ^{1}H and ^{31}P NMR spectra of the white solid, in C_6D_6, are shown in Figures A30 and A31. As can be seen, the former contains strong, well-resolved multiplets at δ 2.17, 2.43, 7.13 and 7.91 while the ^{31}P spectrum exhibits only a very weak resonance at δ 30.0.

2.5.3 Attempted synthesis of Ni(I) species $NiI(dppp)_n$/$[NiI(dppp)_n]_x$

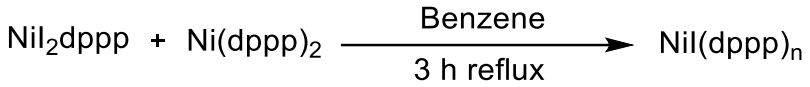

Figure 25. Attempted synthesis of Ni(I) species $NiI(dppp)_n$ (n=1, 2)

Under an argon atmosphere, a mixture of 0.73 g NiI_2dppp (1.0 mmol) and 0.88 g $Ni(dppp)_2$ (1.0 mmol) in 55 mL anhydrous benzene was refluxed for 3 h as the colour changed from brown-yellow to beige-brown and a beige-brown precipitate developed. The precipitate was filtrated and dried under vacuum to give 0.40 g of product, and the filtrate was evaporated to give a pale-yellow solid. The ^{1}H and ^{31}P NMR spectra of the precipitate were run in CD_2Cl_2 on a Bruker AV 500 (Figure A32, A33), and both exhibit broad, featureless bands. The ^{1}H and ^{31}P NMR spectra of the pale-yellow solid were carried out in benzene-d_6 using Bruker AV500 (Figure A34, A35), and the former exhibits broad multiplets with chemical shifts similar to those in Figure A30 although very broad, weak resonances are also apparent at δ 6.1, 7.7, 8.8, 13.1 and 13.9 while the ^{31}P NMR spectrum exhibits only extremely broad bands in the region δ ~0 and ~40.

2.6 Cross-Coupling Reactions

2.6.1 Methodology for Monitoring Buchwald-Hartwig Amination Cross-Coupling Reactions of Morpholine.

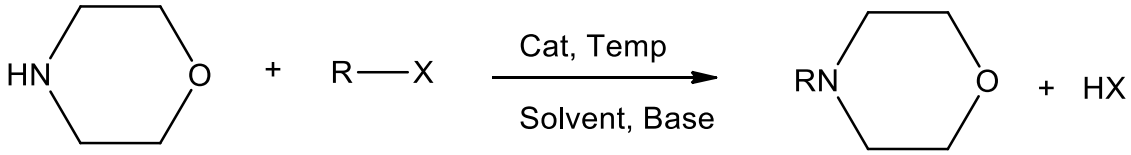

Figure 26. General Amination cross-coupling reaction

As a general procedure, 0.18 g preformed $Ni(dppp)_2$ (0.2 mmol), 0.37 g 4-bromoanisole (2 mmol), 0.21 g morpholine (2.4 mmol) and 0.27 g NaOtBu (2.8 mmol) were combined in 6 mL of anhydrous dioxane in a Schlenk tube, and the mixture was stirred for 24 h at 75 ^{o}C in an oil bath under an argon atmosphere. Aliquots (0.1 mL) were periodically taken from the mixture, diluted with 10 mL dioxane and analysed by GC to monitor the reaction. The reaction of bromoanisole was repeated at 90 ^{o}C in dioxane and at 75 ^{o}C in anhydrous toluene.

A similar procedure was carried out with 2-iodopropane at 85 ^{o}C in dioxane, with 1-iodobutane at 75 ^{o}C in toluene, with 1-iodobutane at 85 ^{o}C in dioxane, and in the presence of an excess free dppp (1 mmol eq). $NiCl_2$dppp was similarly assessed for catalytic activity.

2.6.2 Methodology for Monitoring Suzuki-Miyaura Cross-Coupling Reactions of Phenylboronic Acid

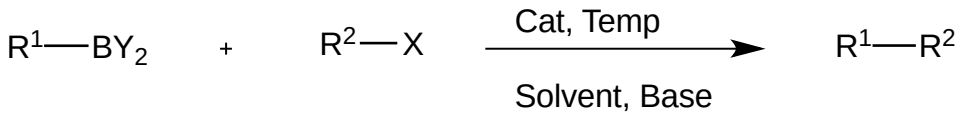

R^1= aryl; R^2= alkyl, aryl; Y_2=OH, R; X=Br, I.

Figure 27. General Suzuki-Miyaura cross-coupling reaction.

As a general procedure, 0.54 g $NiCl_2$dppp (1 mmol), 0.41 g dppp (1 mmol) and 0.30 g zinc dust (4.6 mmol) were combined in 30 mL anhydrous THF under argon. The mixture was stirred for 2 h, and the resulting yellow solution of $Ni(dppp)_2$ was filtered to remove unreacted zinc and then combined with 1.87 g 4-bromoanisole (10 mmol), 1.22 g phenylboronic acid (10 mmol) and 6.5 Cs_2CO_3 (20 mmol). The mixture was stirred at 60 ^oC for 24 h, 0.1 mL aliquots being periodically removed, diluted in 10 mL of THF and analysed by GC. Similar procedures were also carried out in benzene, dioxane and acetonitrile, as were reactions using $NiBr(dppp)_2$ in dioxane at 60 ^oC. Cross-coupling with 1-iodobutane and bromobenzene were also attempted using $Ni(dppp)_2$ formed in situ as above.

2.6.3 Methodology for Monitoring Heck-Mizoroki Cross-Coupling Reactions

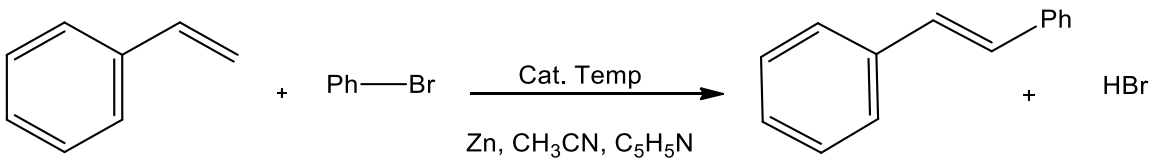

Figure 28. General Heck- Mizoroki cross-coupling reaction.

As a general methodology, a mixture of 0.46 mL styrene (4 mmol), 0.105 mL bromobenzene (1 mmol), anhydrous pyridine (4 mmol) and 0.065 g dust zinc in 3 mL of anhydrous acetonitrile was stirred for 10 min at room temperature and then 0.054 g of $NiCl_2$dppp (0.1 mmol) was added. The resulting mixture was stirred at 65 °C for 4 h, the stirring being stopped periodically to allow the solids to settle so that 0.1 mL aliquots could be removed, diluted in 10 mL of acetonitrile and analyzed by GC.

Chapter 3

Results and Discussion

3.1 Syntheses and properties of NiX_2dppp (X = Cl, Br, I)

3.1.1 $NiCl_2dppp$

The synthesis of $NiCl_2dppp$ was taken from the literature,[22a] and the compound was obtained in 85 % yield as a red, air stable, crystalline solid which was recrystallized from dichloromethane. The compound exists in solution as a rapidly equilibrating mixture of diamagnetic square planar and paramagnetic tetrahedral isomers,[22a] and thus solution NMR spectra are weighted averages of the spectra of the two isomers (Figure 29).

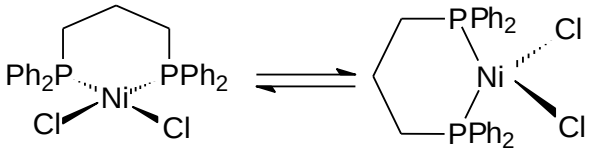

Figure 29. Square planar-tetrahedral equilibrium of $NiCl_2dppp$

The ^1H NMR spectrum of $NiCl_2dppp$ was run in CD_2Cl_2, and is shown in Figure A3 which is reproduced here to facilitate discussion.

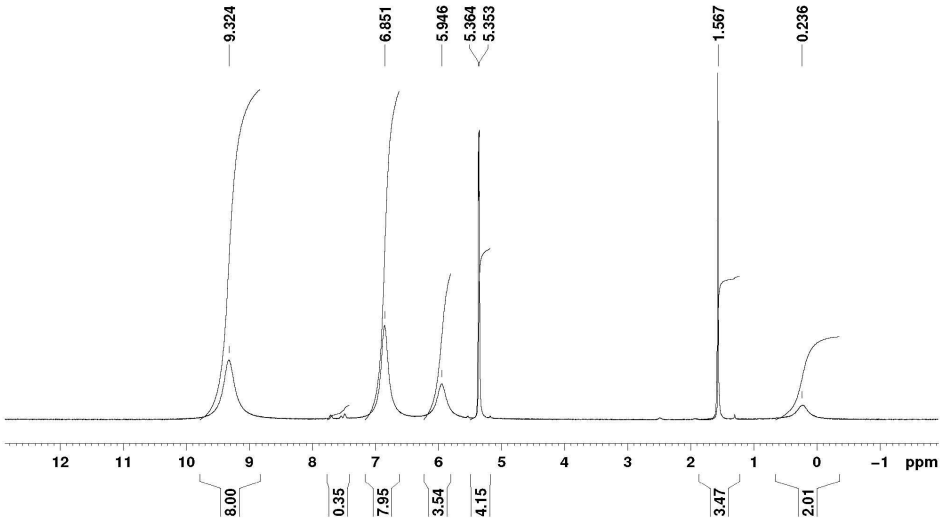

Figure A3: ^1H NMR spectrum of $NiCl_2dppp$ spectrum in CD_2Cl_2 (AV500).

In addition to sharp resonances of $CHDCl_2$ and HDO at δ 5.36 and 1.57, respectively, broad resonances are also observed at δ 0.24 (2H, -CH_2*CH_2*CH_2-), 5.95 (4H, *p*-H), 6.85 (8H, *o*- or *m*-H), and 9.32 (8H, *m*- or *o*-H) and are tentatively assigned as suggested. The resonances are very broad because of the paramagnetism,[22a] and that of the four -*CH_2*-CH_2-*CH_2*- hydrogens is apparently too broad to be observed as is the ^{31}P resonance (Figure A5). Note that contributions to the observed, averaged spectra of the paramagnetic isomer result in unusual, by the norms of diamagnetic organic compounds, chemical shifts, i.e. δ 9.32 for an aromatic H atom. The resonance of this H atom in the NMR spectrum of the tetrahedral isomer would lie much farther downfield, of course,[22a] but discussion of this issue is beyond the scope of this thesis.

We note that the ^{1}H NMR spectrum of $NiCl_2$dppp was not reported in the original 1966 publication.[22a] The compound exhibits low solubility and the non-FT NMR instrumentation available at the time was insufficiently sensitive for the resonances to be observed. The spectrum shown in Figure A3 is, however, very similar to a spectrum presented in an otherwise unpublished 2009 M.S. thesis.[22b]

As mentioned above, $NiCl_2$dppp exists in the solid state as the diamagnetic, square planar isomer and ^{13}C and ^{31}P NMR spectra were obtained in the solid state (Figures A5, A6). The ^{13}C NMR spectrum exhibited poorly resolved resonances in the aromatic (δ 120-142) and aliphatic (δ 16-22, m) regions, the ^{31}P NMR spectrum a resonance at δ 0.59. Both spectra were complicated by spinning sidebands.

3.1.2 $NiBr_2$dppp

The synthesis of $NiBr_2$dppp was taken from the literature.[22a] It also exists in solution as a rapidly equilibrating mixture of diamagnetic square planar and paramagnetic

tetrahedral isomers, in the solid state as the diamagnetic square planar isomer. $NiBr_2$dppp was obtained in 81 % yield as a deep red powder, and ^{1}H NMR spectra were run in $CDCl_3$ and CD_2Cl_2 on a Bruker AV 500 (Figures A7a, A7b). The ^{1}H NMR spectrum run in $CDCl_3$ (Figure A7a) exhibited broad resonances at δ –4.83 (2H, -CH_2*CH_2*CH_2-), –0.29 (~4H, *p*-H), 1.56 (~2H, probably HDO), 2.61 (~8H, *o*- or *m*-H) and 16.2 (8H, *m*- or *o*-H). and are tentatively assigned as indicated. There was also a relatively sharp resonance at δ 7.26, which we attribute to the solvent, and a weak multiplet at δ ~7.4-7.8 which we attribute to a diamagnetic impurity. The resonances are very broad because of the paramagnetism[22a] and the resonance of the four -*CH_2*CH_2*CH_2*- hydrogens again is apparently too broad to be observed as is the ^{31}P resonance. The chemical shifts of the spectrum run in CD_2Cl_2 were somewhat different. As with $NiCl_2$dppp, the ^{1}H NMR spectrum of $NiBr_2$dppp was not reported in the original 1966 publication.[22a]

Because of the paramagnetism, the ^{31}P resonance is too broad to be observed in solution and ^{13}C and ^{31}P NMR spectra were run in the solid state on a Bruker AV600 (Figures A8, A9). ^{13}C NMR: δ 15-26 (m, CH_2), 120-135 (m, Ph). ^{31}P NMR: δ 17.59 (br), 2.28 (br). These spectra are complicated by spinning sidebands.

3.1.3 NiI_2dppp

The synthesis of NiI_2dppp was taken from the literature[22a] and the compound was obtained in 70 % yield as a dark purple, air-stable solid. It exists in solution as an equilibrium between diamagnetic square planar and paramagnetic tetrahedral isomers, in the solid state as the square planar isomer.[22a] Unfortunately the compound apparently could not be obtained pure. Although a ^{1}H NMR spectrum (Figure A10) did

exhibit resonances at δ18.2, 2.1, −1.8 and −4.1, very close to chemical shifts reported earlier,[22a] these resonances were weak and the spectrum was dominated by strong, broad, unidentifiable resonances at δ 8.0, 7.3 ($CHCl_3$) and 2.5. As with $NiCl_2$dppp and $NiBr_2$dppp, ^{13}C and ^{31}P NMR spectra were run in the solid state (Figures A11, A12). ^{13}C NMR: δ ~16.82 (m, CH_2), 120-140 (m, Ph). ^{31}P NMR: δ ~26 (br).

3.2 Synthesis and properties of $Ni(dppp)_2$

3.2.1 $Ni(dppp)_2$ via reduction of $NiCl_2$dppp

$Ni(dppp)_2$ has previously been synthesized by treating nickelocene with dppp[22a] and by co-condensing Ni atoms with dppp at 77 K followed by warming to room temperature.[23] We developed a much more convenient procedure which involves reduction of $NiCl_2$dppp with zinc dust in the presence of excess of dppp (Figure A13). Various solvents were used, benzene, toluene, dioxane, and THF, and the best was found to be benzene. $Ni(dppp)_2$ could be obtained in 68 % yield as an orange-yellow, air-sensitive solid.

The ^1H NMR spectrum of $Ni(dppp)_2$ appears not to have been reported previously, and was found to exhibit somewhat broad resonances at δ 1.58 ($PCH_2\mathit{CH_2}CH_2P$), 2.34 ($P\mathit{CH_2}CH_2\mathit{CH_2}P$) and 7.10-7.61 (Ph) while the ^{31}P NMR spectrum exhibited a singlet at δ 13.6 in agreement with the literature.[23] An HMBC spectrum (Figure A15) showed that the ^1H resonances at δ 7.61 and 2.34 correlate with ^{31}P the resonance at δ 13.56; it seems reasonable that the hydrogen atoms of the central CH_2 group couple relatively weakly with the phosphorus atom.

An X-ray crystal structure of $Ni(dppp)_2$ was obtained prior to our realizing that the structure had already been reported in the literature.[25] The structure is shown in Figure

A17, bond lengths and angles in Appendix B.

The distorted tetrahedral coordination geometry found for $Ni(dppp)_2$ is essentially that reported previously in the literature,[24] and confirms the identity of the zinc reduction product. The Ni-P bond lengths vary between 2.1731(4) Å and 2.1763(5) Å, the P-Ni-P angles between 99.689(16) and 115.217(16). Thus the structure is unexceptional and will not be discussed further.

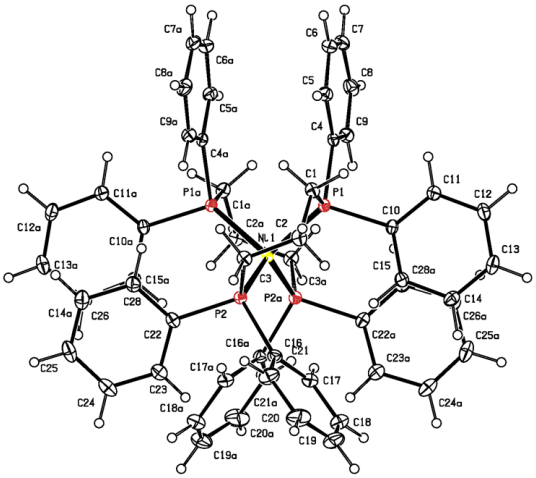

Figure A17. The X-ray crystal structure of $Ni(dppp)_2$

Some of our initial experiments involving the zinc reduction of $NiCl_2$dppp resulted in apparently incomplete reduction, with the possibility of nickel(I) species being formed. To confirm this, an EPR spectrum of a crude sample was obtained and is shown in Figure A16. Although we are not in a position to interpret the spectrum in terms of any particular structure, the approximate *g* value (2.11) is consistent with the presence of a nickel(I) species of some kind.[25] Unfortunately, attempts to recrystallize and identify the compound failed although we did attempt some catalytic runs using crude compounds (see below).

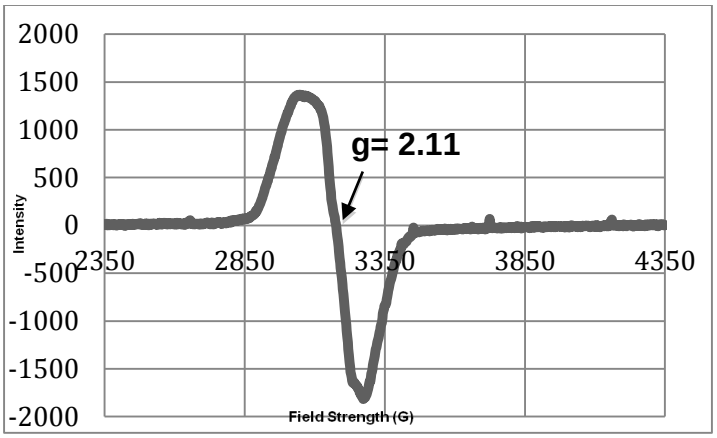

Figure A16: EPR spectra of Ni(I) complex while synthesized Ni(0) complex ($Ni(dppp)_2$)

3.2.2 Attempted Syntheses of $Ni(dppp)_2$ via reduction of $NiBr_2$dppp and NiI_2dppp.

$Ni(dppp)_2$ was obtained in 55 % yield from $NiBr_2$dppp, and was identified as above from its ^1H and ^{31}P NMR spectra (Figures A18, A19). In contrast, a similar procedure with NiI_2dppp resulted in mixtures of products (Figures A20, A21).

3.3 Attempted Syntheses of Ni(I) species $NiX(dppp)_n$

As mentioned above, a crude nickel(I) species could be obtained via incomplete reduction of $NiCl_2$dppp. Comproportionation reactions between molar equivalents of $Ni(dppp)_2$ and $NiCl_2$dppp were also attempted as described in the Experimental Section, and ^1H and ^{31}P NMR spectra of a beige precipitate obtained in this way, of very low solubility, exhibited weak peaks which were very broad (Figures A22, A23), consistent with its being paramagnetic, but not the resonances of the starting compounds $Ni(dppp)_2$ and $NiCl_2$dppp. The material, unfortunately, could not be recrystallized and thus its stoichiometry, and whether it is monomeric or dimeric with bridging chlorides, cannot be determined.

This reaction also yielded a small amount of yellow soluble material, the ^{1}H spectrum exhibited broad aromatic resonances in addition to several broad resonances in the region δ 0.4-2.5. The ^{31}P spectrum, in contrast exhibited a sharp resonances at δ 30.3 (s) in addition to a resonance at δ 13.6 which is attributed to a small amount of $Ni(dppp)_2$. The identities of the major species in solution could not be determined.

A similar comproportionation reaction between $Ni(dppp)_2$ and $NiBr_2$dppp gave a beige precipitate, the NMR spectra of which were also broad and featureless, consistent with paramagnetism (Figures A26, A27). No resonance was observed in the ^{31}P NMR spectrum. Alternatively, a mixture of anhydrous $NiBr_2$ and $Ni(dppp)_2$ in anhydrous toluene was stirred overnight at room temperature as the colour changed from yellow to brown and a beige precipitate formed. The precipitate was filtered to give a beige product and the solvent was removed from the filtrate under reduced pressure to give a white solid. The ^{1}H and ^{31}P NMR spectra of the beige precipitate were run in CD_2Cl_2 and are shown in Figures A28 and A29. As can be seen, very broad resonances were observed in the ^{1}H spectrum while no peaks were observed in the ^{31}P spectrum, consistent with paramagnetic species although otherwise uninformative. The ^{1}H and ^{31}P NMR spectra of the white solid, in C_6D_6, are shown in Figures A30 and A31. The ^{1}H spectrum exhibits broad and sharp resonances while the ^{31}P spectrum exhibits only a very weak resonance, but interpretation is uncertain.

An attempted comproportionation reaction between equimolar amounts of $Ni(dppp)_2$ and NiI_2dppp also gave a beige precipitate while evaporation from the filtrate gave a pale yellow solid. The ^{1}H and ^{31}P NMR spectra of the precipitate were carried out in CD_2Cl_2 on a Bruker AV 500, giving too broad peaks in (Figure A32, A33) while the ^{1}H

and ^{31}P NMR spectra of the pale-yellow solid were carried out in benzene-d_6 using Bruker AV500 (Figure A34, A35). The spectra again indicate the presence of a major paramagnetic species, but unfortunately are not otherwise informative.

It can be concluded that comproportionation reactions do yield paramagnetic nickel(I) species, but all attempts to purify the products failed and none can be identified properly. Elemental analyses did not correspond to expected stoichiometries such as NiCldppp or $Ni(dppp)_2Cl$, but corresponded approximately to Ni_4Cl_3dppp. It was therefore a mixture, which could not be separated into components or purified because of its low solubility. As a result, we assume the formula of Ni(I) compound such as $NiX(dppp)_2$ to test the activation of Ni(I) in cross-coupling reactions.

3.4 Cross-coupling reactions

3.4.1 Buchwald–Hartwig amination reactions using morpholine

Catalytic activities of $Ni(dppp)_2$ under various conditions and using various bases were assessed as shown in Table 3.

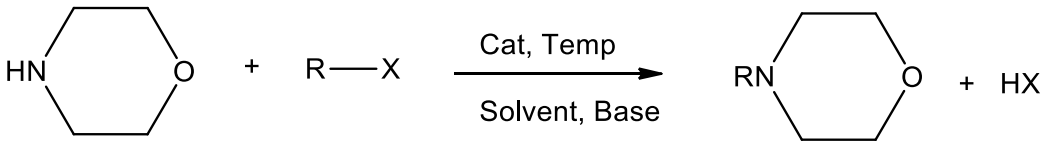

Figure 30. General amination cross-coupling reaction

Table 3. Nickel complexes catalyzed amination reactions.

Entry	Catalyst * 10 (mol%)	Organohalide	Base (equiv)	Anhydrous Solvent	Temp (°C)	Yield[a] (%)
1	$Ni(dppp)_2$	4-Bromoanisole	NaOtBu	Dioxane	75	NR
2	$Ni(dppp)_2$	4-Bromoanisole	NaOtBu	Toluene	75	NR
3	$Ni(dppp)_2$	2-Iodopropane	NaOtBu	Dioxane	85	NR
4	$Ni(dppp)_2$	1-Iodobutane	NaOtBu	Toluene	85	100
5	$NiCl_2$dppp	4-Bromoanisole	LiOtBu	Dioxane	90	NR
6	$Ni(dppp)_2$	1-Iodobutane	LiOtBu	Dioxane[c]	85	100
7	$Ni(dppp)_2$[b]	1-Iodobutane	LiOtBu	Dioxane[c]	85	100
8	$Ni(dppp)_2$[b]	1-Iodobutane	LiOtBu	Dioxane	85	100
9	$NiCl_2$dppp	1-Iodobutane	LiOtBu	Dioxane[c]	85	100
10	$NiCl_2$dppp	1-Iodobutane	LiOtBu	Dioxane	85	100
11	No cat	1-Iodobutane	LiOtBu	Toluene	75	100

a= Determined by GC analysis, b= addition of dppp, c= wet solvent.

As can be seen, no catalysis was observed with 4-bromoanisole, and it was eventually realized that the apparent catalysis using alkyl halides occurred in the absence of $Ni(dppp)_2$ (Figure 30, Table 3, control experiment #11) and were thus a result of conventional non-catalyzed S_N2 reactions.

The lack of catalytic activity with 4-bromoanisole was disappointing, but the reason for failure is not obvious since any of the steps in the catalytic cycle (oxidative addition, nucleophilic attack, reductive elimination) may be the culprit.

3.4.2 Suzuki–Miyaura Reactions

The experiments investigated utilized the chemistry shown in Figure 31, with results as shown in Table 4.

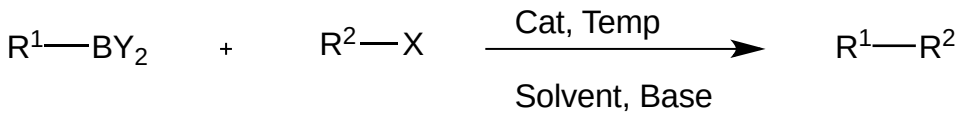

R^1= aryl; R^2= alkyl, aryl; Y_2=OH, R; X=Br, I.

Figure 31. General Suzuki-Miyaura cross-coupling reaction

Table 4. Nickel complexes (*) catalyzed Suzuki–Miyaura reactions.

Entry	Catalyst * 10 (mol%)	Organohalide	Base (equiv)	Anhydrous Solvent	Temp (°C)	Yield[a] (%)
1	$Ni(dppp)_2$	4-Bromoanisole	Cs_2CO_3	THF	60	5%
2	$Ni(dppp)_2$	4-Bromoanisole	Cs_2CO_3	Benzene	60	NR
3	$Ni(dppp)_2$	4-Bromoanisole	Cs_2CO_3	Dioxane	60	NR
4	$Ni(dppp)_2$	4-Bromoanisole	Cs_2CO_3	Acetonitrile	60	NR
5	Ni(I)[d]	4-Bromoanisole	Cs_2CO_3	Dioxane	60	NR
6	Ni(I)[e]	4-Bromoanisole	Cs_2CO_3	THF	60	NR
7	$Ni(dppp)_2$	1-iodobutane	Cs_2CO_3	THF	60	3%
8	$NiCl_2$dppp	Bromobenzene	Cs_2CO_3	THF	60	2%
9	$NiCl_2$dppp	Bromobenzene	K_2CO_3	Dioxane[c]	65	NR
10	$Ni(dppp)_2$	Bromobenzene	Cs_2CO_3	Dioxane	60	NR

a= Determined by GC analysis. c= wet solvent. d= $NiBr(dppp)_2$. e= $NiCl(dppp)_2$

As can be seen, none of the experiments attempted were successful, the best resulting in yields ≤5 %. It seemed futile to attempt to optimize these reactions, and the study was terminated.

3.4.3 Heck Reactions

The experiments investigated utilized the chemistry shown in Figure 32, with results as shown in Table 5.

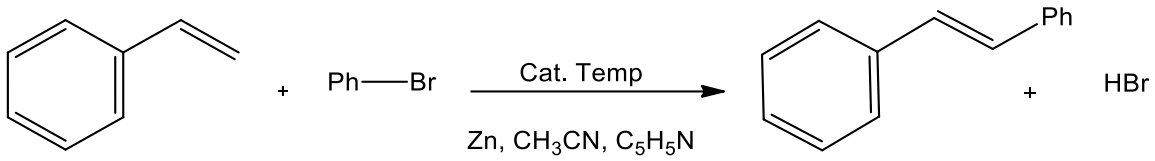

Figure 32. General Heck- Mizoroki cross-coupling reaction

Table 5: Nickel complexes catalyzed Heck reactions.

Entry	Catalyst 10(mol%)	Organhalide	Base (equiv)	Anhydrous Solvent	Temp (°C)	Yield[a] (%)
1	Ni(0)[b]	C_6H_5Br	Pyridine	Acetonitrile	65	97
2	Ni(0)[c]	C_6H_5Br	Pyridine	Acetonitrile	65	97
3	Ni(I)[d]	C_6H_5Br	Pyridine	Acetonitrile	65	NR
4	Ni(I)[e]	C_6H_5Br	Pyridine	Acetonitrile	65	NR

a= Determined by GC analysis. b= $Ni(dppp)_2$ without addition of zinc. c= $NiCl_2$dppp with addition of Zn. d= $NiCl(dppp)_2$. e= $NiBr(dppp)_2$.

As can be seen, the Ni(0) complex $Ni(dppp)_2$ was found to be a good catalyst for the Heck reaction between styrene ($C_6H_5CH=CH_2$) and bromobenzene (C_6H_5Br) in the presence of pyridine (C_5H_5N) and acetonitrile (CH_3CN) (Scheme 6). A yield of 97% was obtained for the product. On the other hand, the Ni(I) complexes $NiCl(dppp)_2$ and $NiBr(dppp)_2$ were completely ineffective under the same conditions.

As shown in Scheme 6, The mechanism of the nickel(0)-catalyzed Heck reaction involves four steps.[18b]

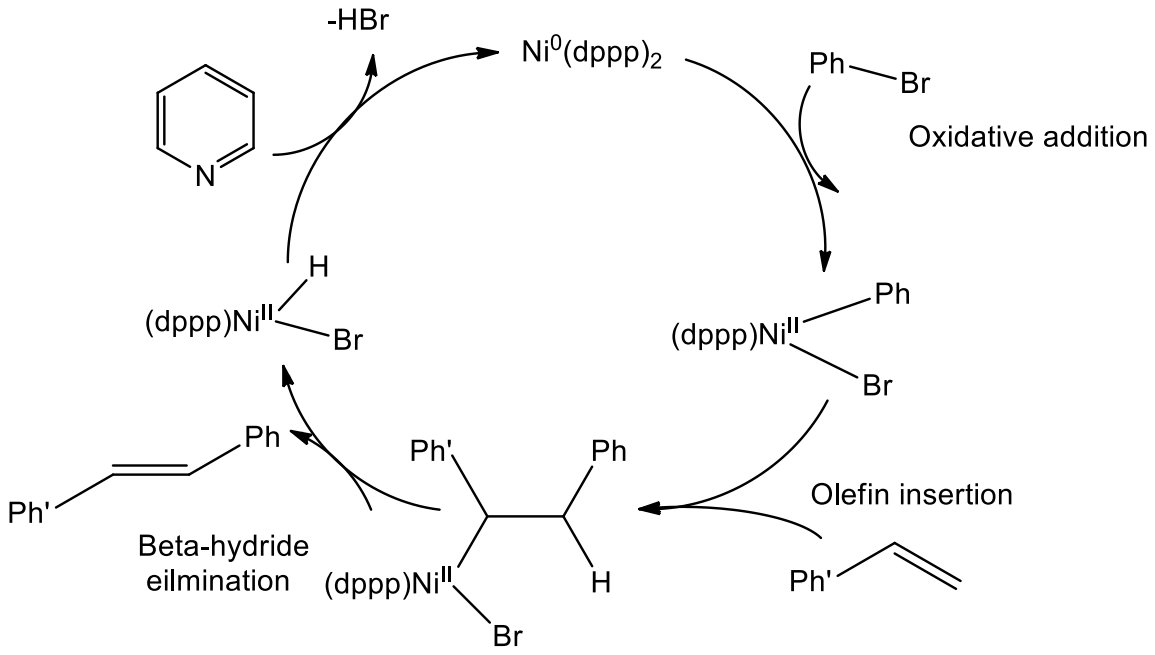

Scheme 6. Mechanism for nickel(0)-catalyzed Heck cross-coupling reactions.

The first of these probably invlolves loss of a dppp ligand followed by oxidative addition of bromobenzene (C_6H_5Br) to form *cis*-Ph-NiBr(dppp), There follows styrene ($C_6H_5CH=CH_2$) coordination to the Ni, insertion of the styrene into the C-Ni bond and β-hydride elimination to form the substituted olefin product which dissociates. The final step involves pyridine (C_5H_5N) removing HBr from the nickel hydride intermediate to regenerate the $Ni(dppp)_2$ catalyst.

Chapter 4

4.1 Conclusions

We have successfully reduced Ni(II) by zinc in presence of an excess of the ligand to form the Ni(0) complex $Ni(dppp)_2$ which had previously been synthesized utilizing a much more difficult process. We have also successfully produced Ni(I) compounds of unfortunately unknown structures via comproportionation reactions involving Ni(II) complexes and $Ni(dppp)_2$. Elemental analyses (C, H, Cl) of the EPR-active chloronickel(I) species were inconsistent with any anticipated stoichiometry, and the material was probably a mixture which could not be purified by recrystallization because of solubility problems.

The nickel(0) compound $Ni(dppp)_2$ was found to be a good catalyst for the Heck coupling of bromobenzene and styrene but not for Suzuki-Miyaura coupling of phenylboronic acid with bromobenzene, or for the Buchwald-Hartwig coupling of morpholine with 4-bromoanisole and 2-Iodopropane.

Unfortunately, the chloronickel(I) species and bromonickel(I) species exhibited no catalytic activity.

4.2 Future work

Further investigations the ability of $Ni(dppp)_2$ to catalyze Heck reactions seem warranted. As indicated above, the catalytic cross-coupling of bromobenzene and styrene was successful and extensions to other alkenes and aryl halides should be attempted in order to assess possible substituent effects. Extensions to alkyl halides should also be attempted since, as indicated above, alkyl halide cross-coupling tends to be more successful with Ni(0)-based than Pd(0)-based catalysts.

Our use of comproportionation reactions of Ni(II) and Ni(0) precursors to form Ni(I) products should be extended to other phosphines in hope of finding and better characterizing new, soluble Ni(I) compounds which can be purified by recrystallization. Any new compounds formed in this way would be characterized by NMR and EPR spectroscopy, and assessed for cross-coupling catalytic abilities.

References

(1) (a) de Mejiere, A., Diederich, F., Eds.; Metal Catalyzed Cross-Coupling Reactions; 2nd ed., John Wiley & Sons: New York, **2004.** (b) Tamao, K.; Norio, M.; Miyaura, N., Ed.; Cross-Coupling Reactions: A Practical Guide*,* Springer Berlin / Heidelberg: **2002**; Vol. 219, p 1. (c) de Meijere A, Bräse S, Oestreich M, editors. Metal Catalyzed Cross-Coupling Reactions and More, 3 Volume Set. John Wiley & Sons; **2013**. (d) Yasushi, N. *Applied Cross-Coupling Reactions*; Springer Science & Business Media, **2012**.

(2) (a) Colacot, T., New Trends in Cross-Coupling: Theory and Applications. No. 21. Royal Society of Chemistry, **2014**, p 5. (b) Tamao, K.; Norio, M.; Miyaura, N., Ed.; Cross-Coupling Reactions: A Practical Guide*,* Springer Berlin / Heidelberg: **2002**; Vol. 219, p 4.

(3) (a) Tasker, S. Z.; Standley, E. A.; Jamison, T. F. *Nature* **2014**, *509* (7500), 299. (b) Cárdenas, D. J. *Angew. Chem. Int. Ed.* **2003**, *42*, 384. (c) Yamaguchi, J.;Muto, K.; Itami,K. *Eur. J. Org. Chem*. **2013**, 19. (d) Ananikov, V.P. *Catalysis*. **2015**, 5, 1964. (e) Phapale, V. B.; Cárdenas, D. J. *Chem. Soc. Rev.* **2009**, *38*, 1598. (f) Luh, T.-Y.; Leung, M.-K; Wong, K.-T. *Chem. Rev.* **2000**, *100*, 3187. (g) Netherton, M. R.; Fu, G. C *Adv. Synth. Catal.* **2004**, *346*, 1525. (h) Frisch, A. C.; Beller, M. *Angew. Chem. Int. Ed.* **2005**, *44*, 674. (i) Takahashi, T.; Kanno, K.-I. in Modern Organonickel Chemistry, Tamaru, Y. editor, Wiley-VCH, New York, **2005**, p. 41. (j) Rudolph, A.; Lautens, M. *Angew. Chem. Int. Ed.* **2009**, *48*, 2656. (k) Rosen, B. M.; Quasdorf, K. W.; Wilson, D. A.; Zhang, N.; Resmerita, A.-M.; Garg, N. K.; Percec, V. *Chem. Rev.* **2011**, *111*, 1346. (l) Jana, R.; Pathak, T. P.;

Sigman, M. S. *Chem. Rev.* **2011**, *111*, 1417. (m) Taylor, B. L. H.; Jarvo, E. R. *Synlett* **2011**, 2761. (n) Wang, Z.-X.; Liu, N., *Eur. J. Inorg. Chem.* **2012**, 901. (o) Everson, D.; Weix D.*J. Org. Chem.* **2014**, *79*, 4793. (p) Henrion, M.; Ritleng, V.; Chetcuti, M.J. *Catalysis*, **2015**, *5*, 1283. (q) Weix , D.*J. Acc. Chem. Res*. **2015**, *48,* 1767. (r) Standley, E.A.; Tasker, S.Z.; Jensen. K.L.; Jamison. T.F. *Acc. Chem. Res*. **2015**, *48*, 1503. (s) Tobisu, M.; Chatani. N. *Acc. Chem. Res*. **2015**, *48*, 1717. (t) Cherney, A. H.; Kadunce, N. T.; Reisman, S. E. *Chem. Rev.* **2015**, *115*, 9587. (u) Yu, D.-G.; Li, B.-J.; Shi, Z.-J. *Acc. Chem. Res.* **2010**, *43*, 1486. (w) Klein, A.; Budnikova, Y. H.; S., Oleg G. *J. Organomet. Chem.* **2007**, *692*, 3156. (x) Klein, A.; Kaiser, A.; Sarkar, B.; Wanner, M.; Fiedler, J. *Eur. J. Inorg. Chem.* **2007**, *7*, 965.

(4) Cárdenas, D. *Angew. Chem. Int. Ed. Engl.* **1999**, *38* (20), 3018.

(5) (a) Saraev, V. V.; Kraikivskii, P. B.; Bocharova, V. V.; Matveev, D. a. *Kinet. Catal.* **2012**, *53* (4), 486. (b) Saraev, V. V.; Kraikivskii, P. B.; Matveev, D. A.; Kuzakov, A. S.; Vil'ms. A. I.; Fedonina, A. A. *Rus. J. Coord. Chem*. **2008**, *34*, 438. (c) Saraev, V. V.; Kraikivskii, P. B.; Zelinskii, S. N.; Tkach, V. S.; Shmidt, F. K. *Rus. J. Coord. Chem.* **2001**, *27,* 136.

(6) Zultanski, S. L.; Fu, G. C. *J. Am. Chem. Soc.* **2013**, *135* (2), 624.

(7) (a) Dudnik, A. S.; Fu, G. C. *J. Am. Chem. Soc.* **2012**, *134* (25), 10693.(b) Zhang, C. P.; Wang, H.; Klein, A.; Biewer, C.; Stirnat, K.; Yamaguchi, Y.; Xu, L.; Gomez-Benitez, V.; Vicic, D. a. *J. Am. Chem. Soc.* **2013**, *135* (22), 8141. (c) Jones, G. D.; Martin, J. L.; McFarland, C.; Allen, O. R.; Hall, R. E.; Haley, A. D.; Brandon, R. J.; Konovalova, T.; Desrochers, P. J.; Pulay, P.; Vicic, D. a. *J. Am. Chem. Soc.* **2006**, *128* (40), 13175.

(8) Tamao, K.; Sumitani, K.; Kumada, M. *J. Am. Chem. Soc.* **1972**, *94* (12), 4374.

(9) Tamao, K.; Sumitani, K. *Org. Synth.* **1978**, *58* (September), 127.

(10) Ye, X.; Yuan, Z.; Zhou, Y.; Yang, Q.; Xie, Y.; Deng, Z.; Peng, Y. *J. Heterocycl. Chem.* **2015**, n/a.

(11) Tamao, K.; Sumitani, K.; Kiso, Y.; Zembayashi, M.; Fujioka, A.; Kodama, S.; Nakajima, I.; Minato, A.; Kumada, M. *Bull. Chem. Soc. Jpn*. **1976**, pp 1958.

(12) Kumada, M. *Pure Appl. Chem.* **1980**, *52* (7), 669.

(13) Gao, H.; Li, Y.; Zhou, Y.-G.; Han, F.-S.; Lin, Y.-J. *Adv. Synth. Catal.* **2011**, *353* (2-3), 309.

(14) Saito, S.; Sakai, M.; Miyaura, N. *Tetrahedron Lett.* **1996**, *37* (17), 2993.

(15) Suzuki, A. *Chem. Commun. (Camb).* **2005**, No. 38, 4759.

(16) Liu, L.; Fu, Y.; Luo, S.-W.; Chen, Q.; Guo, Q.-X. *Organometallics* **2004**, *23* (9), 2114.

(17) Boldrini, G. P.; Savoia, D.; Tagliavini, E.; Trombini, C.; Ronchi, A. U. *J. Organomet. Chem.* **1986**, *301* (3), C62.

(18) (a) Ma, S.; Wang, H.; Gao, K.; Zhao, F. *J. Mol. Catal. A Chem.* **2006**, *248* (1- 2), 17. (b) Lebedev, S. a.; Lopatina, V. S.; Petrov, E. S.; Beletskaya, I. P. J. Organomet. Chem. **1988**, 344 (2), 253.

(19) (a) Wolfe, J. P.; Buchwald, S. L. *J. Am. Chem. Soc.* **1997**, *119* (26), 6054. (b) Surry, D. S.; Buchwald, S. L., Chem. Sci. **2011**, 2 (1), 27. (c) Louie, J.; Hartwig, J. F. Tetrahedron Lett. **1995**, 36 (21), 3609.

(20) Hewertson, W.; Watson, H. R. *J. Chem. Soc.* **1962**, 1490.

(21) Brandsma, L.; Vasilevsky, S. F.; Verkruijsse, H. D. *Application of Transition Metal*

Catalysts in Organic Synthesis; Springer Science & Business Media, **2012**.

(22) (a) Van Hecke, G. R.; Horrocks, W. D. *Inorg. Chem.* **1966**, *5* (11), 1968.(b) McDaniel, A. L. "Synthesis and Characterization of Bis-Phosphine Complexes with Transition Metals" (**2009**). *Masters Theses & Specialist Projects.* Paper 110. http://digitalcommons.wku.edu/theses/110.

(23) Fisher, K. J.; Alyea, E. C. *Polyhedron* **1989**, *8* (1), 13.

(24) Davies, S. C.; Duff, S. E.; Evans, D. J. *Acta Crystallogr. Sect. E Struct. Reports Online* **2005**, *61* (3), m571.

(25) Carter, E.; Murphy, D. M. *Top. Catal.* **2015**, *58* (12-13), 759.

Appendix A:

NMR Spectra

EPR Spectra

X-ray Structure of $Ni(dppp)_2$

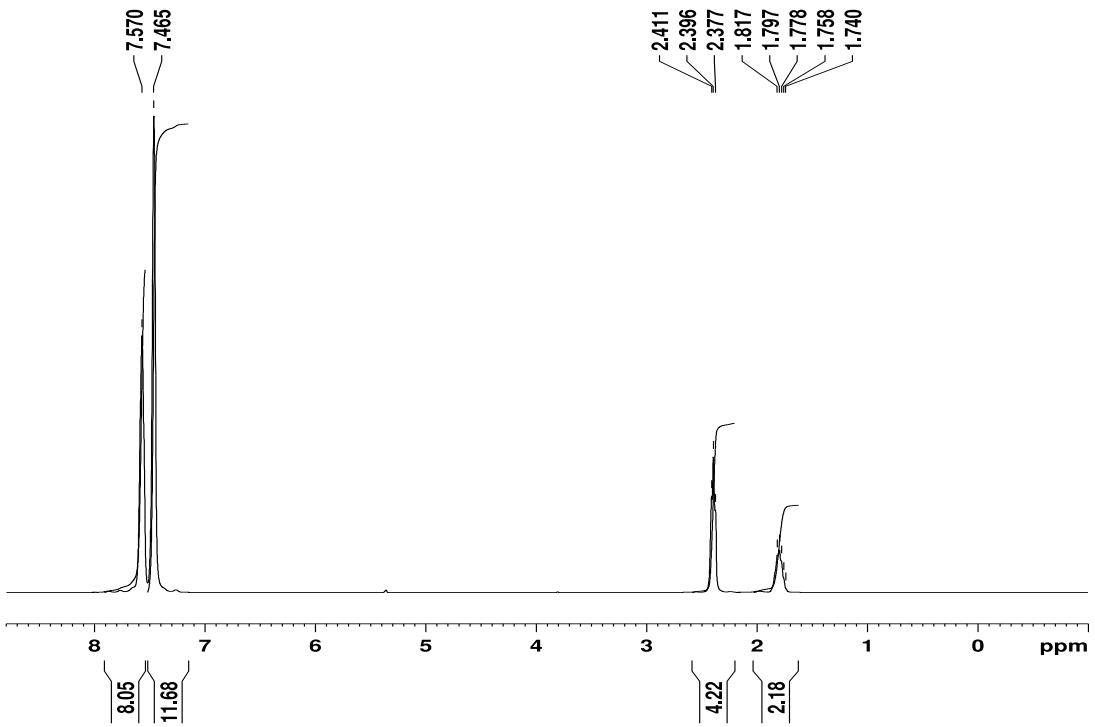

Figure A1: ^{1}H NMR spectrum of dppp in CD_2Cl_2 (AV500).

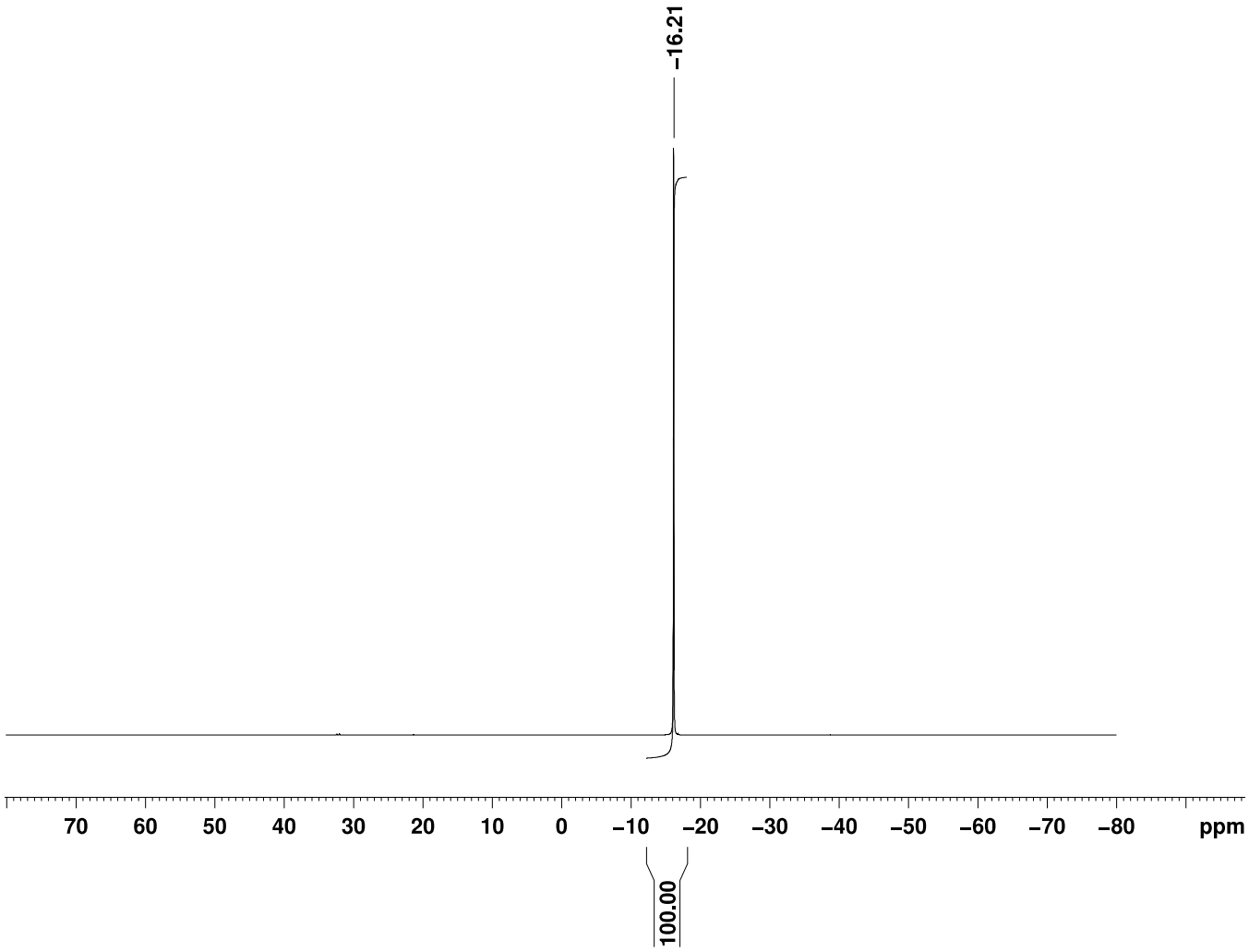

Figure A2: ^{31}P NMR spectrum of dppp in CD_2Cl_2 (AV500).

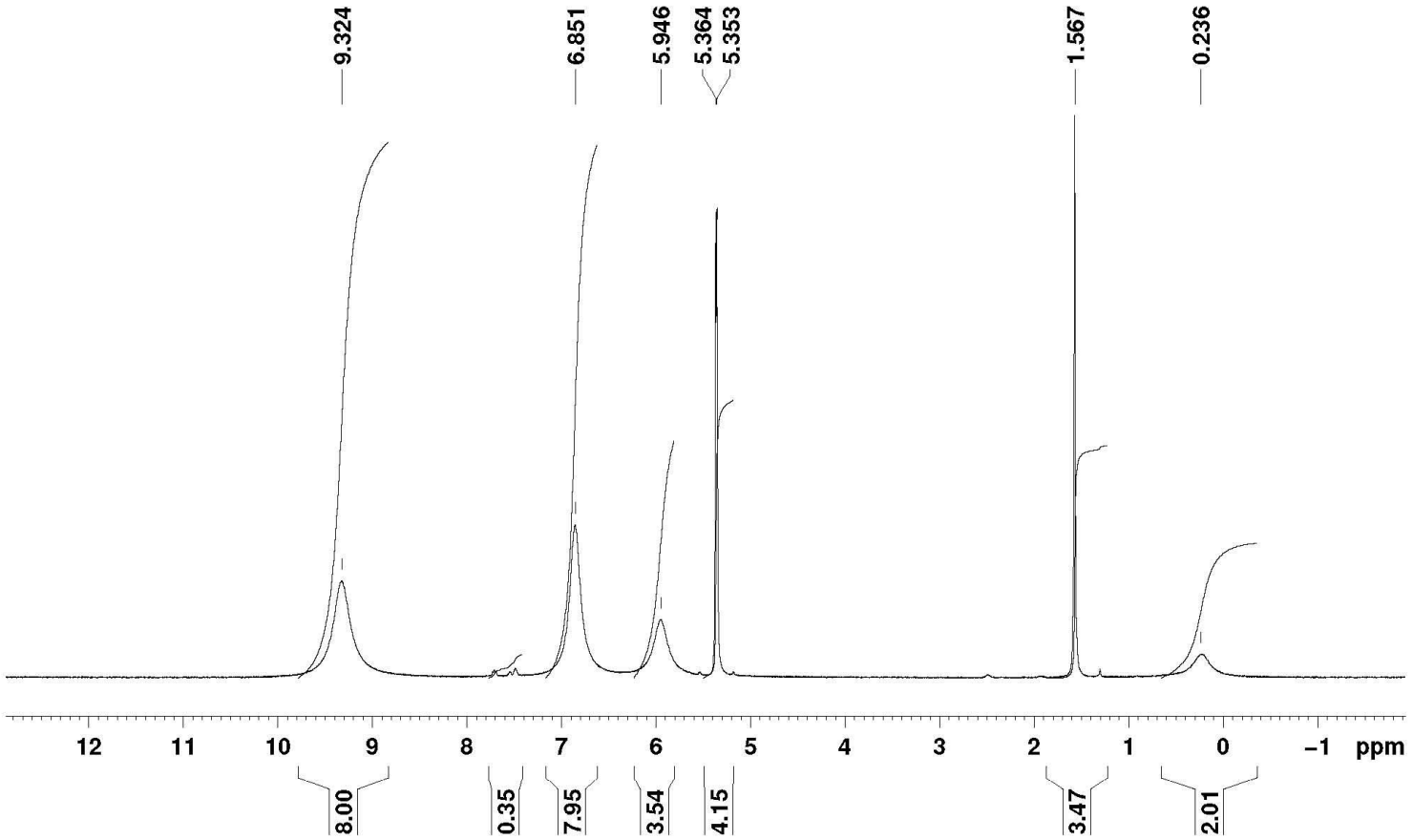

Figure A3: ^{1}H NMR spectrum of $NiCl_2$dppp spectrum in CD_2Cl_2 (AV500).

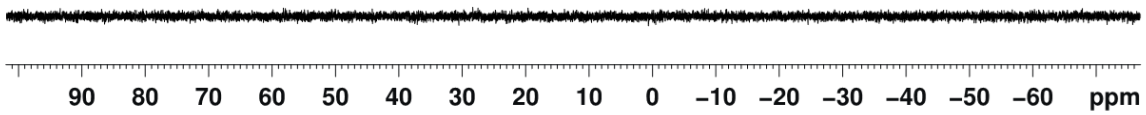

Figure A4: ^{31}P NMR spectrum of $NiCl_2$dppp spectrum in CD_2Cl_2 (AV500).

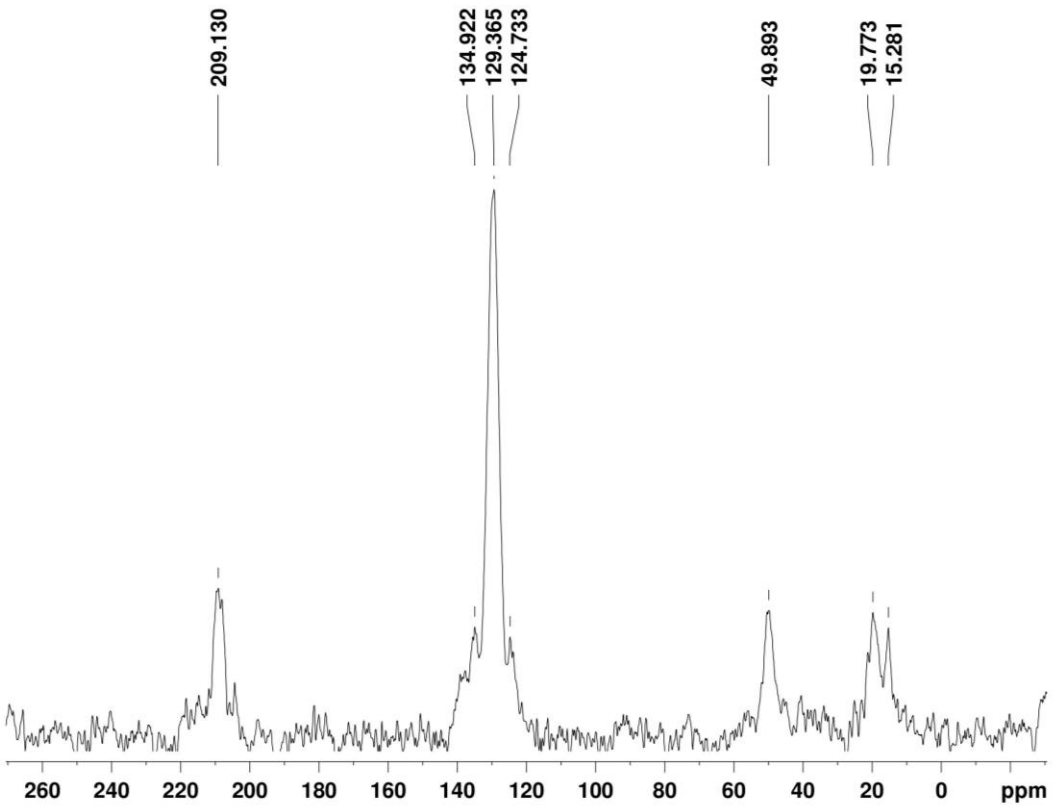

Figure A5: ^{13}C NMR spectrum of $NiCl_2$dppp in solid state (AV600).

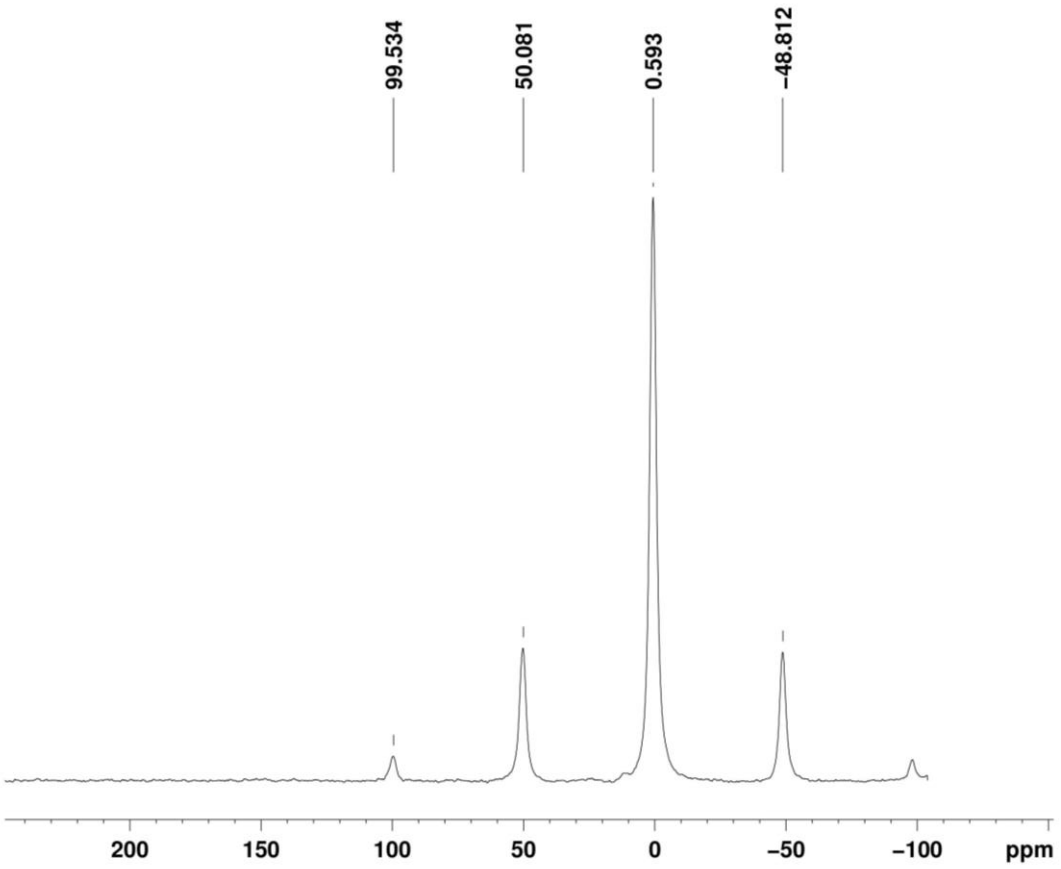

Figure A6: ^{31}P NMR spectrum of $NiCl_2$dppp in solid state (AV600).

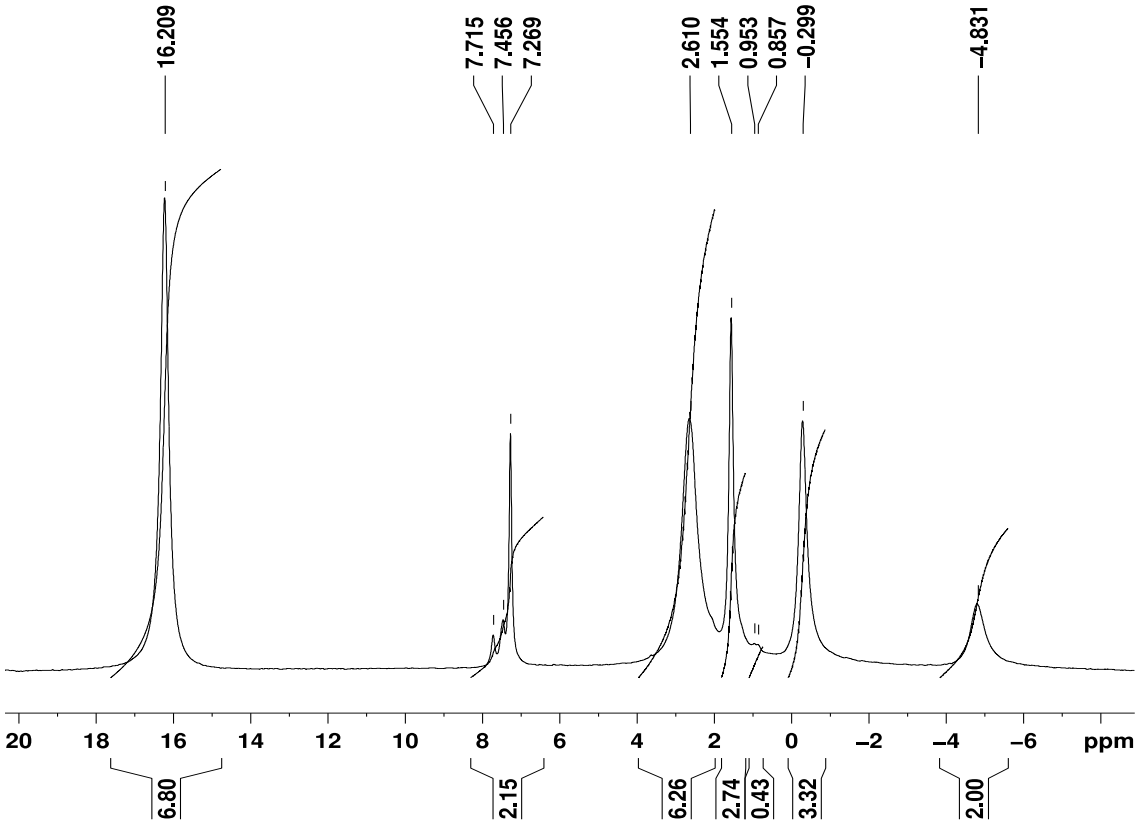

Figure A7a: ^{1}H NMR spectrum of $NiBr_2$dppp spectrum in $CDCl_3$ (AV400).

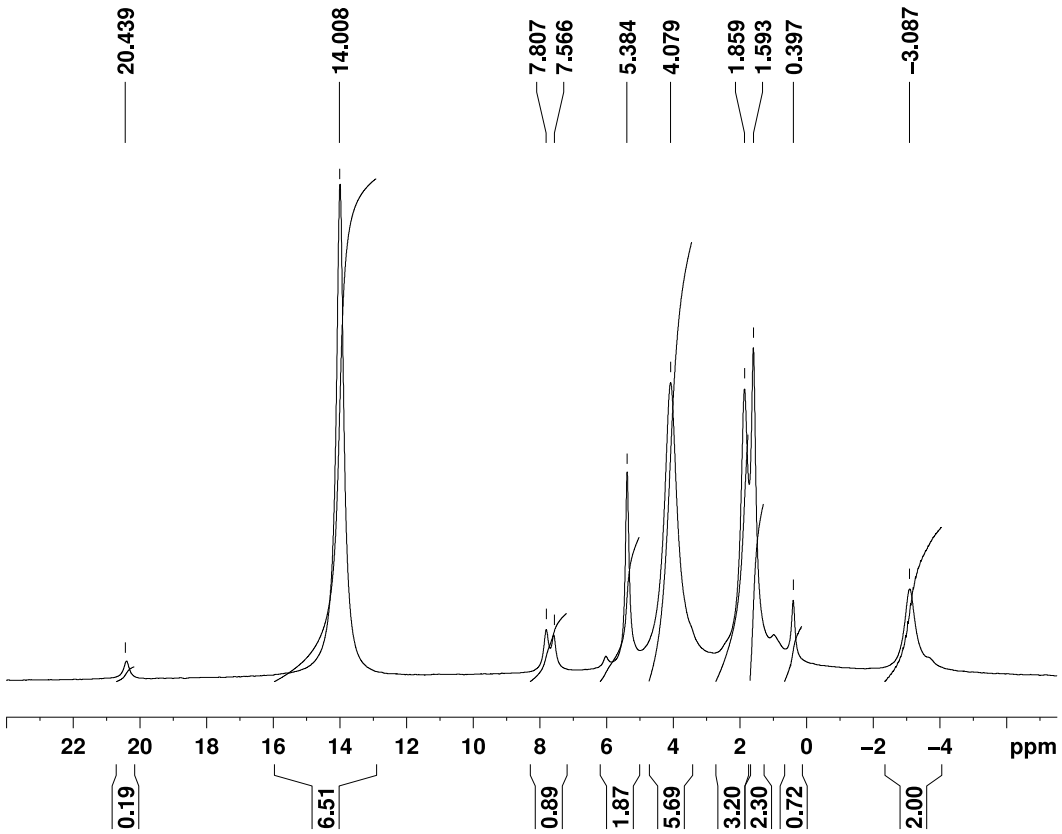

Figure A7b: ^{1}H NMR spectrum of $NiBr_2$dppp spectrum in CD_2Cl_2 (AV400).

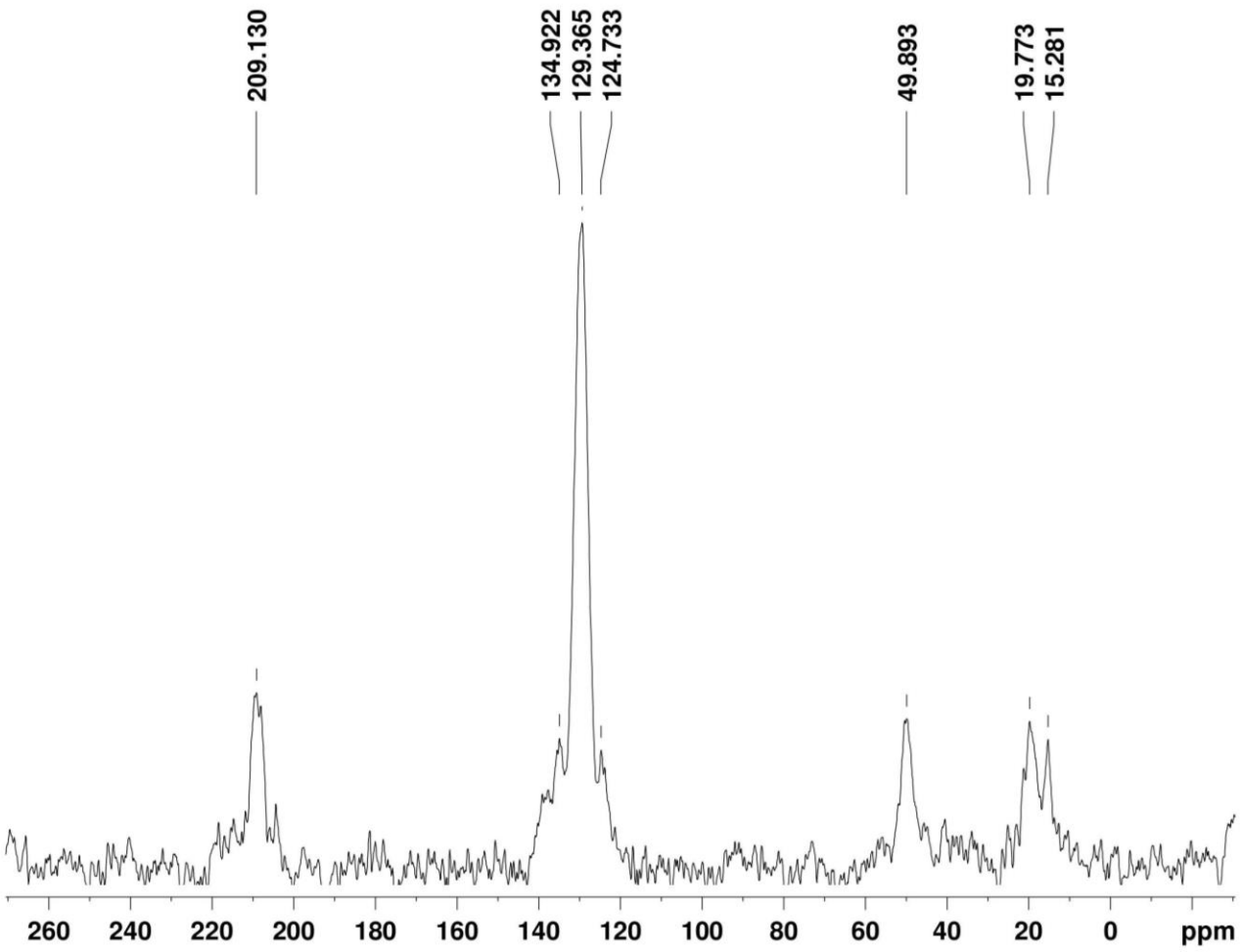

Figure A8: ^{13}C NMR spectrum of $NiBr_2$dppp in solid state (AV600).

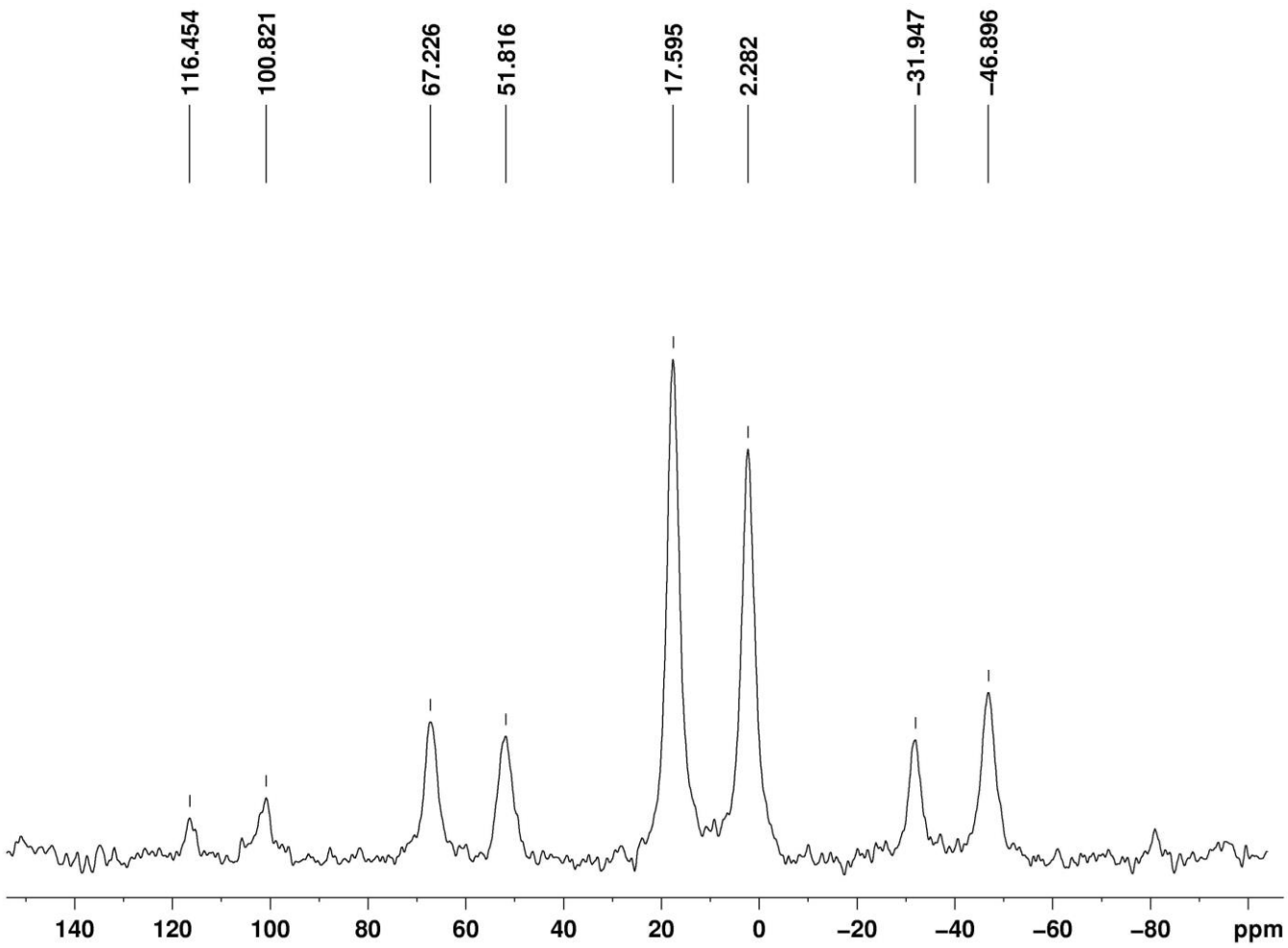

Figure A9: ^{31}P NMR spectrum of $NiBr_2$dppp in solid state (AV600).

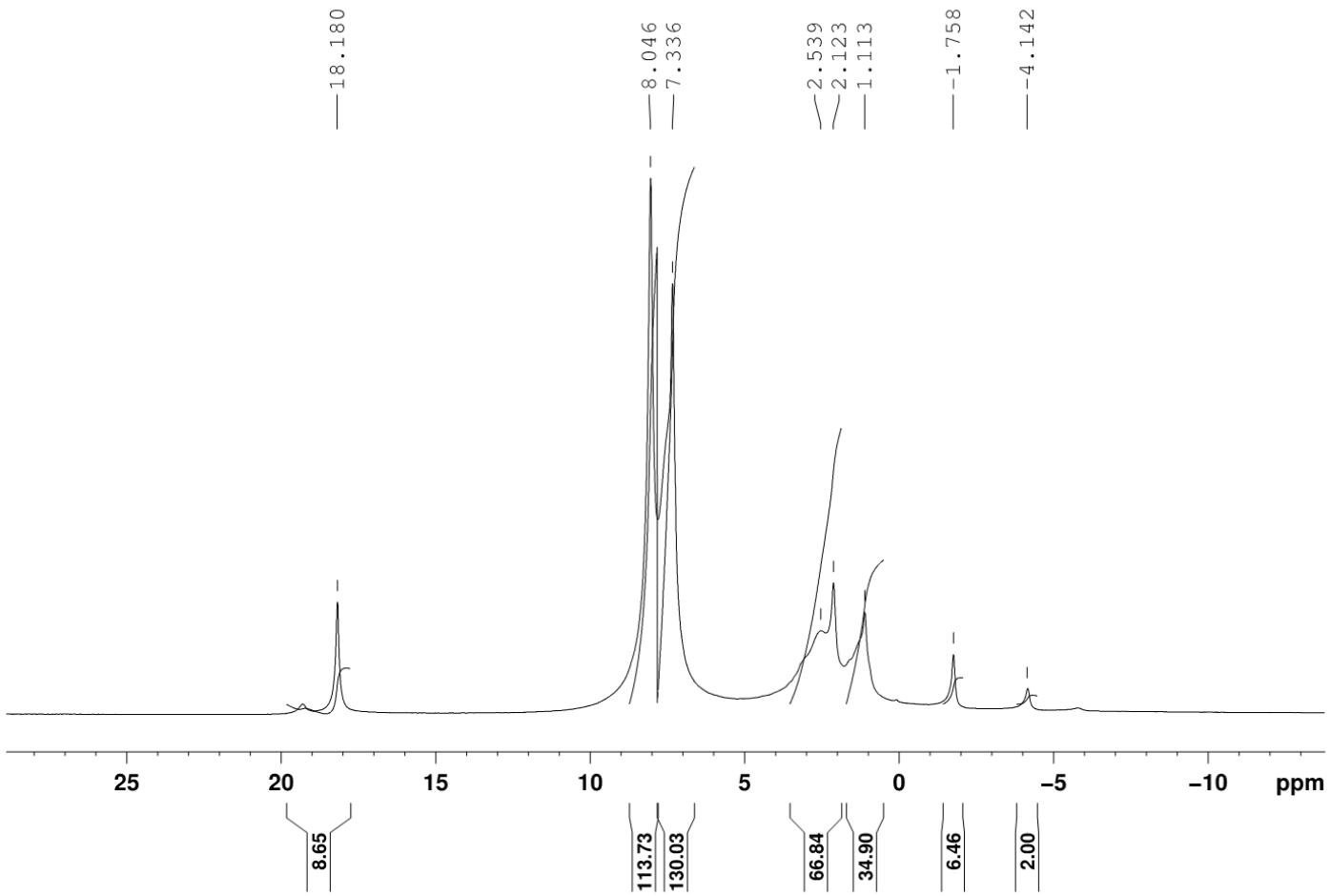

Figure A10: ^{1}H NMR spectrum of NiI_2dppp in $CDCl_3$ (AV500).

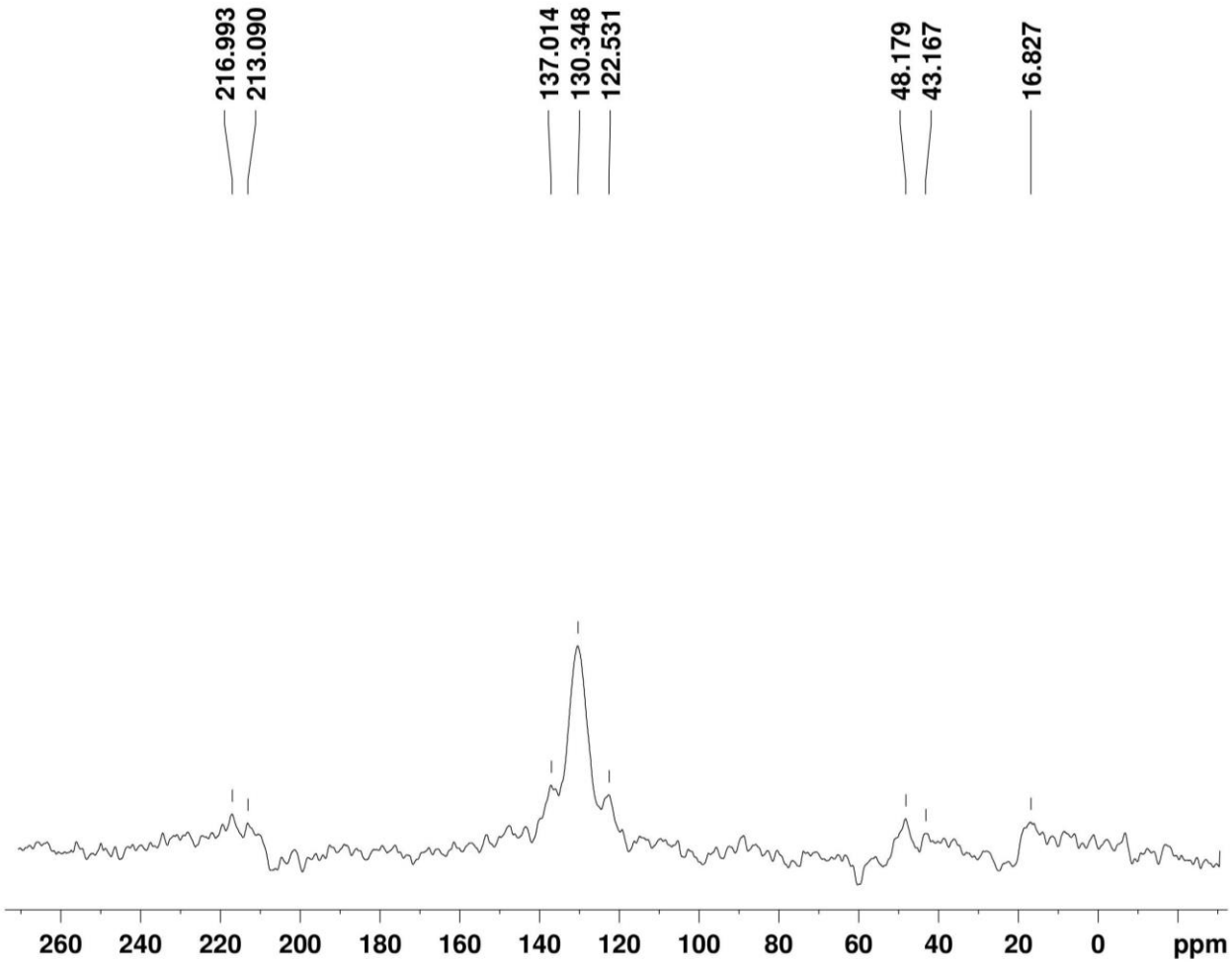

Figure A11: ^{13}C NMR spectrum of NiI_2dppp in solid state (AV600).

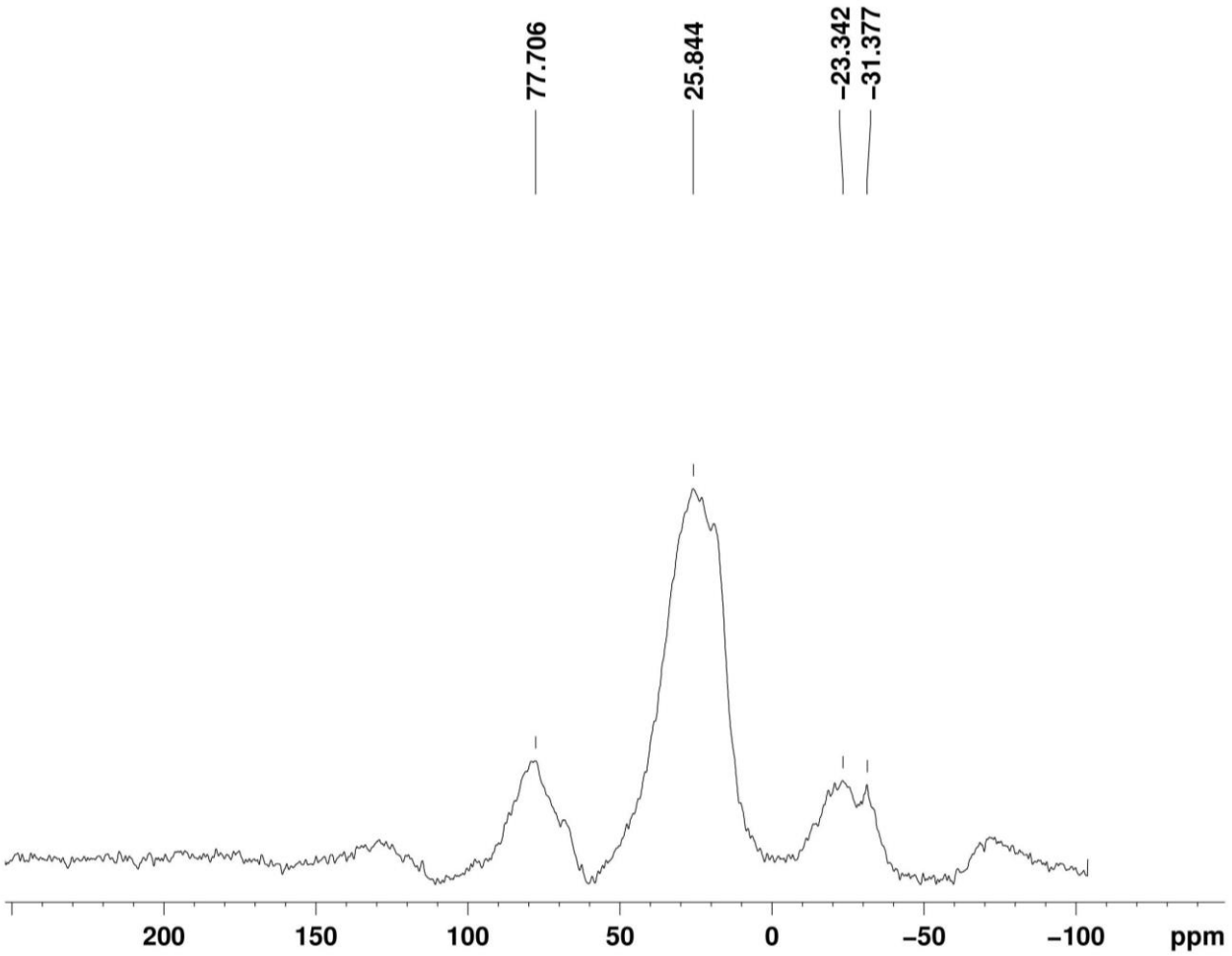

Figure A12: ^{31}P NMR spectrum of NiI_2dppp in solid state (AV600).

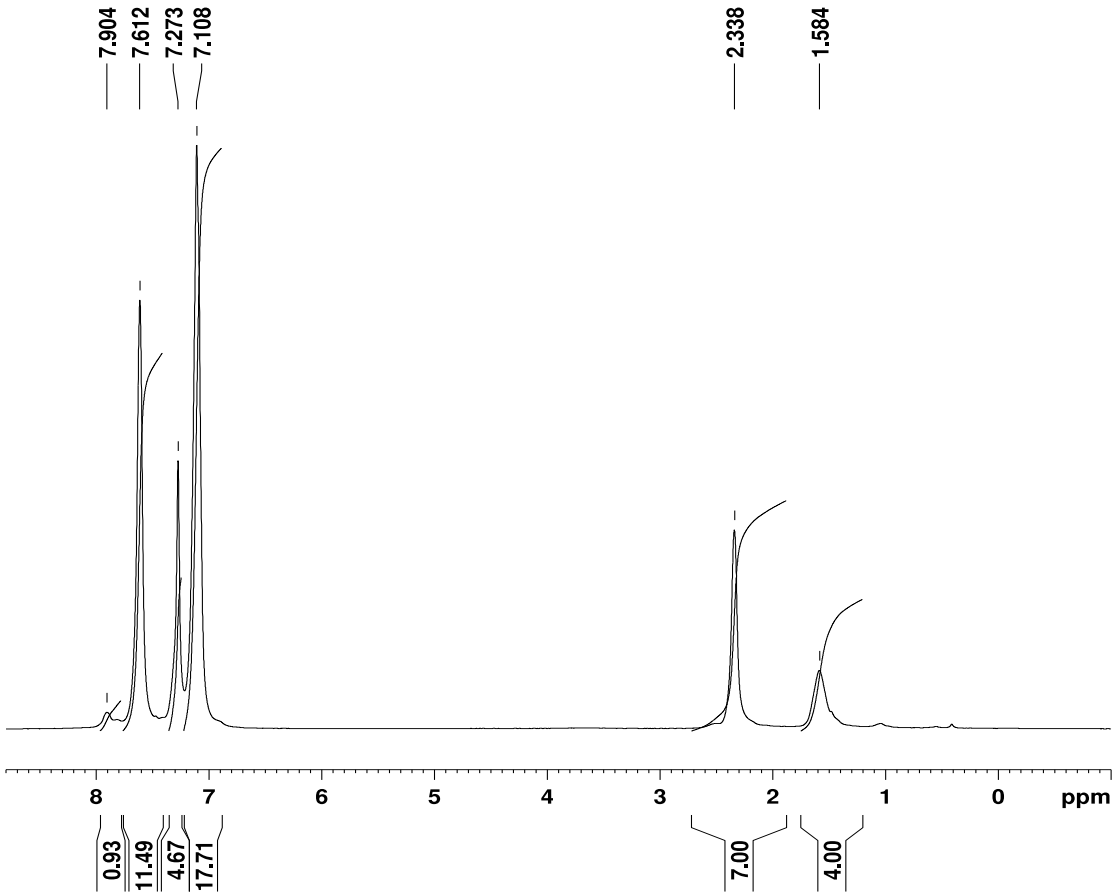

Figure A13: ^{1}H NMR spectrum of Ni(dppp)$_2$ was synthesized by NiCl$_2$dppp in C$_6$D$_6$ (AV600).

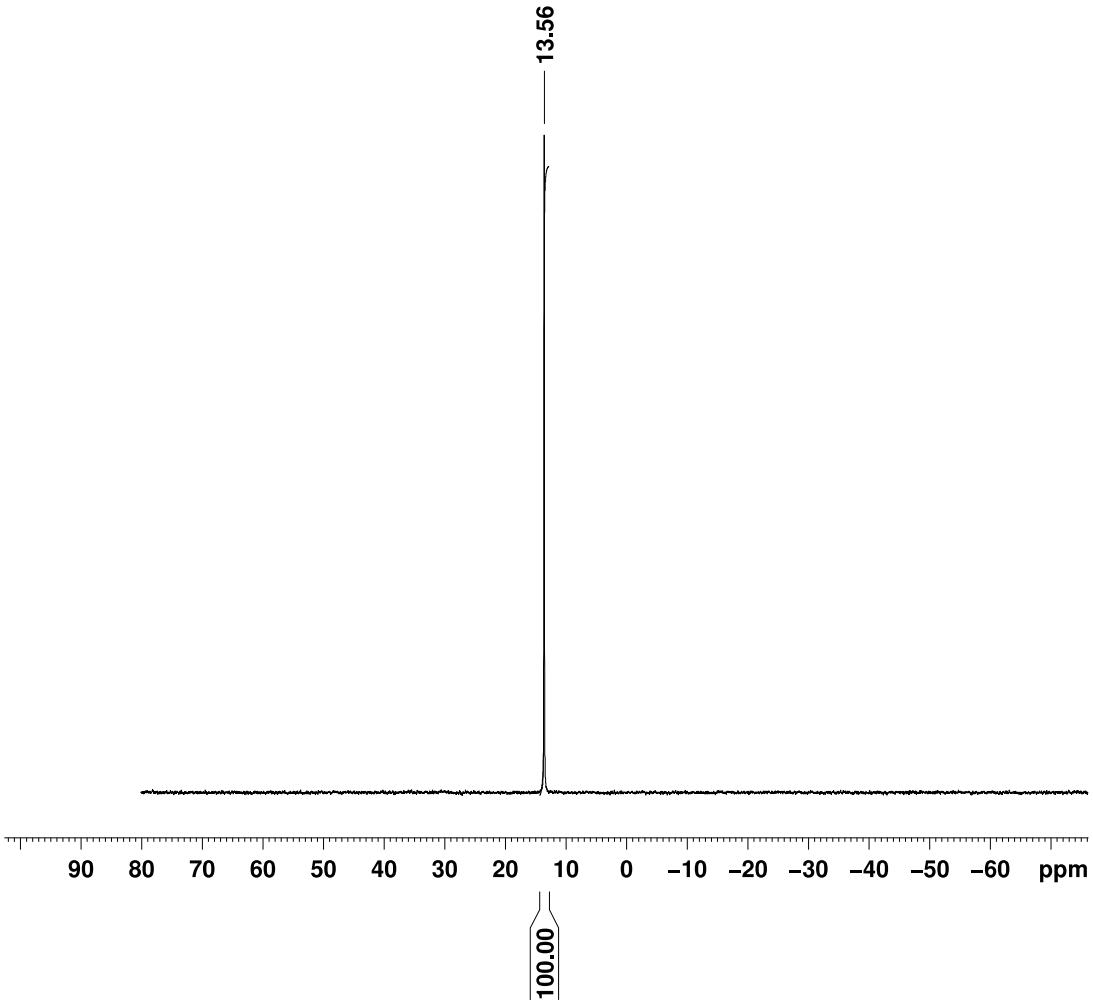

Figure A14: ^{31} P NMR spectrum of $Ni(dppp)_2$ was synthesized via $NiCl_2$dppp in C_6D_6 (AV600).

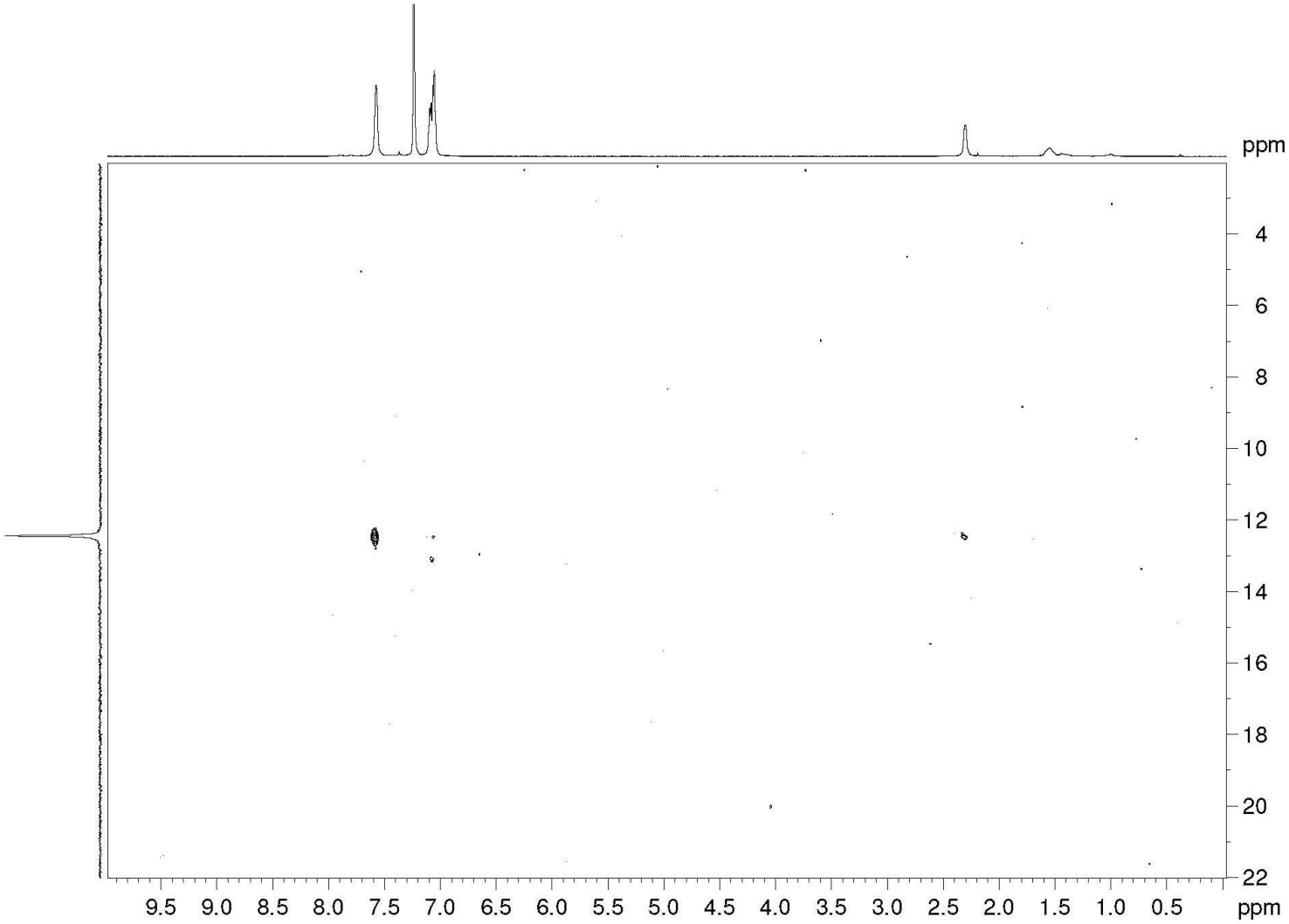

Figure A15: ^{1}H-^{31}P HMBC spectrum of $Ni(dppp)_2$ in C_6D_6 (AV600).

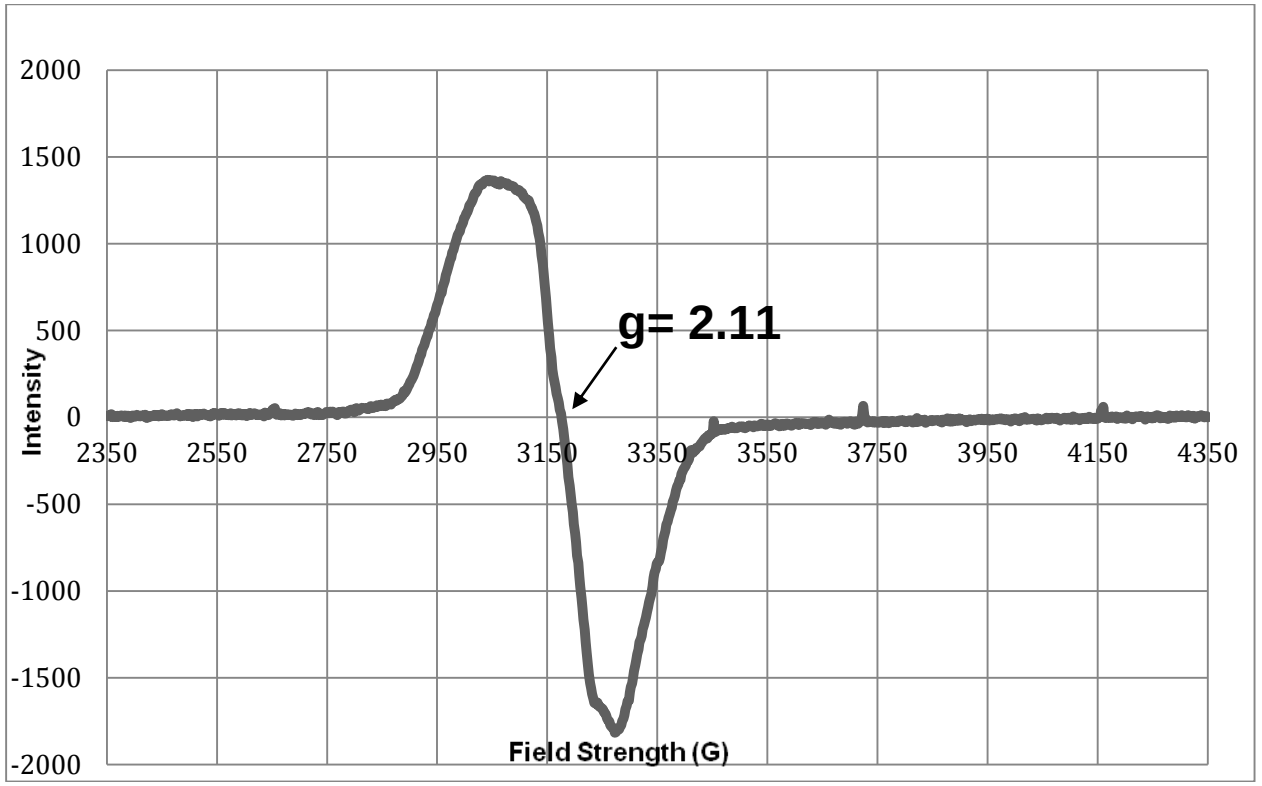

Figure A16: EPR spectra of Ni(I) complex while synthesized Ni(0) complexe ($Ni(dppp)_2$)

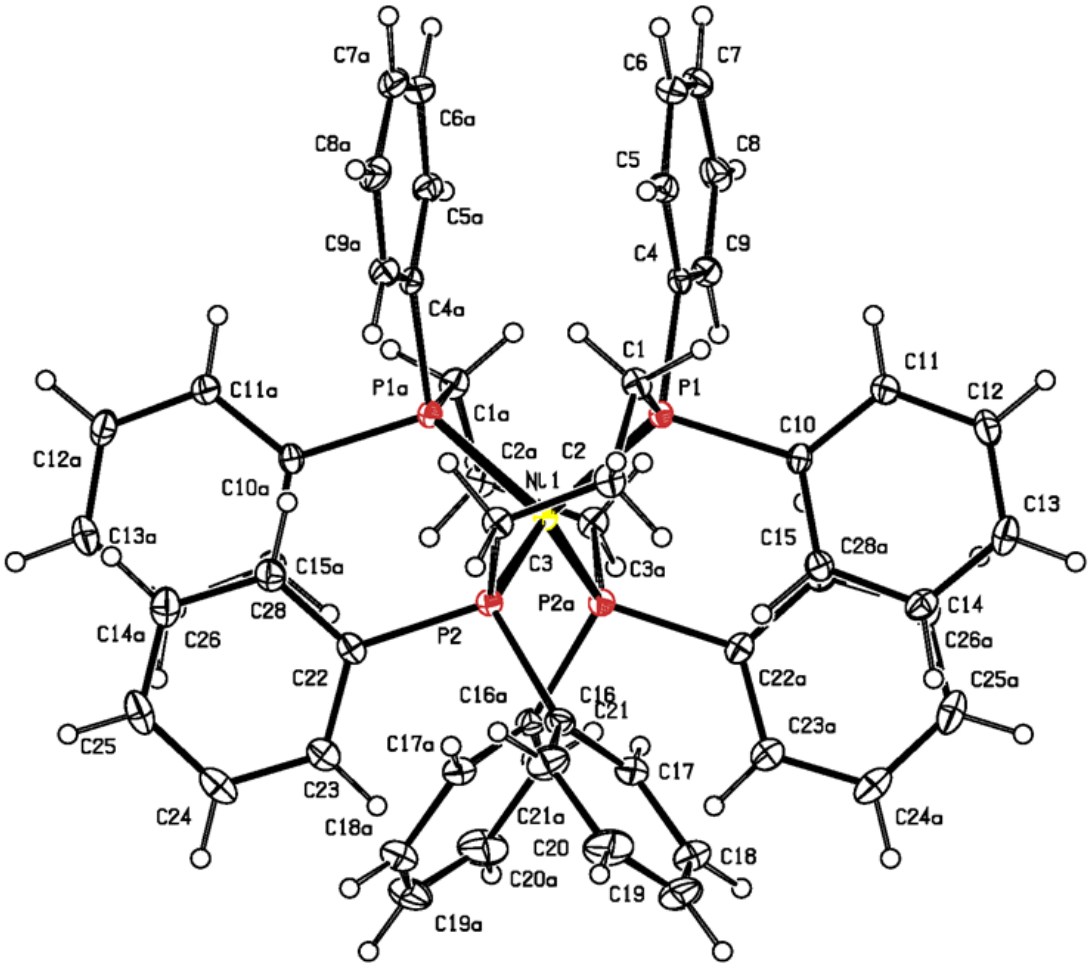

Figure A17: X-ray structure of Ni(dppp)$_2$ was synthesized via NiCl$_2$dppp.

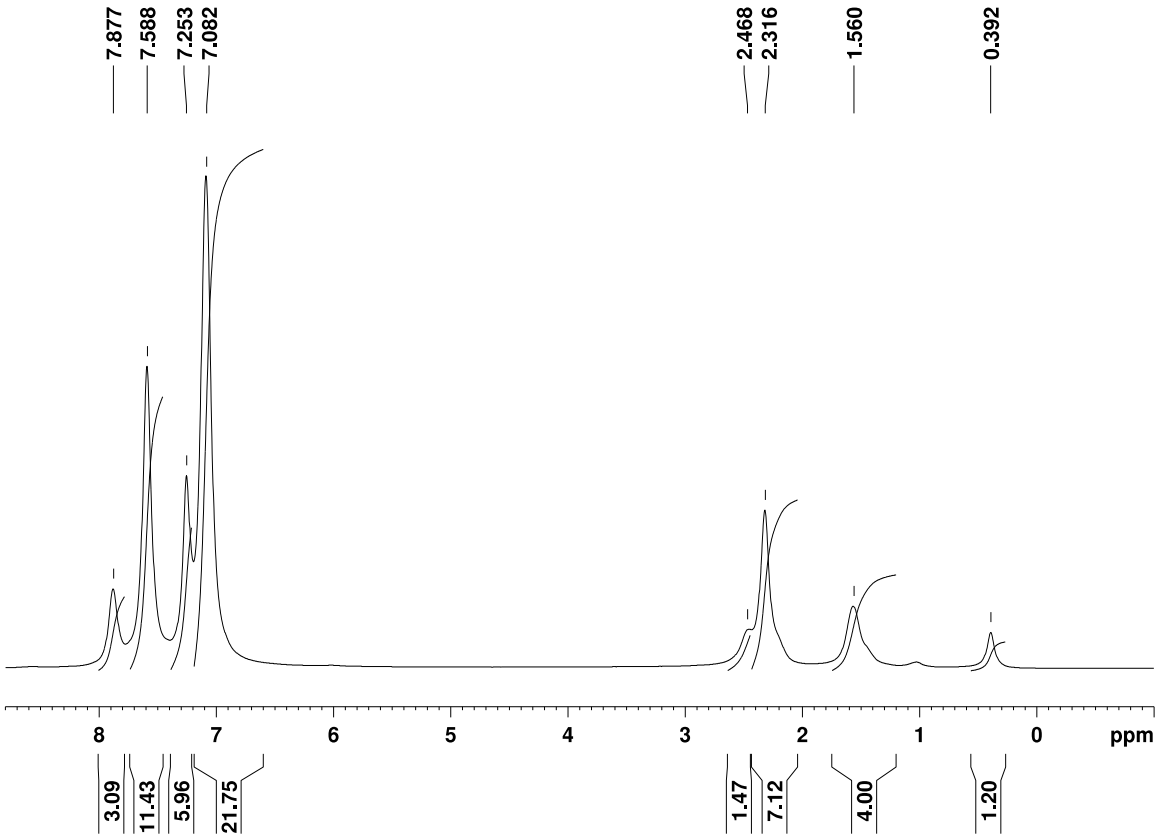

Figure A18: ^{1}H NMR spectrum of Ni(dppp)$_2$ synthesized via NiBr$_2$dppp in C_6D_6 (AV500).

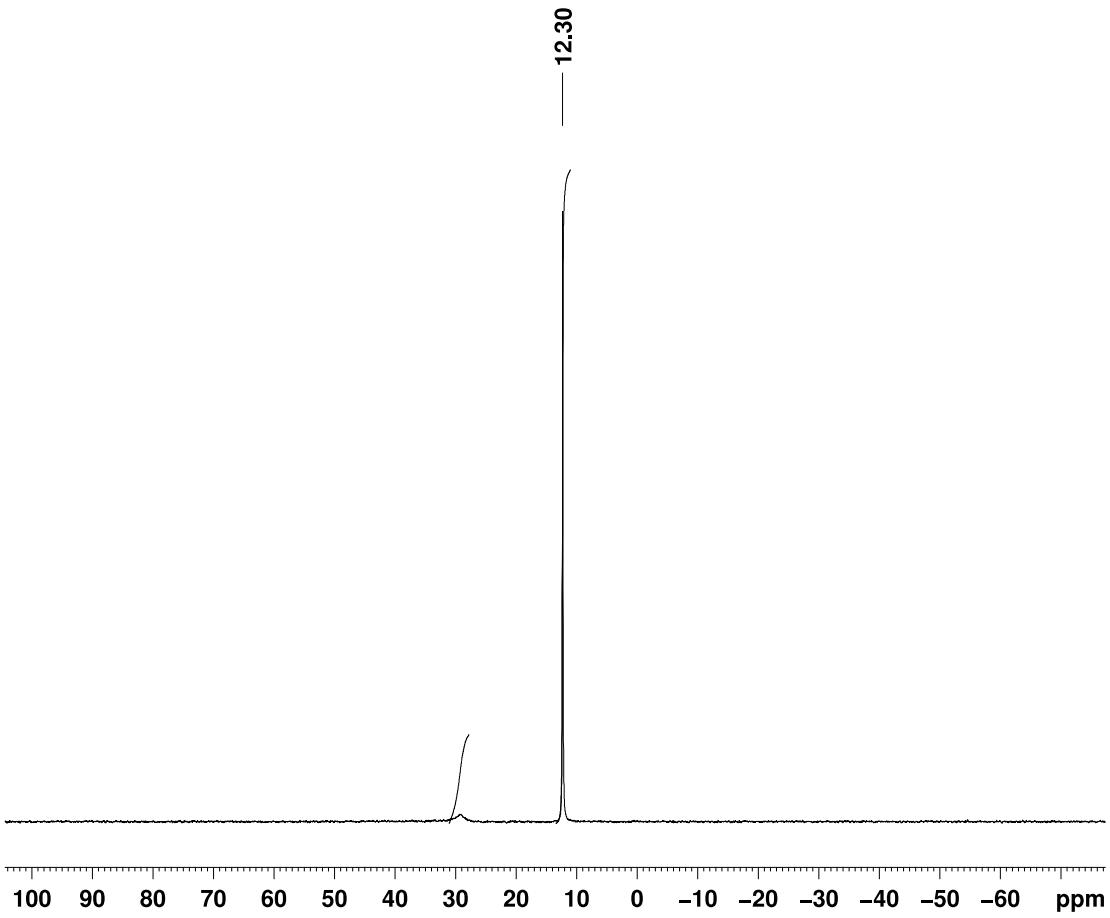

Figure A19: ^{31}P NMR spectrum of Ni(dppp)$_2$ synthesized via NiBr$_2$dppp in C$_6$D$_6$ (AV500).

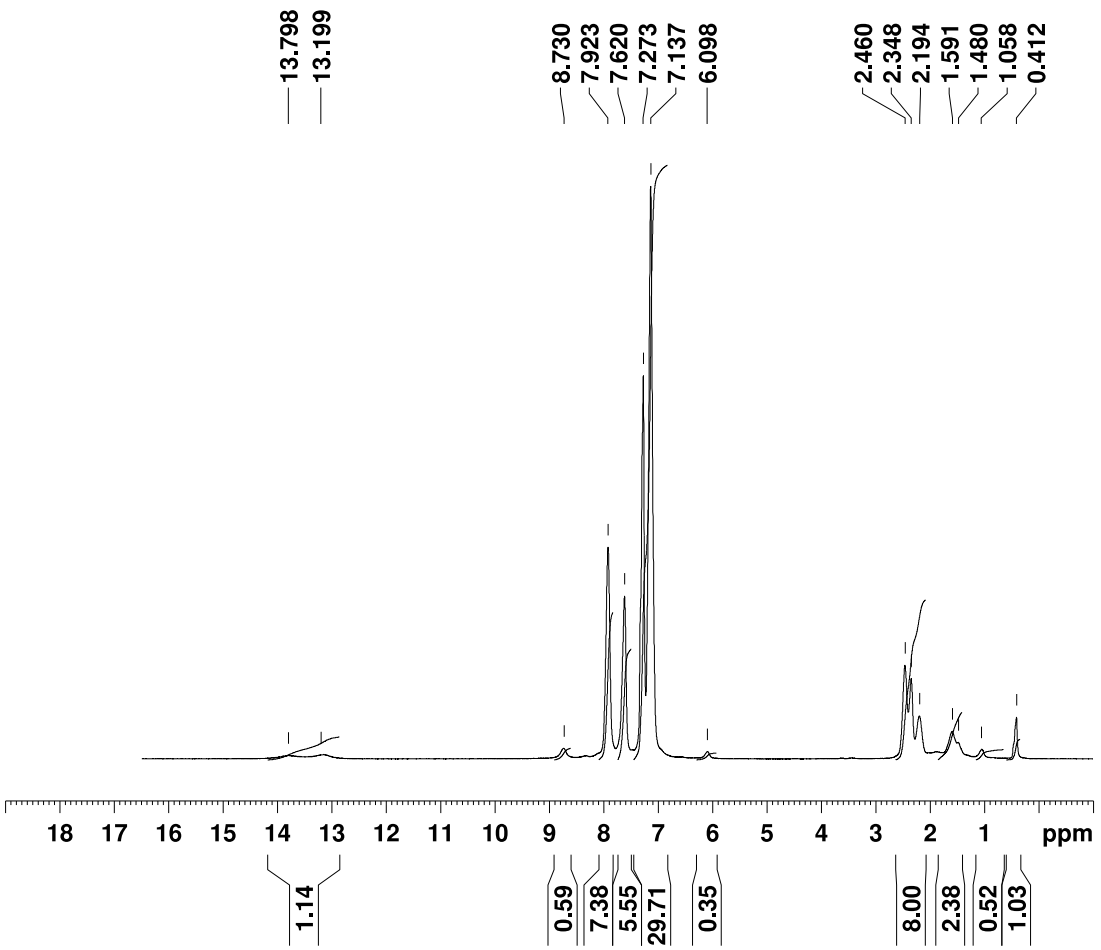

Figure A20: ^{1}H NMR spectrum of attempted synthesis of Ni(dppp)$_2$ via NiI$_2$dppp in C$_6$D$_6$ (AV500).

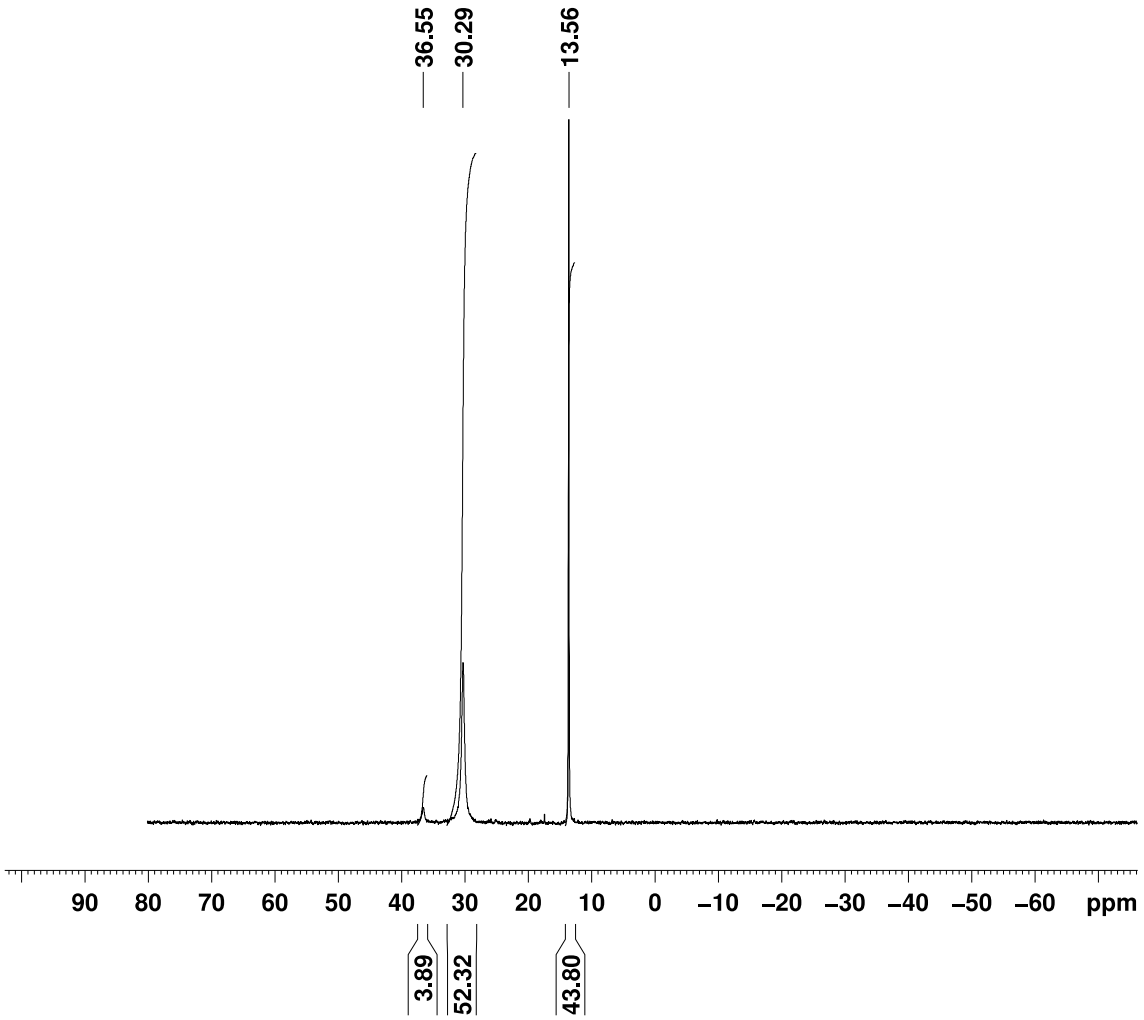

Figure A21: ^{31}P NMR spectrum of attempted synthesis of Ni(dppp)$_2$ via NiI$_2$dppp in C$_6$D$_6$ (AV500).

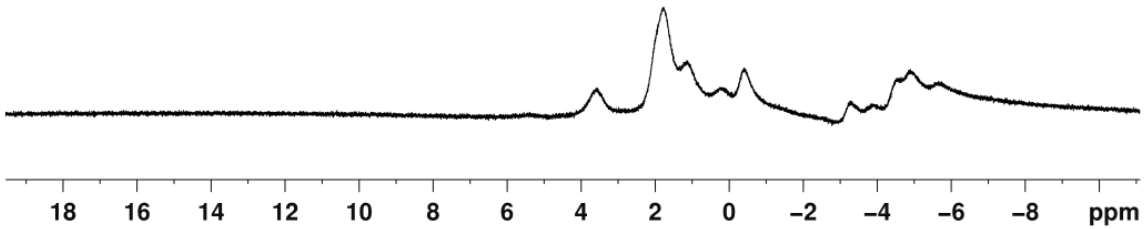

Figure A22: ^{1}H NMR spectrum of precipitate of $NiCl(dppp)_n$ in CD_2Cl_2 (AV400).

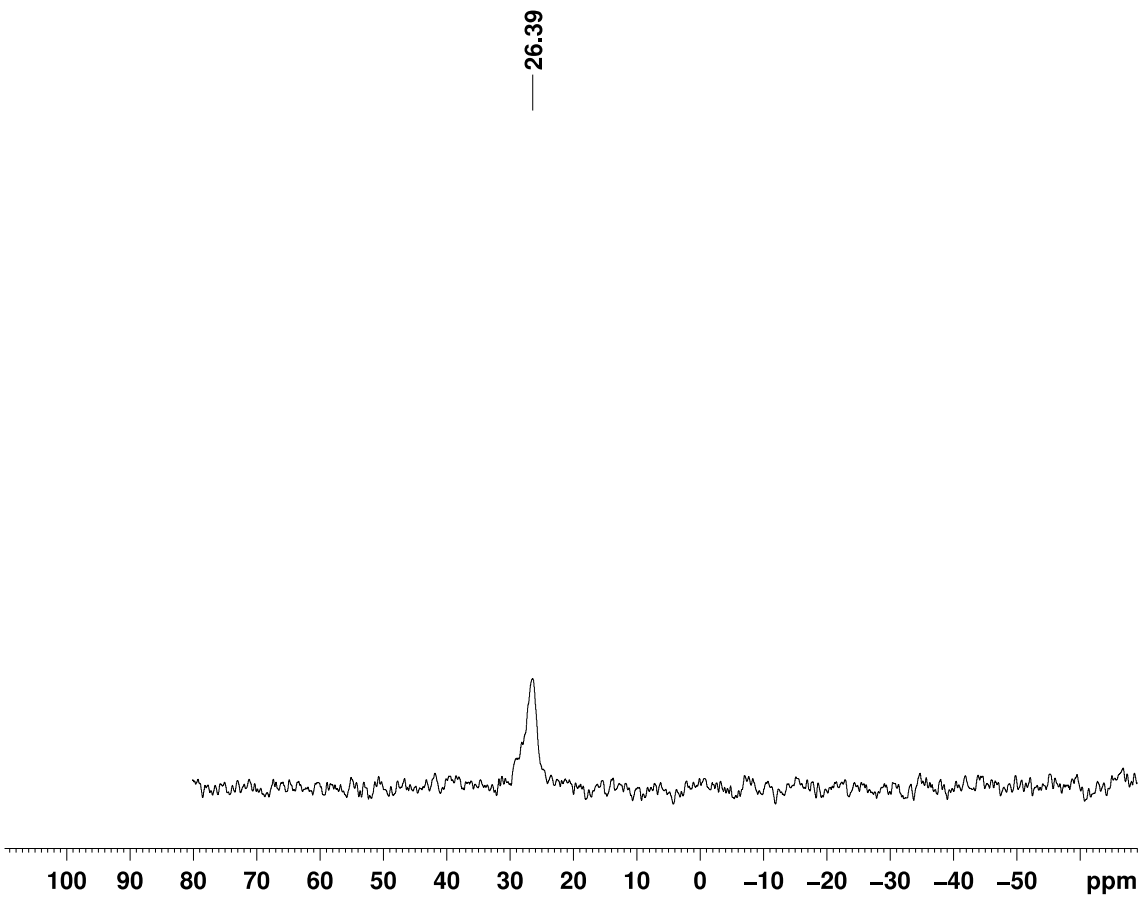

Figure A23: ^{31}P NMR spectrum of precipitate of NiCl(dppp)$_n$ in CD_2Cl_2 (AV400).

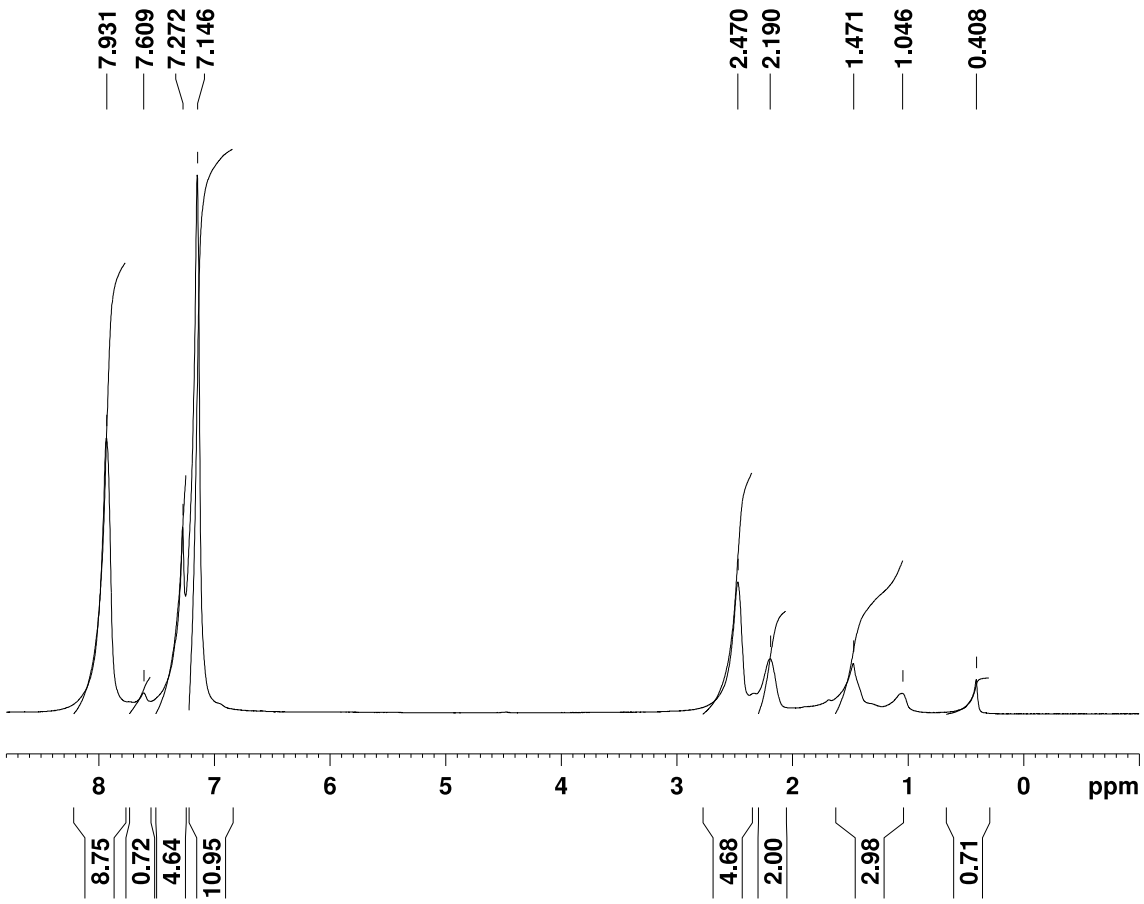

Figure A24: ^{1}H NMR spectrum of pale-yellow solid of NiCl(dppp)$_n$ in C_6D_6 (AV400).

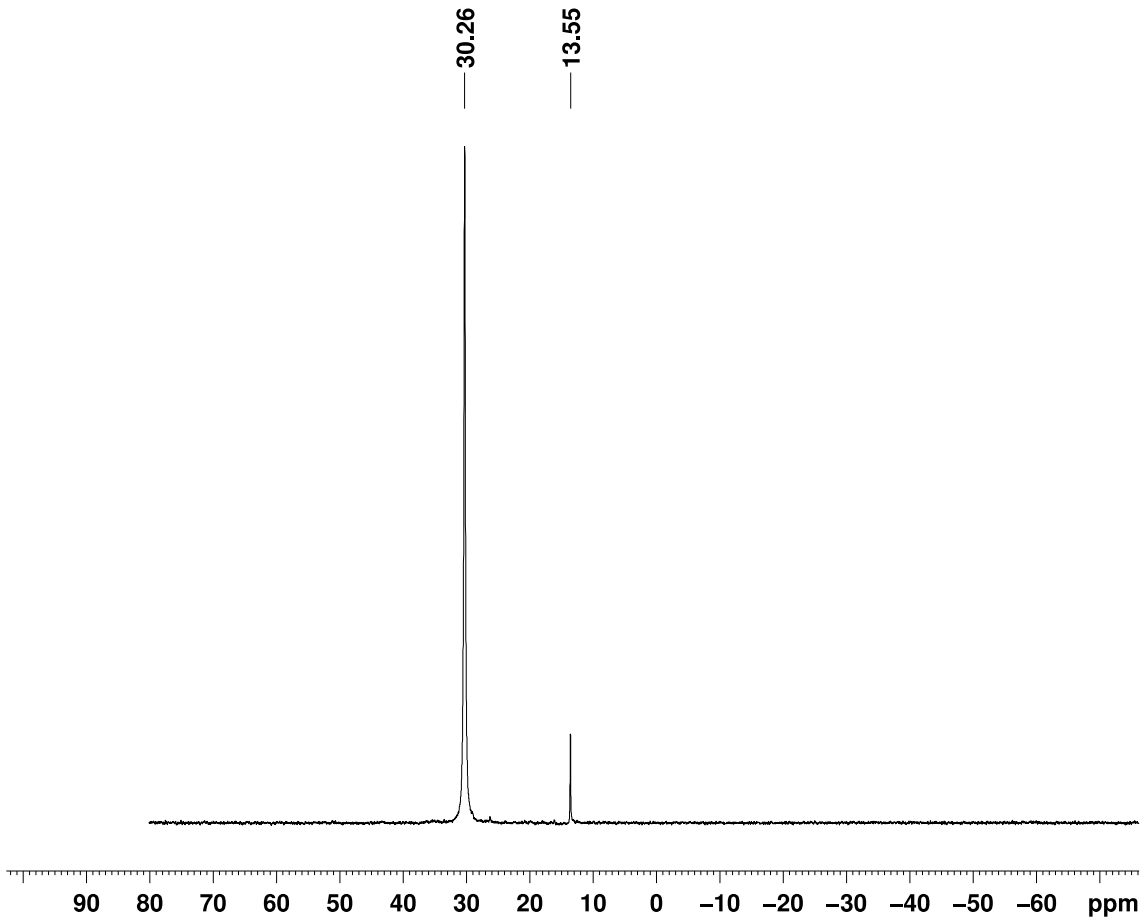

Figure A25: ^{31}P NMR spectrum of pale-yellow solid of NiCl(dppp)$_n$ in C_6D_6 (AV400).

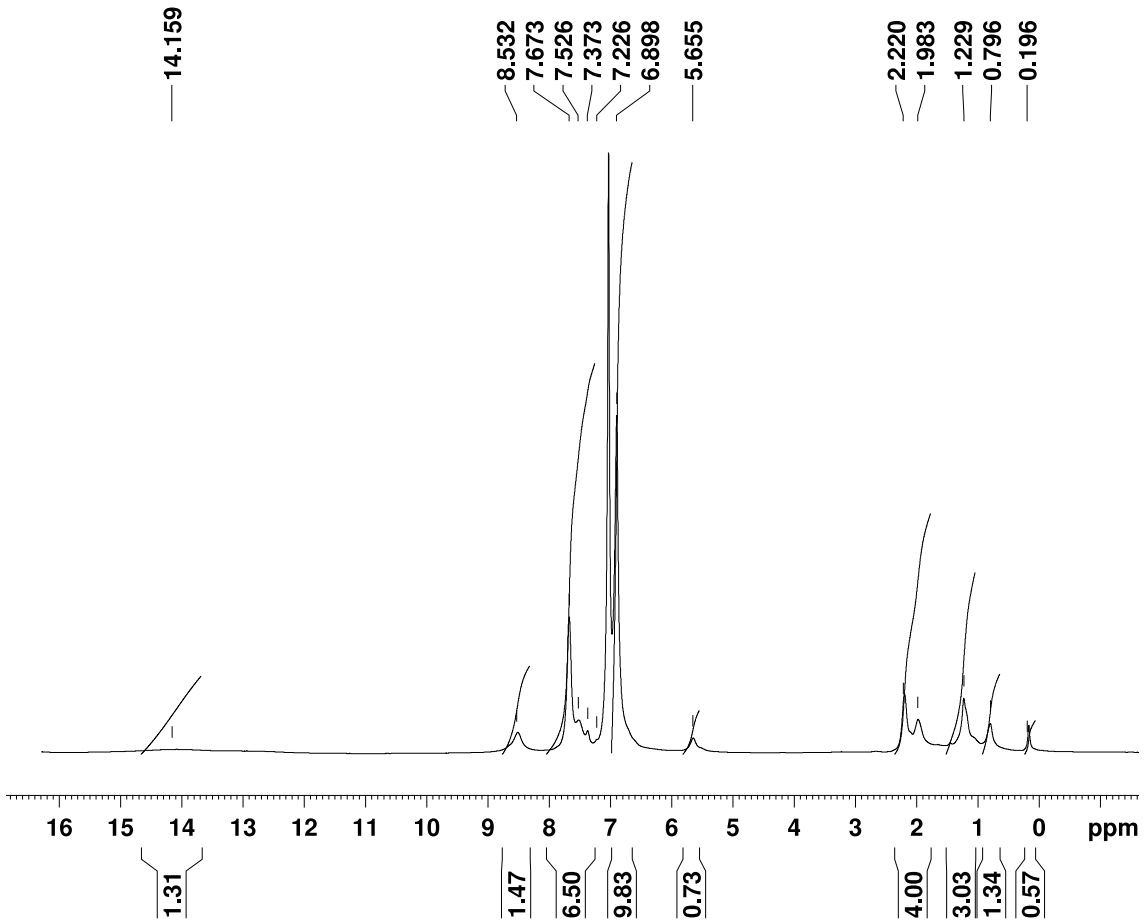

Figure A26: ^{1}H NMR spectrum of precipitate of NiBr(dppp)$_n$ in C_6D_6 (AV400).

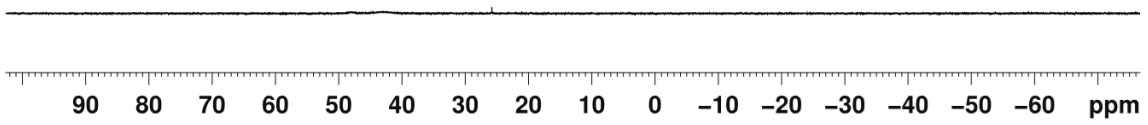

Figure A27: ^{31}P NMR spectrum of precipitate of NiBr(dppp)$_n$ in C_6D_6 (AV400).

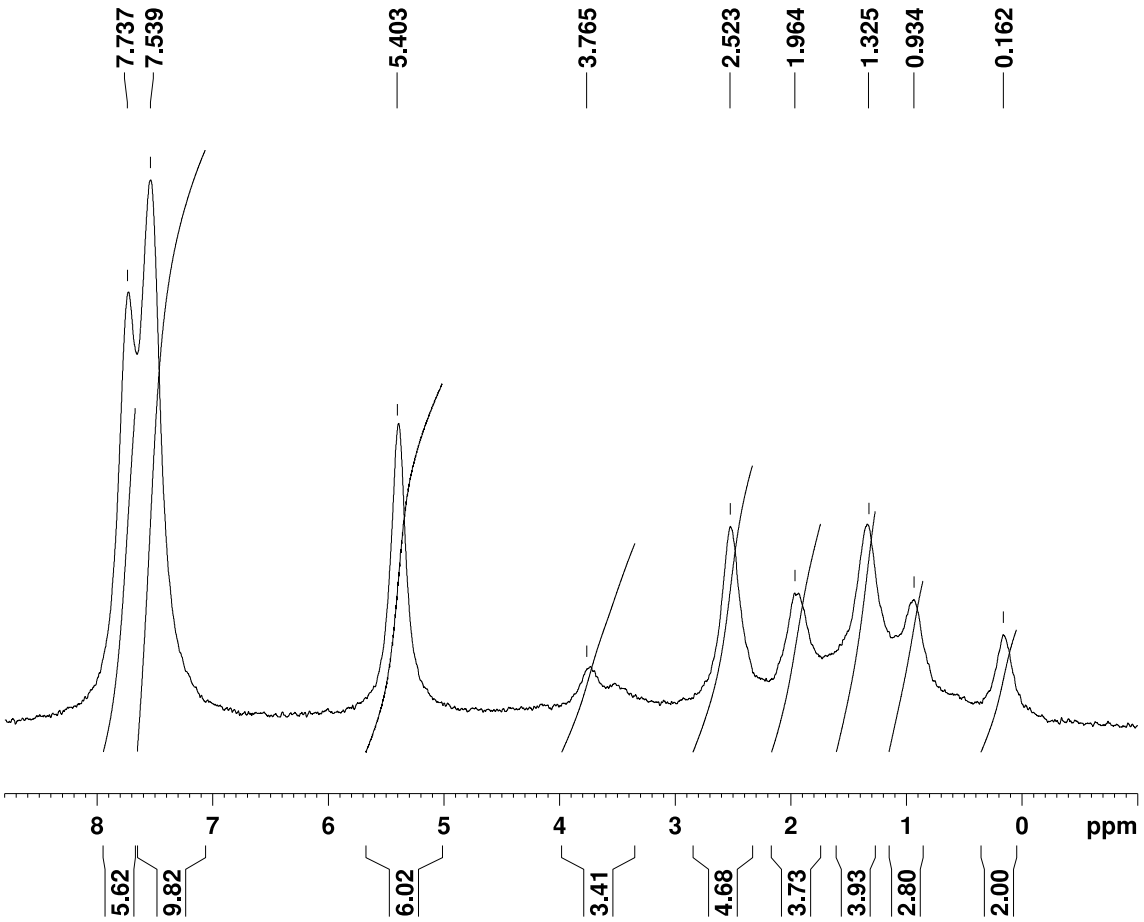

Figure A28: ^{1}H NMR spectrum of precipitate of $NiBr(dppp)_n$ in CD_2Cl_2 (AV400).

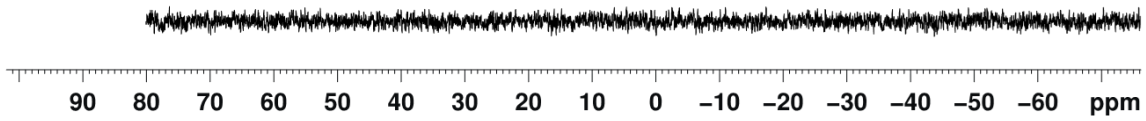

Figure A29: ^{31}P NMR spectrum of precipitate of NiBr(dppp)$_n$ in CD_2Cl_2 (AV500).

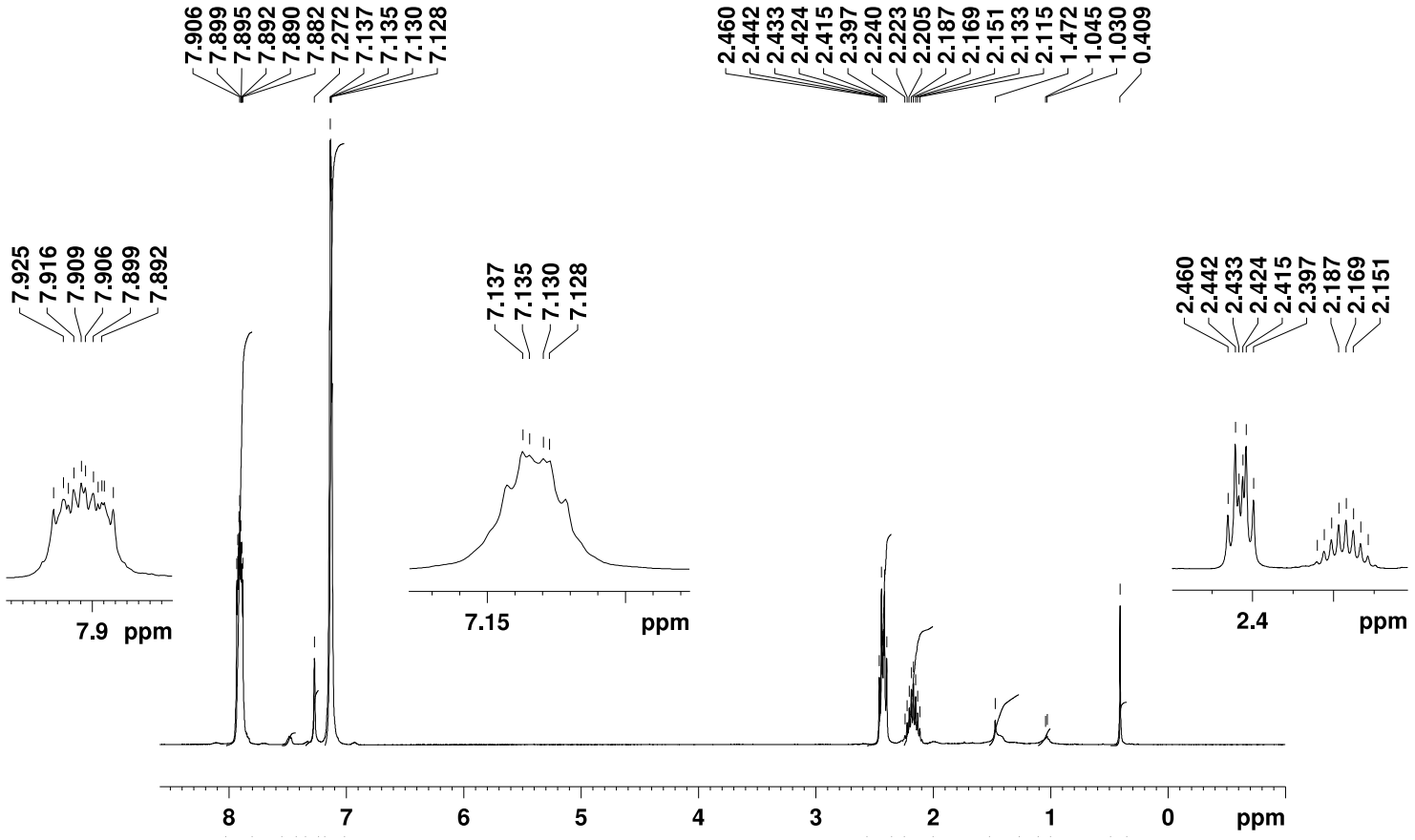

Figure A30: ^{1}H NMR spectrum of white solid of NiBr(dppp)$_n$ in C_6D_6 (AV400).

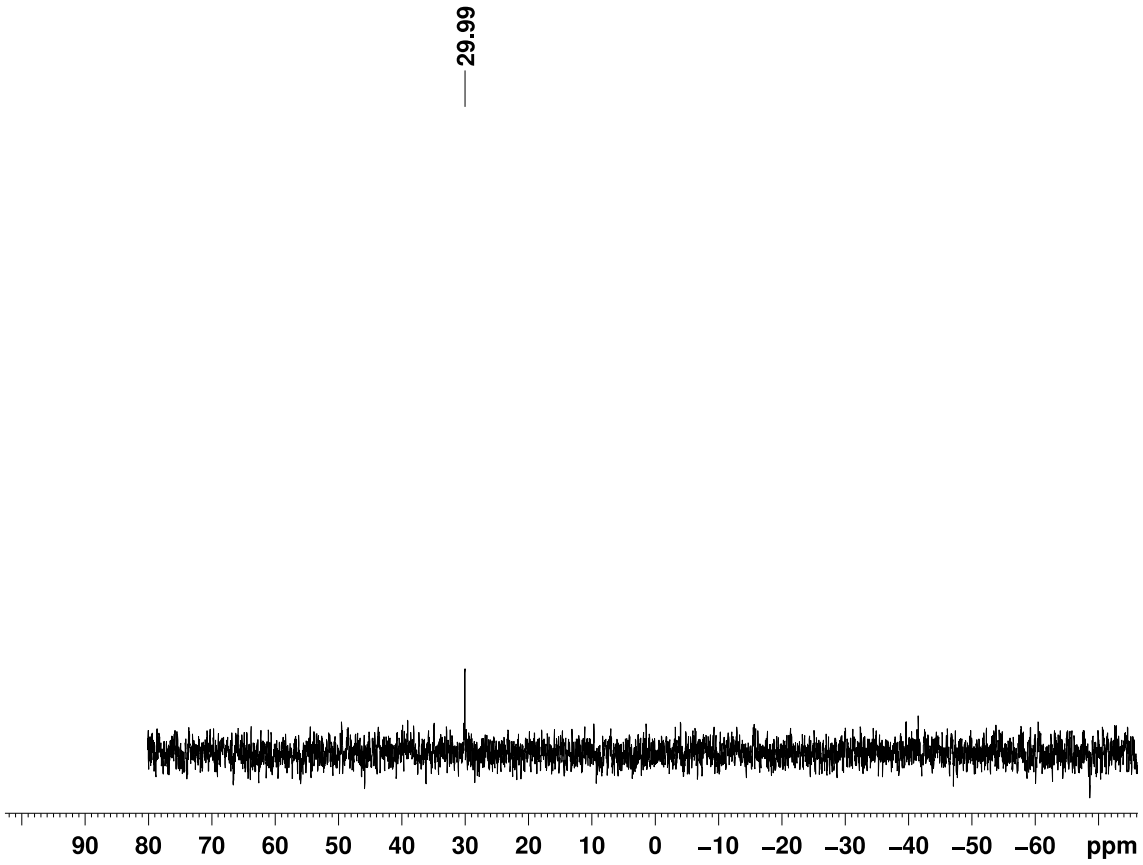

Figure A31: ^{31}P NMR spectrum of white solid of NiBr(dppp)$_n$ in C_6D_6 (AV400).

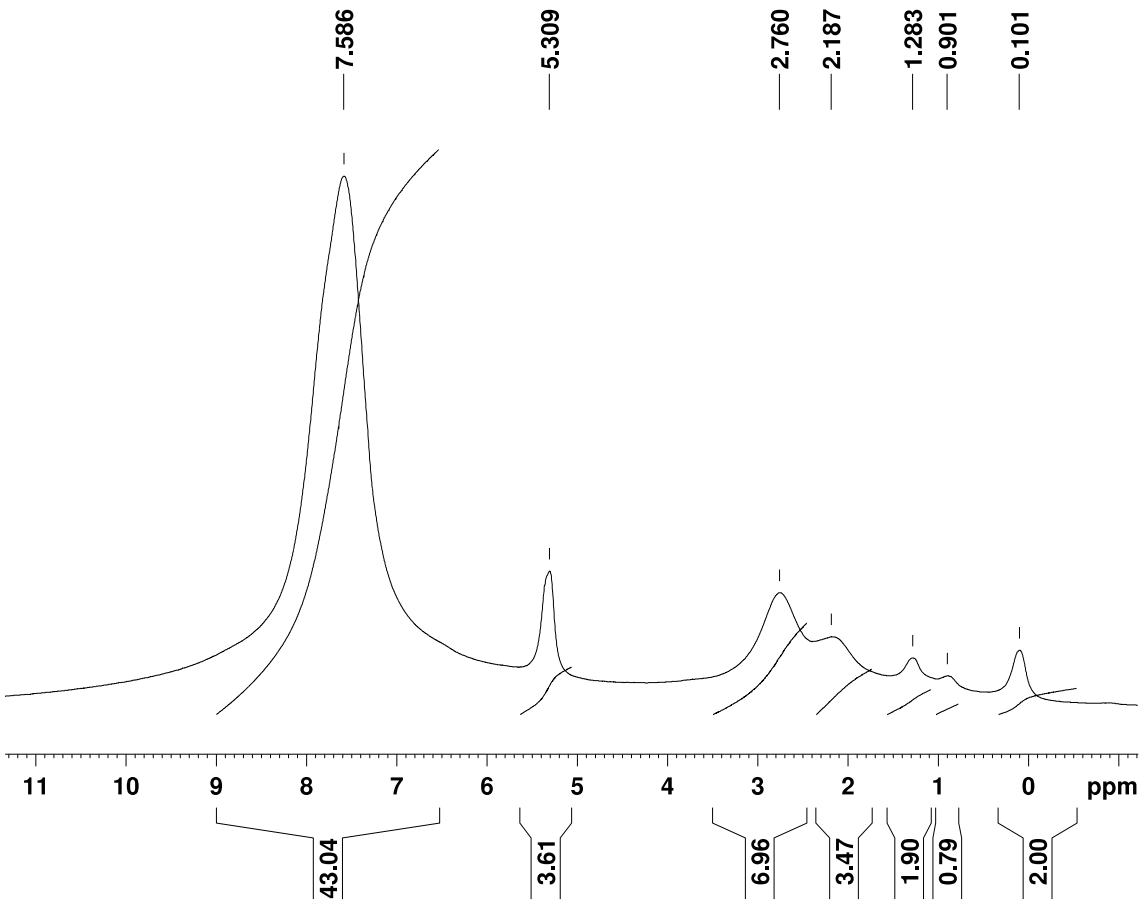

Figure A32: ^{1}H NMR spectrum of precipitate of NiI(dppp)$_n$ in CD_2Cl_2 (AV500).

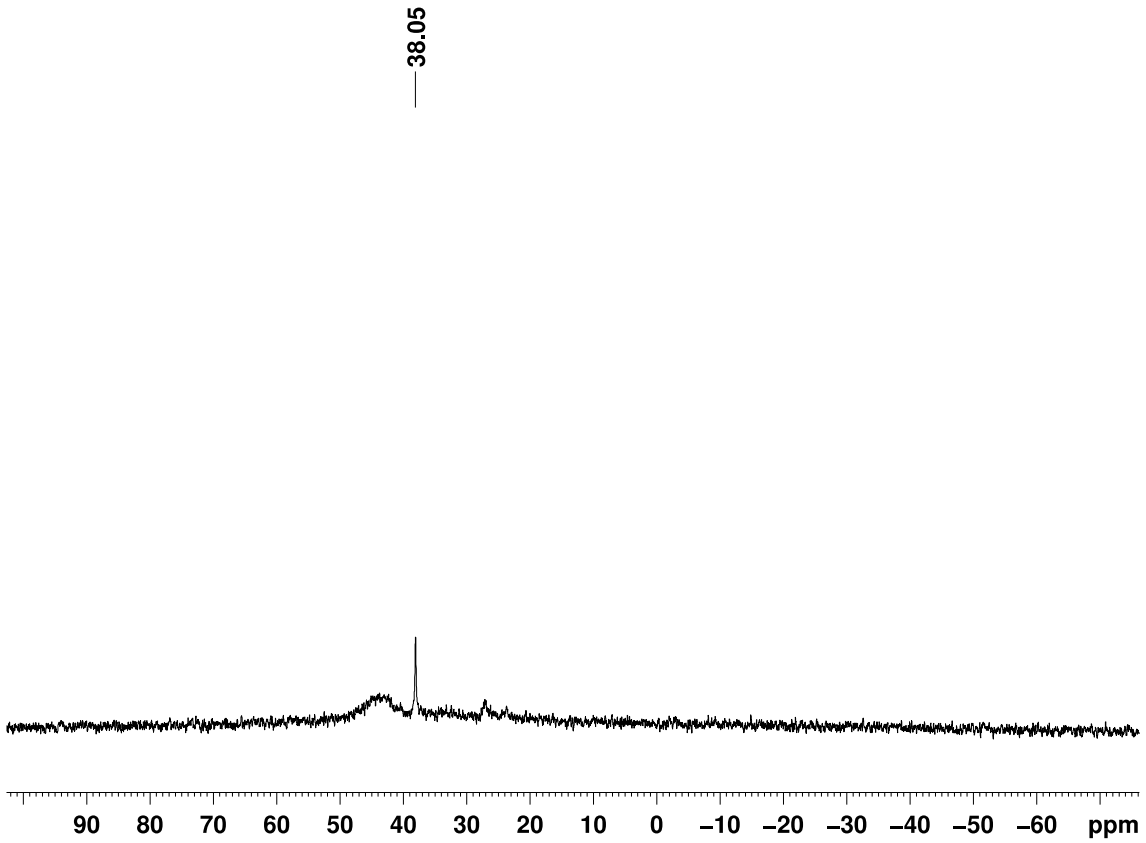

Figure A33: ^{31}P NMR spectrum of precipitate of NiI(dppp)$_n$ in CD_2Cl_2 (AV500).

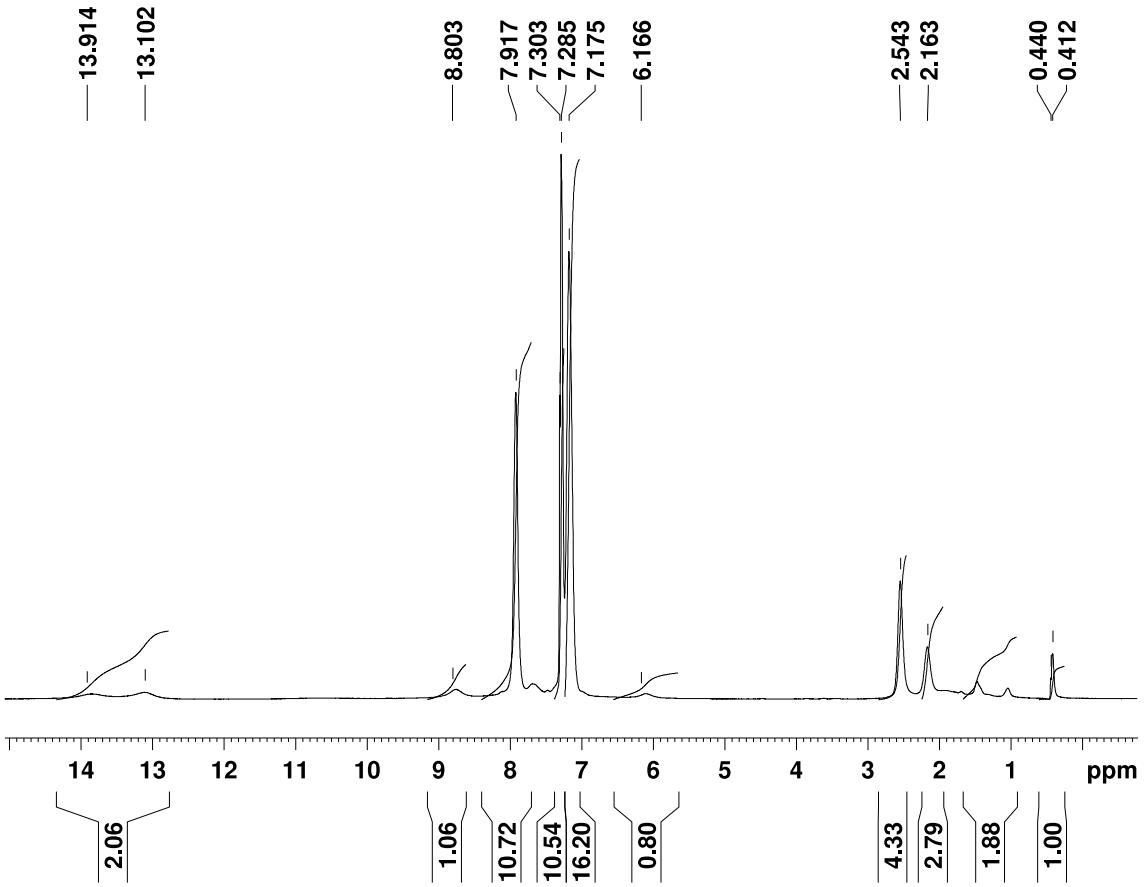

Figure A34: ^{1}H NMR spectrum of pale-yellow solid of NiI(dppp)$_n$ in C_6D_6 (AV500).

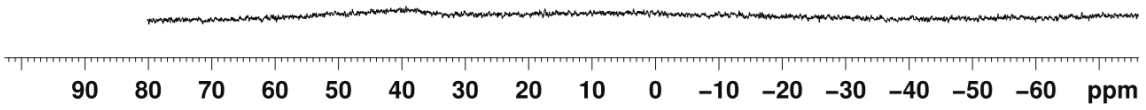

Figure A35: ^{31}P NMR spectrum of pale-yellow solid of NiI(dppp)$_n$ in C_6D_6 (AV500).

Appendix B:
Crystal Structure Data for $Ni(dppp)_2$

Table B1. Crystal data and structure refinement for $Ni(dppp)_2$.

A. Crystal Data

Empirical formula	$C_{54}H_{52}Ni_1P_4$
Formula weight	883.54
Crystal Color, Habit	orange, block-like
Crystal dimensions (mm)	$0.127 \times 0.120 \times 0.088$
Crystal system	monoclinic
Space group	*C*2/*c* [15]
Unit cell parameters[a]	
a (Å)	18.1596(3)
b (Å)	13.2018(2)
c (Å)	19.8852(3)
α (°)	90
β (°)	109.6880(10)
γ (°)	90
V (Å^3)	4488.58(12)
Z[b]	4
F(000)	1856
Density (ρ_{calcd})	1.034 Mg/m^3
Absorption coefficient (μ)	0.612 mm^{-1}

B. Data Collection and Refinement Conditions

Diffractometer	Bruker-AXS Smart Apex II diffractometer[c]
Radiation	monochromated Mo K_α
Wavelength (Mo K_α)	0.71073 Å
Temperature	-93(2) °C [180(2) K]
Scan type	ω-and φ-scans (0.5º/frame, 40 s exposure/frame, 4 sets)
Theta range for data collection	1.949 to 26.758°
Completeness to theta = 25.242°	100.0%
Reflections collected[d]	18474
Index ranges	$-22 \le h \le 22$, $-12 \le k \le 16$, $-20 \le l \le 25$
Independent reflections [$F_o^2 \ge -3\sigma(F_o^2)$][e]	4742 [R_{int} = 0.0243][f]
Observed reflections [$F_o^2 > 2\sigma(F_o^2)$][g]	3993
Absorption correction method	multi-scan [SADABS][k]
Anomalous Dispersion	For all non-hydrogen atoms
Structure solution method	Direct methods (SHELXT-2014)[h]
Refinement method	Full-matrix least-squares on F^2 (SHELXL-2014)[i]
Function Minimized	$\Sigma w(\lvert F_o\rvert^2 - \lvert kF_c\rvert^2)^2$ (k: overall scale factor)
Weighing scheme, w $w = [\sigma(F_o^2) + (a\,P)^2 + (b\,P)]^{-1}$	$w = [\sigma(F_o^2) + (0.0307\,P)^2 + (4.4551\,P)]^{-1}$
P-factor	$[\mathrm{Max}(F_o^2,0) + 2\,F_c^2]/3$
Data / restraints / parameters	4742 [$F_o^2 \ge -3\sigma(F_o^2)$] / 0 / 267
Reflection (observed)/parameter ratio	15:1
Reflection (data)/parameter ratio	18:1

Goodness-of-fit[j] on F^2	1.034
$GooF = \{\Sigma[w(F_o^2-F_c^2)^2]/(n - p)\}^{1/2}$	
n: number of reflections, p: number of parameters	
Final R indices	
$R_1 = [\Sigma\|\|F_o\|-\|F_c\|\|]/[\Sigma\|F_o\|]$ for $[F_o^2 > 2\sigma(F_o^2)]$[i]	0.0309
$wR_2 = \{[\Sigma w(F_o^2-F_c^2)^2]/[\Sigma w(F_o^2)^2]\}^{1/2}$ [all data]	0.0740
Max. Shift/Error in Final Cycle	0.001
Largest difference peak and hole	0.382 and -0.221 $e^-/Å^3$
Transmission factor (min)	0.7070 [SADABS][k]
Transmission factor (max)	0.7454 [SADABS][k]

Table B2. Atomic coordinates ($\times 10^4$), equivalent isotropic displacement parameters ($Å^2 \times 10^3$) and site occupancy factors for $Ni(dppp)_2$.

U(eq) is defined as one third of the trace of the orthogonalized U^{ij} tensor.

Atom	x	y	z	U(eq)
Ni(1)	5000	5033(1)	2500	15(1)
P(1)	4554(1)	6019(1)	1577(1)	16(1)
P(2)	5887(1)	4216(1)	2205(1)	17(1)
C(1)	5248(1)	6313(1)	1107(1)	22(1)
C(2)	5676(1)	5385(1)	964(1)	24(1)
C(3)	6303(1)	4979(1)	1641(1)	22(1)
C(4)	4232(1)	7302(1)	1709(1)	19(1)
C(5)	4551(1)	8195(1)	1552(1)	25(1)
C(6)	4309(1)	9131(1)	1718(1)	31(1)
C(7)	3741(1)	9198(2)	2031(1)	31(1)
C(8)	3406(1)	8326(2)	2175(1)	30(1)
C(9)	3652(1)	7389(1)	2020(1)	24(1)
C(10)	3717(1)	5596(1)	807(1)	19(1)
C(11)	3203(1)	6259(2)	327(1)	31(1)
C(12)	2590(1)	5890(2)	-245(1)	36(1)
C(13)	2482(1)	4858(2)	-347(1)	31(1)
C(14)	2992(1)	4196(2)	117(1)	27(1)
C(15)	3603(1)	4567(1)	691(1)	22(1)
C(16)	5622(1)	3068(1)	1633(1)	23(1)
C(17)	4912(1)	2598(1)	1539(1)	28(1)
C(18)	4663(1)	1784(2)	1077(1)	41(1)
C(19)	5124(2)	1422(2)	707(1)	48(1)
C(20)	5839(2)	1864(2)	802(1)	48(1)
C(21)	6089(1)	2678(2)	1263(1)	36(1)
C(22)	6808(1)	3776(1)	2876(1)	20(1)
C(23)	6945(1)	2759(1)	3068(1)	26(1)

C(24)	7632(1)	2458(2)	3595(1)	33(1)
C(25)	8192(1)	3162(2)	3938(1)	36(1)
C(26)	8070(1)	4171(2)	3758(1)	33(1)
C(28)	7380(1)	4478(2)	3236(1)	26(1)

Table B3. Interatomic Angles [°] for $Ni(dppp)_2$.

P(1)-Ni(1)-P(1)*	106.34(3)
P(1)-Ni(1)-P(2)*	115.217(16)
P(1)*-Ni(1)-P(2)*	99.689(16)
P(1)-Ni(1)-P(2)	99.689(16)
P(1)*-Ni(1)-P(2)	115.216(16)
P(2)*-Ni(1)-P(2)	120.56(3)
C(4)-P(1)-C(10)	100.62(7)
C(4)-P(1)-C(1)	100.61(8)
C(10)-P(1)-C(1)	98.97(8)
C(4)-P(1)-Ni(1)	118.48(5)
C(10)-P(1)-Ni(1)	119.22(6)
C(1)-P(1)-Ni(1)	115.48(6)
C(22)-P(2)-C(3)	98.82(8)
C(22)-P(2)-C(16)	99.80(8)
C(3)-P(2)-C(16)	98.47(8)
C(22)-P(2)-Ni(1)	122.28(6)
C(3)-P(2)-Ni(1)	112.58(6)
C(16)-P(2)-Ni(1)	120.45(6)
C(2)-C(1)-P(1)	113.75(12)
C(1)-C(2)-C(3)	112.94(14)
C(2)-C(3)-P(2)	112.84(12)
C(9)-C(4)-C(5)	117.55(16)
C(9)-C(4)-P(1)	117.68(13)
C(5)-C(4)-P(1)	124.70(14)
C(6)-C(5)-C(4)	120.72(18)
C(7)-C(6)-C(5)	120.67(19)
C(6)-C(7)-C(8)	119.47(18)

C(7)-C(8)-C(9)	120.13(18)
C(8)-C(9)-C(4)	121.43(18)
C(15)-C(10)-C(11)	118.32(15)
C(15)-C(10)-P(1)	118.15(12)
C(11)-C(10)-P(1)	123.51(14)
C(12)-C(11)-C(10)	120.57(18)
C(13)-C(12)-C(11)	120.12(18)
C(14)-C(13)-C(12)	119.88(17)
C(13)-C(14)-C(15)	119.88(18)
C(10)-C(15)-C(14)	121.22(16)
C(17)-C(16)-C(21)	117.82(17)
C(17)-C(16)-P(2)	119.01(14)
C(21)-C(16)-P(2)	123.11(14)
C(16)-C(17)-C(18)	121.11(19)
C(19)-C(18)-C(17)	120.3(2)
C(18)-C(19)-C(20)	119.7(2)
C(19)-C(20)-C(21)	120.2(2)
C(20)-C(21)-C(16)	120.8(2)
C(23)-C(22)-C(28)	117.76(16)
C(23)-C(22)-P(2)	122.31(14)
C(28)-C(22)-P(2)	119.85(13)
C(24)-C(23)-C(22)	120.86(18)
C(25)-C(24)-C(23)	120.42(19)
C(24)-C(25)-C(26)	119.77(17)
C(25)-C(26)-C(28)	120.11(19)
C(26)-C(28)-C(22)	121.07(18)

Symmetry transformations used to generate equivalent atoms:

*: -x + 1, y, -z + ½

Table B4. Anisotropic displacement parameters ($Å^2 \times 10^3$) $Ni(dppp)_2$.

The anisotropic displacement factor exponent takes the form:

$$[-2\pi^2(h^2a^{*2}U_{11} + k^2b^{*2}U_{22} + l^2c^{*2}U_{33} + 2klb^*c^*U_{23} + 2hla^*c^*U_{13} + 2hka^*b^*U_{12})]$$

Atom	U^{11}	U^{22}	U^{33}	U^{23}	U^{13}	U^{12}
Ni(1)	14(1)	16(1)	14(1)	0	5(1)	0
P(1)	16(1)	18(1)	15(1)	1(1)	5(1)	0(1)
P(2)	16(1)	19(1)	18(1)	-1(1)	7(1)	1(1)
C(1)	21(1)	26(1)	21(1)	5(1)	10(1)	0(1)
C(2)	24(1)	31(1)	20(1)	2(1)	12(1)	1(1)
C(3)	20(1)	26(1)	24(1)	1(1)	12(1)	2(1)
C(4)	19(1)	20(1)	15(1)	1(1)	2(1)	2(1)
C(5)	24(1)	23(1)	27(1)	4(1)	6(1)	0(1)
C(6)	35(1)	21(1)	31(1)	4(1)	3(1)	-1(1)
C(7)	35(1)	24(1)	26(1)	-2(1)	1(1)	9(1)
C(8)	30(1)	34(1)	25(1)	-1(1)	9(1)	10(1)
C(9)	25(1)	24(1)	23(1)	2(1)	8(1)	0(1)
C(10)	18(1)	24(1)	15(1)	-1(1)	5(1)	-1(1)
C(11)	34(1)	23(1)	26(1)	-2(1)	-2(1)	3(1)
C(12)	33(1)	36(1)	28(1)	-1(1)	-6(1)	9(1)
C(13)	24(1)	42(1)	23(1)	-7(1)	2(1)	-4(1)
C(14)	32(1)	26(1)	23(1)	-4(1)	10(1)	-6(1)
C(15)	24(1)	25(1)	18(1)	2(1)	7(1)	1(1)
C(16)	26(1)	20(1)	23(1)	-1(1)	8(1)	4(1)
C(17)	30(1)	21(1)	32(1)	0(1)	9(1)	2(1)
C(18)	40(1)	25(1)	51(1)	-5(1)	5(1)	-6(1)
C(19)	65(2)	28(1)	46(1)	-16(1)	11(1)	-2(1)
C(20)	71(2)	35(1)	47(1)	-13(1)	32(1)	5(1)
C(21)	42(1)	32(1)	42(1)	-10(1)	23(1)	-2(1)
C(22)	19(1)	26(1)	19(1)	2(1)	10(1)	6(1)
C(23)	27(1)	28(1)	27(1)	2(1)	14(1)	5(1)

C(24)	37(1)	35(1)	30(1)	11(1)	16(1)	16(1)
C(25)	28(1)	52(1)	25(1)	4(1)	5(1)	16(1)
C(26)	24(1)	43(1)	28(1)	-6(1)	5(1)	4(1)
C(28)	23(1)	28(1)	26(1)	-3(1)	9(1)	5(1)

Table B5. Hydrogen coordinates ($\times 10^4$) and isotropic displacement parameters ($Å^2 \times 10^3$) for $Ni(dppp)_2$.

Atom	x	y	z	U(eq)
H(1A)	4960	6641	645	27
H(1B)	5640	6804	1396	27
H(2A)	5927	5565	609	29
H(2B)	5290	4843	755	29
H(3A)	6595	5558	1924	26
H(3B)	6678	4558	1500	26
H(5)	4938	8162	1329	30
H(6)	4538	9732	1614	37
H(7)	3582	9841	2147	37
H(8)	3006	8367	2382	36
H(9)	3421	6793	2128	29
H(11)	3275	6969	393	37
H(12)	2241	6347	-568	43
H(13)	2058	4606	-737	37
H(14)	2925	3486	43	32
H(15)	3950	4105	1011	27
H(17)	4590	2837	1796	33
H(18)	4172	1476	1016	50
H(19)	4950	870	387	58
H(20)	6161	1610	551	58
H(21)	6585	2974	1328	43
H(23)	6563	2265	2835	31
H(24)	7716	1762	3720	39
H(25)	8662	2952	4297	43
H(26)	8457	4658	3991	39
H(28)	7297	5177	3122	31

Table B6. Selected torsion angles [°] $Ni(dppp)_2$.

C(4)-P(1)-C(1)-C(2)	175.69(12)
C(10)-P(1)-C(1)-C(2)	-81.63(13)
Ni(1)-P(1)-C(1)-C(2)	46.88(13)
P(1)-C(1)-C(2)-C(3)	-73.24(17)
C(1)-C(2)-C(3)-P(2)	78.82(17)
C(22)-P(2)-C(3)-C(2)	174.05(13)
C(16)-P(2)-C(3)-C(2)	72.67(14)
Ni(1)-P(2)-C(3)-C(2)	-55.42(14)
C(10)-P(1)-C(4)-C(9)	74.92(14)
C(1)-P(1)-C(4)-C(9)	176.26(13)
Ni(1)-P(1)-C(4)-C(9)	-56.90(14)
C(10)-P(1)-C(4)-C(5)	-108.33(15)
C(1)-P(1)-C(4)-C(5)	-6.99(15)
Ni(1)-P(1)-C(4)-C(5)	119.85(13)
C(9)-C(4)-C(5)-C(6)	1.5(2)
P(1)-C(4)-C(5)-C(6)	-175.25(13)
C(4)-C(5)-C(6)-C(7)	-0.9(3)
C(5)-C(6)-C(7)-C(8)	-0.5(3)
C(6)-C(7)-C(8)-C(9)	1.4(3)
C(7)-C(8)-C(9)-C(4)	-0.8(3)
C(5)-C(4)-C(9)-C(8)	-0.7(2)
P(1)-C(4)-C(9)-C(8)	176.33(13)
C(4)-P(1)-C(10)-C(15)	-158.21(14)
C(1)-P(1)-C(10)-C(15)	99.12(15)
Ni(1)-P(1)-C(10)-C(15)	-26.85(16)
C(4)-P(1)-C(10)-C(11)	23.21(17)
C(1)-P(1)-C(10)-C(11)	-79.45(17)
Ni(1)-P(1)-C(10)-C(11)	154.57(14)
C(15)-C(10)-C(11)-C(12)	0.8(3)
P(1)-C(10)-C(11)-C(12)	179.39(16)
C(10)-C(11)-C(12)-C(13)	-0.3(3)
C(11)-C(12)-C(13)-C(14)	-0.7(3)
C(12)-C(13)-C(14)-C(15)	1.1(3)

C(11)-C(10)-C(15)-C(14)	-0.4(3)
P(1)-C(10)-C(15)-C(14)	-179.08(14)
C(13)-C(14)-C(15)-C(10)	-0.5(3)
C(22)-P(2)-C(16)-C(17)	121.43(15)
C(3)-P(2)-C(16)-C(17)	-138.02(15)
Ni(1)-P(2)-C(16)-C(17)	-15.47(17)
C(22)-P(2)-C(16)-C(21)	-61.64(17)
C(3)-P(2)-C(16)-C(21)	38.91(17)
Ni(1)-P(2)-C(16)-C(21)	161.45(14)
C(21)-C(16)-C(17)-C(18)	-1.8(3)
P(2)-C(16)-C(17)-C(18)	175.30(15)
C(16)-C(17)-C(18)-C(19)	0.6(3)
C(17)-C(18)-C(19)-C(20)	0.7(3)
C(18)-C(19)-C(20)-C(21)	-0.7(4)
C(19)-C(20)-C(21)-C(16)	-0.5(3)
C(17)-C(16)-C(21)-C(20)	1.7(3)
P(2)-C(16)-C(21)-C(20)	-175.24(17)
C(3)-P(2)-C(22)-C(23)	-130.05(15)
C(16)-P(2)-C(22)-C(23)	-29.79(16)
Ni(1)-P(2)-C(22)-C(23)	106.06(14)
C(3)-P(2)-C(22)-C(28)	53.22(15)
C(16)-P(2)-C(22)-C(28)	153.48(14)
Ni(1)-P(2)-C(22)-C(28)	-70.67(15)
C(28)-C(22)-C(23)-C(24)	-0.6(3)
P(2)-C(22)-C(23)-C(24)	-177.41(14)
C(22)-C(23)-C(24)-C(25)	-0.1(3)
C(23)-C(24)-C(25)-C(26)	0.1(3)
C(24)-C(25)-C(26)-C(28)	0.5(3)
C(25)-C(26)-C(28)-C(22)	-1.2(3)
C(23)-C(22)-C(28)-C(26)	1.2(3)
P(2)-C(22)-C(28)-C(26)	178.12(14)

Table B7. Interatomic Distances [Å] for $Ni(dppp)_2$

Ni(1)-P(1)	2.1731(4)	C(10)-C(15)	1.382(3)
Ni(1)-P(1)*	2.1731(4)	C(10)-C(11)	1.395(2)
Ni(1)-P(2)*	2.1763(5)	C(11)-C(12)	1.386(2)
Ni(1)-P(2)	2.1763(5)	C(12)-C(13)	1.381(3)
P(1)-C(4)	1.8392(18)	C(13)-C(14)	1.377(3)
P(1)-C(10)	1.8436(16)	C(14)-C(15)	1.386(2)
P(1)-C(1)	1.8453(17)	C(16)-C(17)	1.386(3)
P(2)-C(22)	1.8466(17)	C(16)-C(21)	1.395(3)
P(2)-C(3)	1.8493(18)	C(17)-C(18)	1.387(3)
P(2)-C(16)	1.8572(18)	C(18)-C(19)	1.372(3)
C(1)-C(2)	1.527(2)	C(19)-C(20)	1.376(3)
C(2)-C(3)	1.537(2)	C(20)-C(21)	1.386(3)
C(4)-C(9)	1.394(2)	C(22)-C(23)	1.395(3)
C(4)-C(5)	1.395(2)	C(22)-C(28)	1.397(2)
C(5)-C(6)	1.388(3)	C(23)-C(24)	1.391(2)
C(6)-C(7)	1.376(3)	C(24)-C(25)	1.377(3)
C(7)-C(8)	1.377(3)	C(25)-C(26)	1.378(3)
C(8)-C(9)	1.385(3)	C(26)-C(28)	1.391(2)